Technical Support for the Long-Term Deployment of an L-Band Radiometer at Concordia Station

Yearly Report – Data Acquisition and Processing Report
Fifth Year – D3- D6
May 2018

EUROPEAN SPACE AGENCY STUDY
ESTEC Contract 4000105872/12/NL/NF

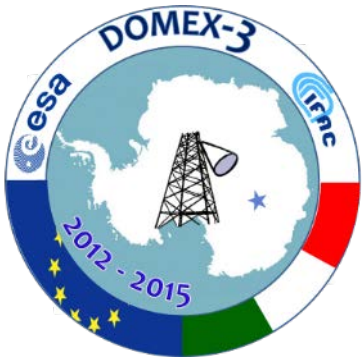

Prepared by
Giovanni MACELLONI, Marco BROGIONI, Francesco Montomoli
IFAC- CNR, Firenze, ITALY

DATE: 28/05/2018
Version: 1.0
Deliverable of the contract: D3-D6

Consiglio Nazionale delle Ricerche
Istituto di **F**isica **A**pplicata "Nello **C**arrara"
VIA MADONNA DEL PIANO N. 10 - CAP 50019 SESTO FIORENTINO FIRENZE

This page is intentionally left blank

ESA STUDY CONTRACT REPORT

ESTEC CONTRACT NO:	SUBJECT:		CONTRACTOR:
4000105872/12/NL/NF	Technical Support for the Long-Term Deployment of an L-Band Radiometer at Concordia Station		IFAC
ESA CR ( )NO:	STAR CODE:	No of volumes: 1 This is volume no: 1	CONTRACTOR'S REF: Deliverable

ABSTRACT:

This document is related to Task2 (Deliverable D6) of the study *Technical Support for the Long-Term Deployment of an L-Band Radiometer at Concordia Station* (ESTEC contract 4000105872/12/NL/NF). It contains the Fifth Year Report of the Domex-3 Experiment. In the document is described the execution of the activity that were carried out in the fifth experimental year of the project (i.e. form January to December 2017). It includes the description of the activity was conducted during of the winter campaign and in Italy. Data analysis and Data Processing Report are reported here too. The Technical Notes 1 and 2 about the absolute calibration technique implemented and the acquisition configurations used are included as annexes to this report in order to provide the reader with all of the tools for understanding the analysis carried out and provide a detailed description of the entire 2017 activity.

The work described in this report was done under ESA Contract. Responsibility for the contents resides in the authors or organisation that prepared it.

PREPARED BY:

GIOVANNI MACELLONI, MARCO BROGIONI, FRANCESCO MONTOMOLI –IFAC

ESA STUDY MANAGER:	ESA BUDGET HEADING:
TANIA CASAL	

DOCUMENT CHANGE LOG

Issue/ Revision	Date	Observations
1/0	28/05/2018	First issue –Draft Version

ABBREVIATIONS

ACL	Active Cold Load
ESA	European Space Agency
IFAC-CNR	Institute of Applied Physics – National Research Council
NS	Noise Source
OMT	OrthoMode Transducer
PI	Polarization Index
PNRA	Programma Nazionale RIcerche in Antartide
SMAP	Soil Moisture Active Passive
SMOS	Soil Moisture Ocean Salinity
UPC	Universitat Politècnica de Catalunya

This page is intentionally left blank.

TABLE OF CONTENTS

Purpose and structure of document

Purpose

This document contains the Fifth Year Report for DOMEX-3 experiment, prepared by the Institute for Applied Physics “Nello Carrara” – Firenze in the framework of the ESA contract N. 4000105872/12/NL/NF.

In the document is described the execution of the activity carried out in the fifth experimental year of the project (i.e. from January to December 2017). It includes also the studies conducted during the fifth year of the winter campaign in Italy.

The document is divided into sections in which the individual points were discussed. At the end, two technical notes about the acquisition configurations and the absolute calibration of Radomex are included as annex.

1 Overview

The Domex-3 experiment is the follow on of two previous experiments called Domex-1 and Domex-2 which were successfully conducted at Concordia base, Antarctica, by IFAC-CNR in cooperation to ESA (contracts N. 18060/04/NL/CB [1] and N. 22046/08/NL/EL, 20066/06/NL/EL [2]) and PNRA. The results obtained in these contracts demonstrated that Dome C represents a unique "high"- temperature (i.e. higher than 150 K), extended target that provides a temporally-stable reference which potentially meets existing requirements for assessing the long-term stability of space-borne L-band radiometric instruments.

In order to meet this objective, co-located ground measurements are required in order to verify target stability over time and to monitor changes in target characteristics that may affect the long-term reference signal: for example, surface roughness or "crusting", which in spite of being quite stable, appears to evolve with time (possibly due to climatic changes) and may affect the brightness temperature. Long-term monitoring of Dome C is also crucial to investigating further and to modeling variations in H-pol observed during the DOMEX-2 experiment. A long-term experiment is also recommended in order to provide a continuous data record of ground-based radiometric measurements covering the SMOS – Aquarius – SMAP era. The resulting data set will support the Level 1C quality assessment for SMOS and SMAP at the accuracy level required for climate applications. In addition, the produced data set will be instrumental for satellite sensor product inter-calibration ensuring a harmonized Level 1 data set of passive microwave observations at L-band for future climate applications.

The objective of DOMEX-3 project is to contribute to the long-term deployment of an L-Band Radiometer at Concordia Station. The activity of the contract is divided in four phases: the first phase deals with the preparation of the instrument and the experiment while the others 3 phases are constituted by the campaign and the analysis of the data acquired during the 5 campaigns 2013 - 2017. Phase-1 of the activity was devoted to the preparation of an improved version of the L-band microwave radiometer RADOMEX as well as the definition of acquisition procedure and campaign execution. Phase-1 started in January 2012 and ended in October 2012, the performed activities were reported in the CIP and RR document of the contract [3],[3],[5].

Phase-2 of the activity is constituted by the deployment of the instrument during the first summer Antarctic campaign 2012, the acquisition of the data during 2013 and its analysis and the preparation for the Austral summer campaign 2013. It started in November 2012 and ended in October 2013. Results are presented in the First Year Report of the project [6].

Phase-3 of the activity is the subject of this document, consists in the execution of the Antarctic summer campaigns (if planned) , data collection and analysis from 2013 to 2017 [6]-[9]. In particular, this document deals with the data acquisition and analysis for year 2017.

It is worth pointing out that during the Antarctic summer 2017/2018 the Domex summer campaign was not conducted. . This is mainly motivated by the fact that the instrument was in nominal conditions and any special activity was required. Moreover, during 2017 Concordia Station was in a strong fuel shortage, forcing PNRA and IPEV to organize a shorter campaign which limited the presence on the field to those projects that requireds mandatory activities.

The data acquisition and analysis (D3) is also contained here and the dataset itself is contained in D5. Due to the lack of the summer campaign, D4 (collection of the photographic material) has not prepared.

2 DOMEX-3 - 2017 DATA ANALYSIS

2.1 Data acquisitions

The acquisition of Domex data have been performed nominally for the entire 2017 year. It is worth recalling that Radomex receiver was upgraded in 2016 to improve its radiometric performances and its robustness to failures. The configuration of the acquisition geometry was scheduled according to TN2. For the first time angular scans were performed once per season throughout the year to allows an assessment of the radiometer absolute calibration and performances. The acquisition was continuous over the entire year even though 15 minor interruptions occurred, mainly caused by the blackouts that took place in power grid of the base, either scheduled or not. The interruptions did not affect the nominal functioning of the system and it automatically rebooted with the standard setup.

In summary an amount of 345437 samples, corresponding to 96.6% of total acquisitions, are currently available. For the entire period Radomex worked with the new total power three loads calibration scheme, nominally the Active Cold load (ACL), the cold load and the hot load. A forth reference load, the switchable Noise Source was acquired. Until 12/06/2017 it was turned on, then it was switched off to allow for the absolute calibration of the radiometer by using the technique reported in TN1 “Technical note on the absolute calibration strategies of Radomex”. The acquisition schedule is reported in TN2 “Technical Note on the Acquisition Plan” and listed here for the sake of convenience (Table 2-1). Angular scans were repeated approximatively once per season with an incidence angle between 20° and 110° with respect to nadir in step of 2°; four clear sky calibrations were performed pointing at 115° usually after the angular scan (only the first one was performed at 110°). In the remaining days the observation angle was at the nominal value of 42°.

Table 2-1: Data acquisition schedule for 2017

ACQUISITION TYPE	VALUE [deg] (MIN/MAX/STEP)	FROM/TO
Angular scan #1	20 - 110 step 2	18 - 28 Jan
Angular scan #2	20 - 110 step 2	1 - 6 Mar
Angular scan #3	20 - 110 step 2	2 - 6 Apr
Angular scan #4	20 - 110 step 2	25 - 28 Jun
Angular scan #5	20 - 110 step 2	31 Aug – 5 Sep
Angular scan #6	20 - 110 step 2	21 – 27 Nov
Clear SKY #1	110	7 – 13 Mar
Clear SKY #2	115	13 – 22 Jun
Clear SKY #3	115	20 – 25 Sep
Clear SKY #4	115	27 Nov – 6 Dec
Nominal Angle	42	elsewhere

2.2 Data processing and calibration

The processing of the 2017 Domex data have been performed by using a slightly different methodology w.r.t. to the previous years. This is due to the absolute calibration procedure adopted which is similar to the one developed by UPC for SMOS [11]. The improved architecture of Radomex is represented in Figure 2-1 in which the various losses and mismatches that are relevant to the measurements of Radomex are represented. There, $S_{11\text{-}V,H}$ are the mismatches at the OMT ports, $L_{ext\ V,H}$ are the external cables losses (i.e. the Phasetrack 210), $L_{int\ V,H}$ are the internal cables losses (i.e. the Sucoform 141) and $S_{xy\text{-}V,H}$ are the losses for each channel of the microwave switch.

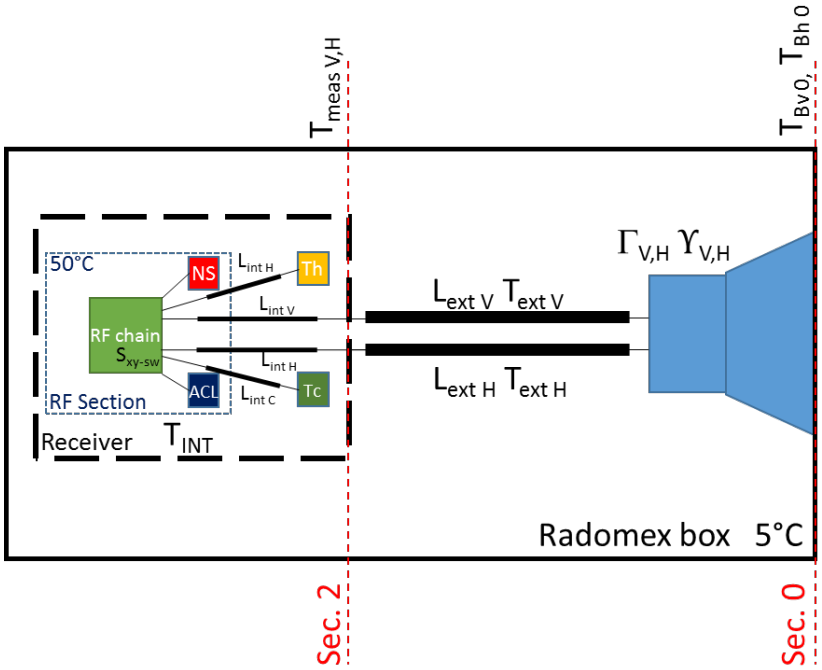

Figure 2-1: The architecture of Radomex with the improved version of the receiver. The sections at which the Tb are referred are represented as long as the nominal operating temperatures.

The general equation relating $T_{meas\ v,h}$ (Figure 2-1, Sec. 2) with the $T_{Bv,h}$ of the scene (Sec. 0) are detailed in Appendix 6 of TN1 and reported here for the sake of convenience.

$$T_{meas\ v} = L_{ext\ v}\,\Upsilon_v\,T_{Bv\ 0} + L_{ext\ v}^2\,\Gamma_v\,T_{REC} + (L_{ext\ v}\,\Gamma_v + 1)\,(1 - L_{ext\ v})T_{ext\ v}$$

$$T_{meas\ h} = L_{ext\ h}\,\Upsilon_h\,T_{Bh\ 0} + L_{ext\ h}^2\,\Gamma_h\,T_{REC} + (L_{ext\ h}\,\Gamma_h + 1)\,(1 - L_{ext\ h})T_{ext\ h}$$

Solving the previous equations for $T_{Bv\ 0}$ and $T_{Bv\ 0}$ (i.e. the brightness temperature of the scene) makes it is possible to compensate the losses of external cables and antenna. The values of L, Γ, Υ parameters are listed in appendix 7 of TN1. It should be noted that these equations taking into account more receiver's parameters (e.g. receiver temperature T_{REC} and antenna parameters $\Gamma_{v,h}$, $\Upsilon_{v,h}$) with respect to the compensation equations used in past years.

2.2.1 Absolute Calibration

While in the past years more attention was devoted to the evaluation of target's stability, this year the SMOS Payload and Calibration Working Group expressed the need to better investigate on the the absolute calibration of the Tb measured at Dome C and to an accurate evaluation of error sources. For this reason a new strategy for the absolute calibration of the Radomex measurements has been implemented. It must be underlined that the new methodology has provided different calibration curves thus the Tb values of DOMEX as delivered in previous D3 deliverables differ from the new one of few Kelvin. This fact will be discussed in section 2.3.1, where an analysis of the entire Domex-3 dataset is provided.

In particular the calibration was used until December 2016 have been derived from a dedicated campaign held on the preparatory phase of DomeX-3 in Italy [6] and from data collected during DOMEX-2 [2]. In that context two reference target namely clear sky and calm water at different incidence angles were used. The so obtained curves have been used for the Antarctic campaigns and the performed clear sky measurement were used as a tool to verify the correct TB values.

The new approach is similar to the traditional one that relies on the measurement of two stable targets (one cold, one hot) outside to the system having a well-known Tb for re-calibrating the collected data. Moreover, it does not make any assumption on the a-priori absolute calibration of the various Radomex sections. As a cold target, the deep sky was used since it has a stable Tb. The plane of the galaxy and other RF emitting natural sources were avoided during the measurements. To observe the sky it is sufficient to rotate the instrument at its highest elevation over the horizon. Regarding the hot target, a direct measure is not possible for Radomex in Antarctica and, like SMOS, an "artificial" one must be simulated. In particular, one of the internal reference loads has been used. Particularly suited to this aim is the noise source that can be electronically switched on and off. In this latter case it is equivalent to a matched load at its thermometric temperature T_{NS} (i.e. about 50°C).

By considering the switch port losses L_{SW}, internal cable losses $L_{INT\,V,H}$, external cable losses $L_{EXT\ V,H}$ and antenna ports mismatch $S_{11\,V,H}$ it is possible to simulate a load at the antenna plane, i.e. in similar conditions of the sky, by means of the Friis formula. The procedure is fully described in TN1. The radiometric schematization of the equivalent hot load chain is represented in the Figure 2-2.

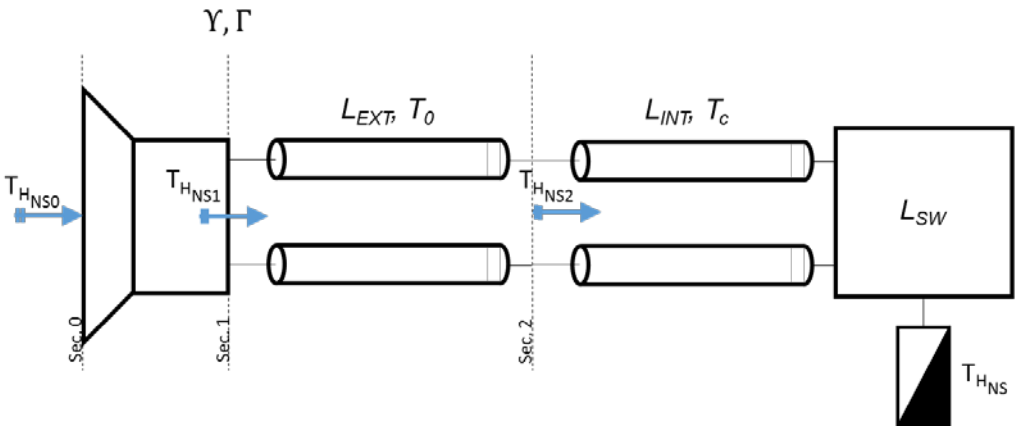

Figure 2-2: Radiometric schematization of the chain losses for the second methodology

In Figure 2-2 the switched-off noise source is represented as a matched load at the RF chain temperature. Since also the switch is at the NS temperature, the chain can be further simplified. The Tb of the pseudo-hot target is expressed by

$$T_{H_{NS0\,\mathrm{v,h}}} = \frac{\beta_{\mathrm{v,h}} - \Gamma_{\mathrm{v,h}}\, T_{REC1}}{1 - \Gamma_{\mathrm{v,h}}}$$

where

$$\beta_{\mathrm{v,h}} = \frac{\alpha_{\mathrm{v,h}} - \left(1 - L_{EXT\,\mathrm{v,h}}\right)\, T_0}{L_{EXT}} \qquad \alpha_{\mathrm{v,h}} = \frac{T_{H_{NS}} - \left(1 - L_{INT\,\mathrm{v,h}}\right)\, T_c}{L_{INT\,\mathrm{v,h}}}$$

In order to get the absolute calibration curves (one per channel), the radiometer must be pointed toward the sky. Then the measured temperature of the sky is related to its theoretical value and the same is done with the noise source turned off. In this way, it is possible to derive the equation for the absolute calibration and correct the entire dataset. The entire procedure is described in deep in TN1 along with the associated error analysis.

The calibration approach has been tested by using the data collected from 31 May to 7 July 2017. On June 14-23, Radomex acquired data looking at the sky with an incidence angle of 115 deg while the internal noise source was turned off (see Figure 2-3).

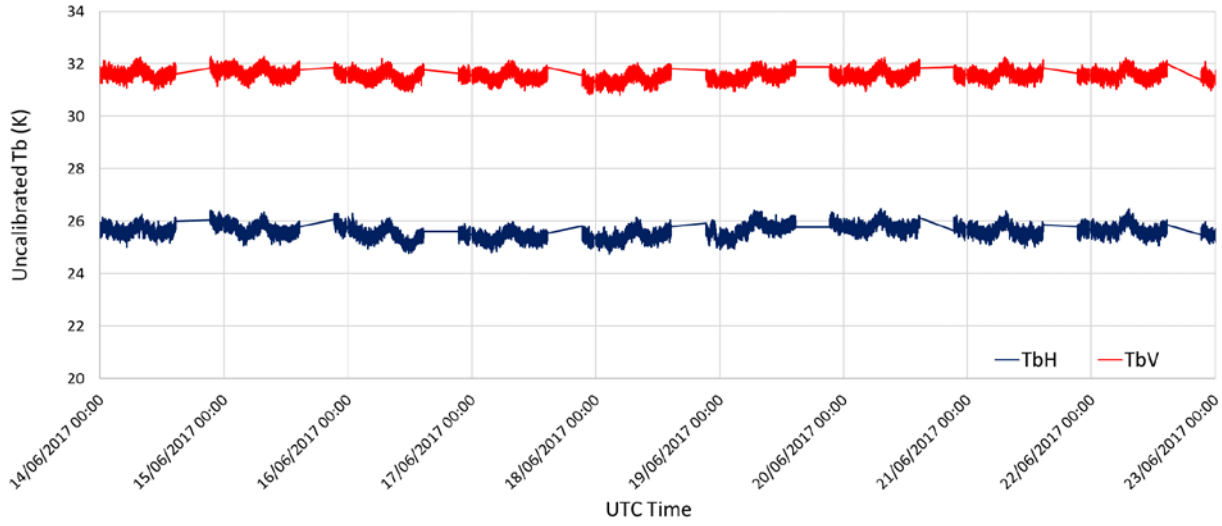

Figure 2-3: Data collected on Jun 14-23 2017 for the absolute calibration test. Data relative to the crossing of the inner galaxy arm were removed.

Only data collected from 21:30 to 14:30 were used since the center of the galaxy is outside the antenna lobe in this period. Before the calibration the Tb of the sky measurements were 31.6K and 21.6K for the V and H pol respectively (standard deviations 0.2K and 0.24K).

The brightness and physical temperature of the equivalent hot targets were 333.8K and 331.9K for the V and H polarization respectively (standard deviation 0.11K and 0.12K respectively).

For the theoretical Tb value of the cold target (clear sky), to be used as secondary reference load, some assumption are needed. Indeed, because of the real aperture of the antenna and giventhat the radiometer was measuring at an elevation of 25 deg above the horizon , the radiometer still collected energy coming from the ice sheet (albeit very small) when it pointing the sky. In order to consider this effect, we have to convolve the antenna lobe with the Tb of a proper synthetic scene. This latter is assumed as composed by Tb of ice sheet and sky as observed by a point antenna. For the ice sheet we used the Tb simulated by using the WALOMIS model [12] Sky emission was obtained by using a radiative transfer model under the assumption of non-scattering plane parallel atmosphere in local thermodynamic equilibrium [13] and two years of Radio-Echo Sounding collected at Dome C by the Italian Meteorological observatory from Jan 2012 to Dec 2013 [14]. Gaseous absorption/emission (mainly water vapor and oxygen) formulas were developed by Rosenkranz [15], cloud layers are identified from radiosonde observations when the atmospheric RH profile exceeds a suitable threshold [16], absorption/emission from Liebe [17] and further modifications. The synthetic scenario is represented in Figure 2-4 along with the antenna gain (Radomex antenna has a symmetrical lobe on the V and H planes) placed at an incidence angle of 115°. Figure shows that at this angle a small part of the lobe (i.e. left side from 90° to 80 °) is still affected by the Tb value of the ice sheet.

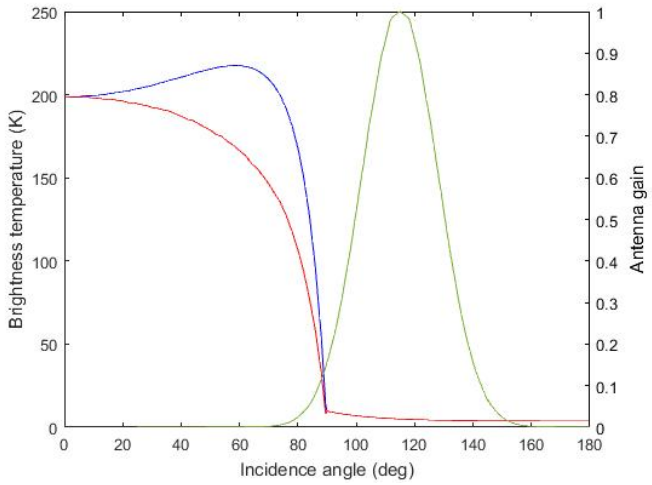

Figure 2-4: The angular trend of the synthetic scenario at V- (blue) and H-pol (red) plotted along with the antenna gain (green) in a linear scale.

By computing the convolution of the antenna on the scenario it is possible to derive the true Tb values observed by the radiometer while looking at 115deg. They resulted in being 7.51K and 6.65K for the V and H pol respectively. With these hot and cold reference target characterized, it was possible to calibrate absolutely Radomex data. As a first test, the data collected fourteen days before (from May 31 00:00 to June 13 10:00) and after (from June 23 3:50 to July 7 23:36) the sky measurements while looking at the ice sheet at 42 deg incidence angle were calibrated absolutely. The average Tb values obtained were 211.14K and 186.32K (pre-calibration period, σ 0.22K and 0.24K) and 211.04K and 186.22K (post-calibration period, σ 0.21K and 0.33K) for the V and H pol respectively. This result confirms that calibration method is stable in time. The values obtained by the new method resulted in being slightly higher with respect to those obtained during the 2016 Antarctic campaign (see Table 2-2) and better in line with SMOS data, especially at V-pol.. It must be underlined that Domex data showed in table were not deconvoluted for the antenna pattern, thus the Tb values will likely increase by a few K.

Table 2-2: Values of Tb after the absolute calibration

Dataset	Tb (K)	
	H pol	V pol
Domex June 2017 new procedure	186.27	211.09
Domex entire 2016 (no sun)	185.24	207.73
SMOS entire 2016	186.3	212.37

The absolute calibrated Domex 3 dataset, acquired ar 42°, for the year 2017 are represented in Figure 2-5. The gaps in figure are related to the angular scans and sky acquisition which are not represented. The spikes

present until March and after mid of September are due to sun emission reflected by the ice sheet into the antennas observed in previous camapigns.

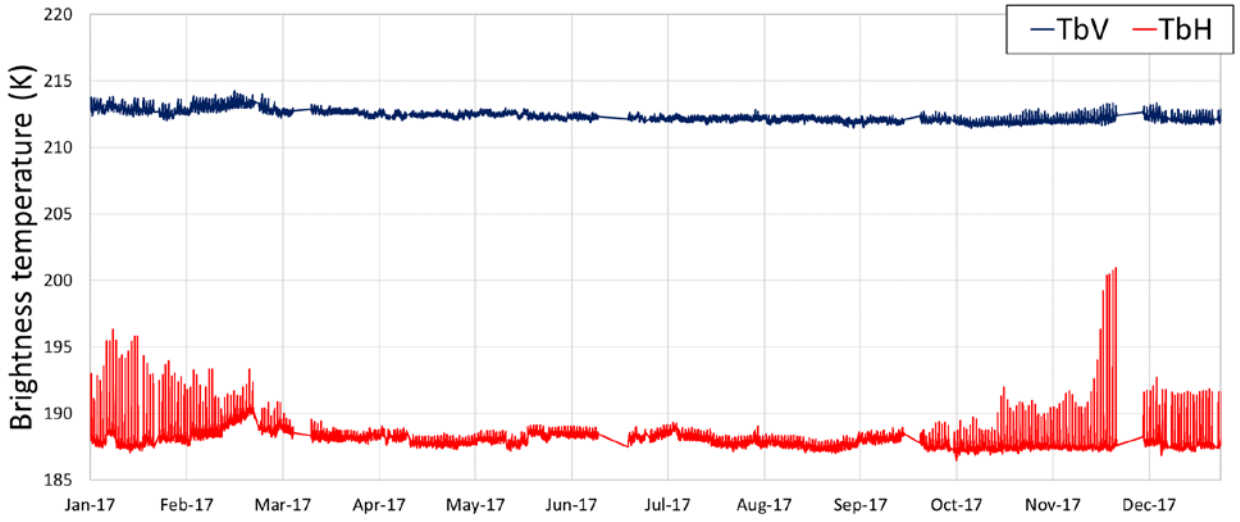

Figure 2-5: Absolute calibrated brightness temperature timeseries at V pol (blue) and H pol (red) collected at 42 deg incidence angle. The spikes are related to the sun emission reflected by the ice sheet into the antenna.

2.2.2 Antenna Deconvolution

After the absolute calibration process, the antenna deconvolution is the remaining step was performed to derive the brightness temperature as emitted from the ice sheet. Albeit having a quite narrow beamwidth (15deg at -3dB), the influence of the Radomex antenna on the ice sheet measurement can be of the order of few K, especially at H polarization. The antenna lobe particularly affects the measurements carried out at incidence anglegreater than 40 - 50 deg, i.e. when the antenna start to illuminate the emission of the sky above the horizon.

Thus, the deconvolution of the Tb measured with the antenna lobe is important to retrieve the “true” brightness temperature value at the various incidence angles. The deconvolution wascomputed for the mean Tb values and the angular correction was then applied to all the data.

In order to perform the deconvolution a consistent data set of Tb measured at different incidence angle was selected. The angular scans that were performed throughout the 2017 campaign are:

- 5 extended scans 20-160 deg in summer
- 35 standard scans 20-115 deg in the entire year (one set of scan per season)

In Figure 2-6 are represented the angular trends for the V and H polarizations, along with the standard deviation of the Tb obtained for each incidence angle. Data at incidence angles below 20 deg, and above 150 deg were artificially introduced in order to complete the angular scan and to allow the deconvolution. Indeed,

because of the influence of the tower structure where the instrument is installed, data at these angles were not acquired.. For the V pol, the std dev of the measurements is around 0.3 K until θ<60deg. Then it increases due to the effect of a small pointing variation of the instrument (i.e. ± 0.5 K with respect to the nominal value) for angle close to the horizon. The H pol shows an increasing trend starting at about 30-40 deg because to the temporal variability of the ice sheet properties throughout the year. It is worth to recall that this variability affects lesser the V pol. e. Overall the std dev of Tb remains lower than 1K over the entire angular scan range.

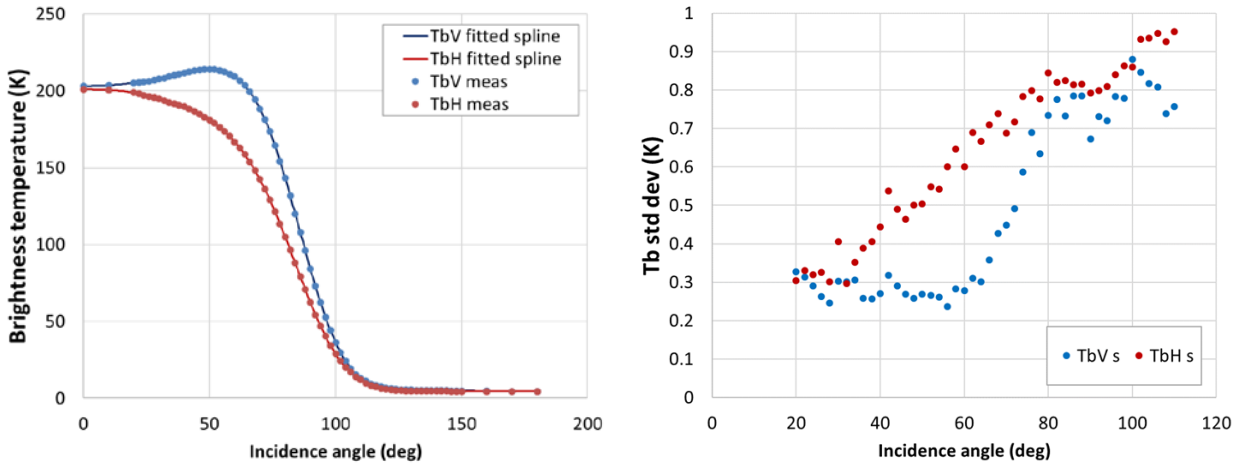

Figure 2-6: Annual average of Tb angular trends (left) and standard deviation of the measurements (right). V and H pol are represented in blue and red respectively. Due to the smaller number of measurements at high incidence angles, the standard deviation is computed only for the angular range 20-110 deg.

The Tb angular trend have been deconvoluted with an iterative process as represented in Figure 2-7: the measured Tb is deconvolved in order to retrieve a first guess of the "true profile". This profile is then modified and convolved again with the antenna lobe until the difference between the measured and convolved profiles is minimized.

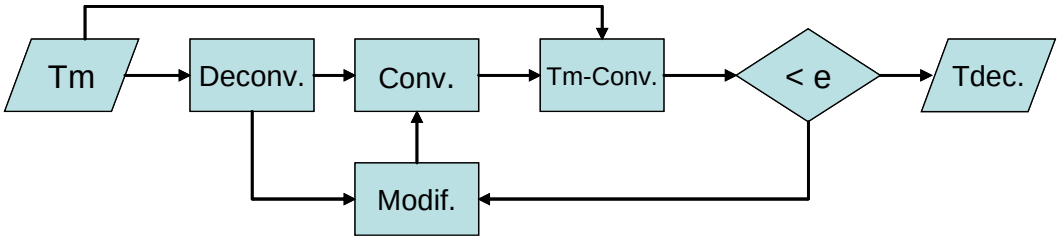

Figure 2-7: Flowchart of the deconvolution procedure.

The starting step was to obtain a first guess of Tb_{deconv} by using the relative increments of Domex-2 deconvolution applied to the 2017 measured Tb. Then:

- for each Tb_{deconv} curve 15 nodes (approximatively every 10 deg) are selected,
- by using a smoothing spline the nodes are interpolated,

- the convolution process is performed and, according to the results, reiterated until the difference between $Tb_{measured}$ and $Tb_{deconvolute\text{-}convoluter}$ is lower than 1K.

This method (based on the nodes and splines) resulted to be the most viable with respect to modify directly the interpolant of the first guess. After having run the procedure for both polarizations, the final deconvolution curves were obtained (Figure 2-8) as well as the relative error in Figure 2-9 (i.e.the difference between measured and deconvoluted values).

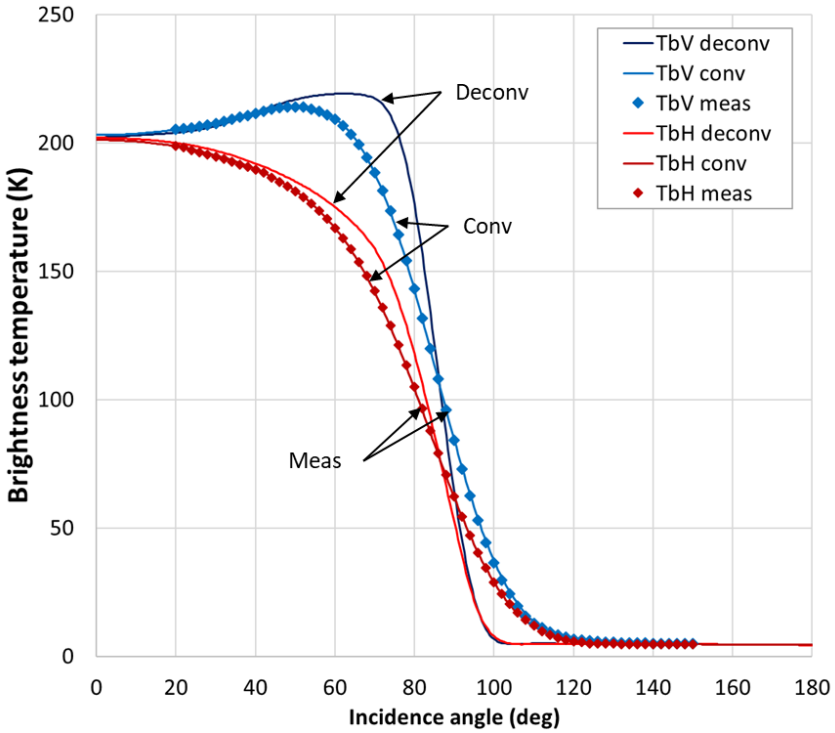

Figure 2-8: Angular trends of Domex Tb. V and H pol are shown in blue and red respectively. Diamond represent measured data, blue and red the deconvoluted trends while light blue and magenta the deconvoluted/convoluted Tb.

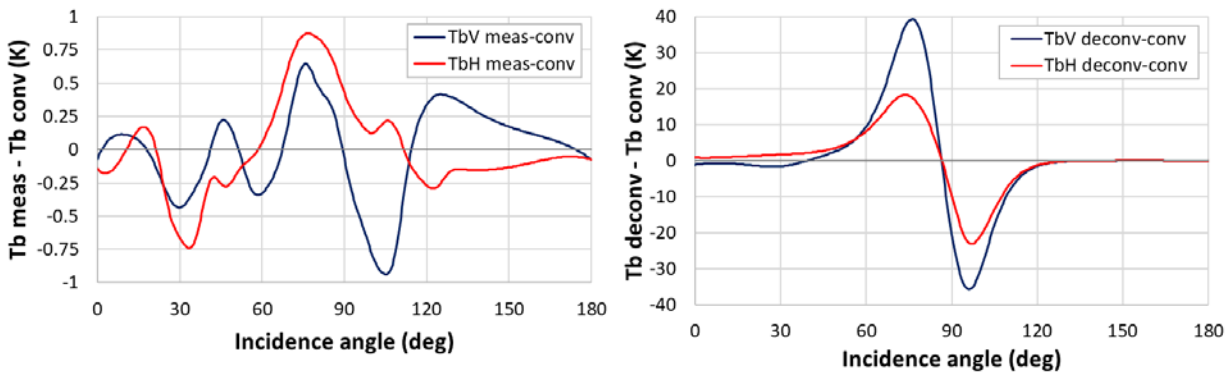

Figure 2-9: Residual errors of the deconvolution process (left) and Tb variations between deconvoluted and convoluted data (right). V and H pol are represented in blue and red respectively.

In Figure 2-10 and Figure 2-11 the Tb deconvolution for the data acquired over the ice sheet (incidence angle between 20 deg and 60 deg) are represented. In this range the maximum error in the procedure is 0.75 K at H pol, while at V pol the error is slightly lower. Focusing on the nominal Domex angle, the error Tb_{meas}-$Tb_{deconv-conv}$ is negligible at V pol and lower than 0.25 K at H pol (Figure 2-11 left). Regarding the correction provided by the deconvolution to the Tb, at 42 deg incidence angle the V pol is increased by 0.65K and 2.4K at Hpol.

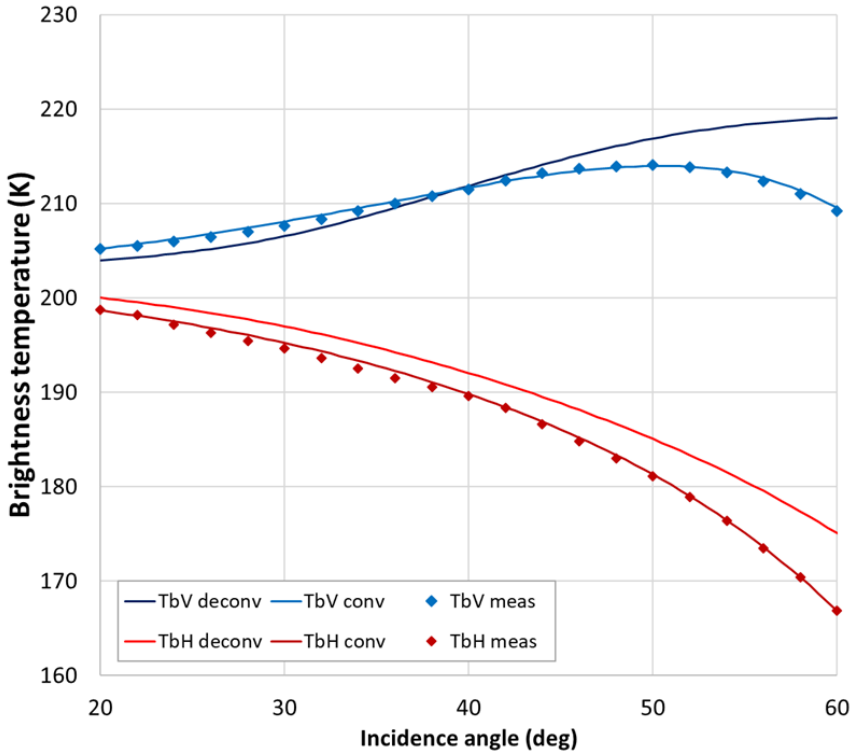

Figure 2-10: Zoom of the angular trend of Domex Tb for the 20-60 deg angle range. V and H pol are shown in blue and red tones. Diamond represent measured data, blue and red the deconvoluted trends while light blue and magenta the deconvoluted-convoluted Tb.

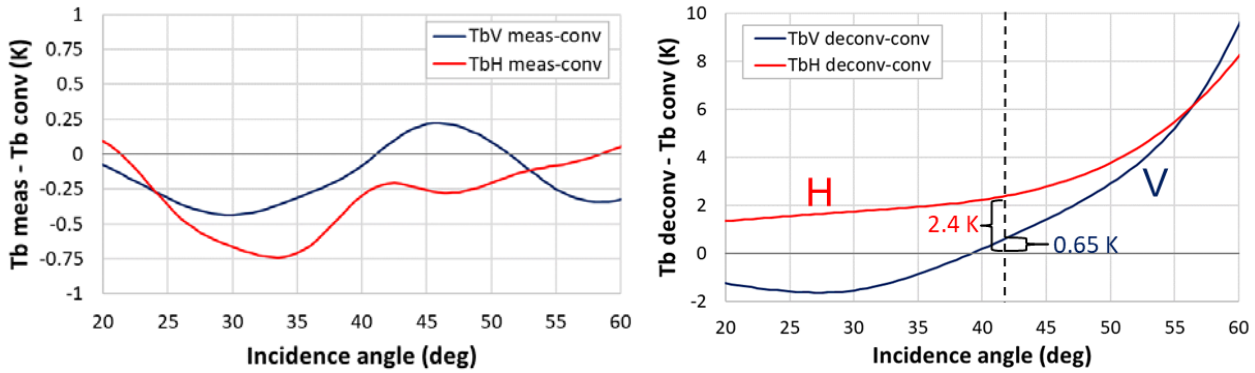

Figure 2-11: Zoom of the residual errors of the deconvolution process (left) and of the Tb variations between deconvoluted and convoluted data (right) for the 20-60 deg angle range. V and H pol are represented in blue and red respectively.

2.2.3 Tb sky correction

The last analysis carried out was the evaluation of the atmospheric contribution which should be added to Domex measurements in order to make them equivalent to a satellite scenario, i.e. Top of the Atmosphere (TOA).

In Figure 2-12 are represented the different atmospheric contributions as seen by Domex and by SMOS (or by any other spaceborne radiometer). In Figure 2-12 T_{up}, T_{dn}, T_{CMB} represent the upwelling, downwelling and cosmic microwave background Tb respectively while *Att* is the integrated atmospheric attenuation and Γ is the reflection coefficient of the ice sheet.

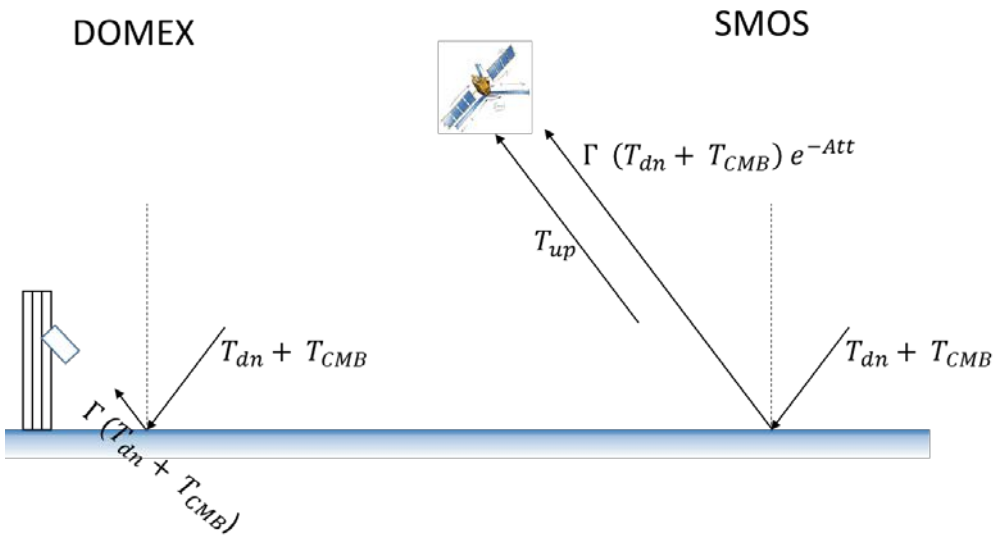

Figure 2-12: Schematization of the atmospheric contribution for the ground (Domex, left) and spaceborne (SMOS, right) scenarios.

By assuming the atmospheric emission to be unpolarized (i.e. $T_{up} = T_{dn}$), its contribution to the Tb measurements is:

- Domex: $T_{atm} = \Gamma_{V,H}\ (T_{dn} + T_{CMB})$
- SMOS: $T_{atm} = T_{up} + \Gamma_{V,H}\ (T_{dn} + T_{CMB})\ e^{-Att}$

At 42 deg incidence angle, the ice sheet and atmospheric parameters are (these latter were obtained by Tb simulated from radiosonde data collected at Dome C from 01/01/2012 to 31/12/2013) [14]:

- $T_{up} = T_{dn} = 1.29\ K\ (\sigma^2 = 0.028\ K)$
- $Att = 5.582\ 10^{-3} Np\ (\sigma^2 = 1.99\ 10^{-4} Np)$
- $\Gamma_V = 0.019$
- $\Gamma_H = 0.16$

- $T_{CMB} = 2.7\ K$

which provide the atmospheric contribution summarized in Table 2-3.

Table 2-3 – Values of Tb after the absolute calibration

Scenario	Tb (K)	
	V pol	H pol
Domex	0.076	0.64
SMOS	1.37	1.92

The difference between SMOS and Domex are 1.29K and 1.28K for the V and H pol respectively. These values represent essentially the upwelling contribution of the atmosphere.

2.3 Data analysis

The entire dataset of absolute calibrate brightness temperature data collected in 2017 is shown in Figure 2-13 at V (blue) and H polarization (red). The time series spans from 1/1/2017 to 31/12/2017 and it contains data averaged every 4 minutes for the acquisitions at 42 deg. No temporal averaging is performed for the observations collected pointing towards clear sky and for the angular scans, in order to ensure a better separation between nominal observations and transitional angles.

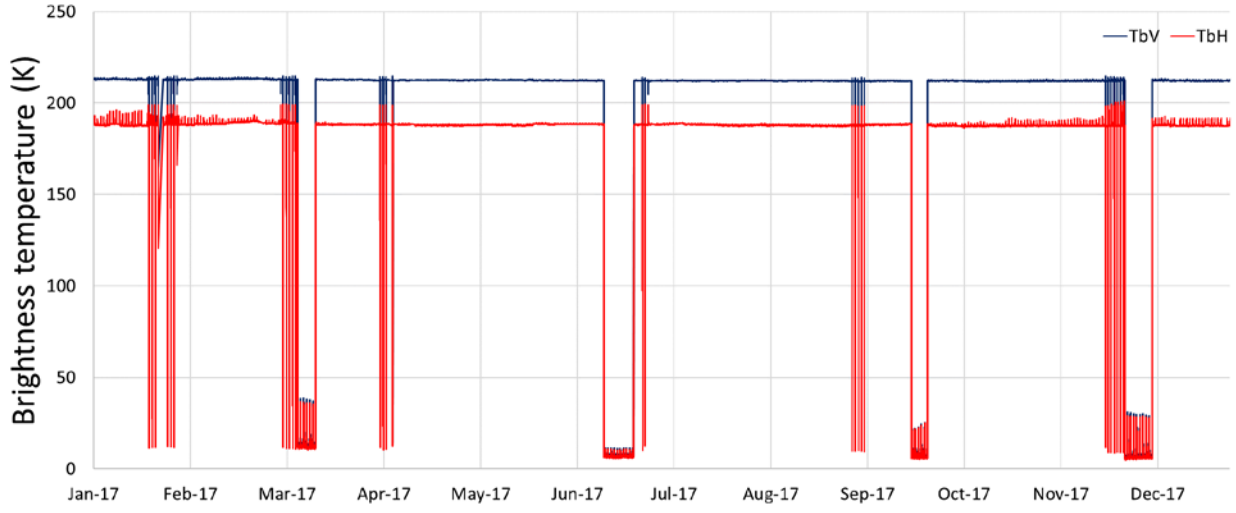

Figure 2-13: Absolute calibrated brightness temperature collected in 2017

Data acquired at 42 deg incidence angle are shown in Figure 2-14. The Tb trend resulted to be quite flat at both polarizations. However it should be noted that starting from mid-January, Tb to increase until end of

February when a sudden decrease took place (noticeable especially at H pol). This phenomenon is similar to what happened in 2015, when particular meteorological conditions affected the surface properties of the snow causing a similar Tb fluctuation [18]. As expected, spikes due to the sun emission reflected by the ice sheet inside of the antenna lobe are present and they disappear only during the Antarctic night (approx. April through September). These peaks can be quite strong at H polarization (up to 10K) even though they are noticeable also at V pol. Given the sun reflections could be hardly compensated without introducing artifacts, in Figure 2-15 is represented the time series of Tb collected when the sun was outside of the antenna lobe (sun above the horizon and associated azimuth between 100 deg and 200 deg). In Figure 2-16 the standard deviation of Tb computed every 20 samples at V and H pol are provided.The quality of data is in agreement with previous years with a typical value of standard deviation of around 0.18 K except few anomalous values due to the restart of the radiometer following the blackouts.

Data acquired at 42 deg incidence angle confirm the high temporal stability for the L-band emission of the ice sheet at V polarization with average and standard deviation values of 212.26K and 0.3K respectively. A similar behavior is observed for H- pol (mean=188.03K and std=0.49K) with only one clear change of the scenario due to a modification on snow surface. The histograms of calibrated V and H pol, showing the data distribution at 42 deg, are reported in Figure 2-17.

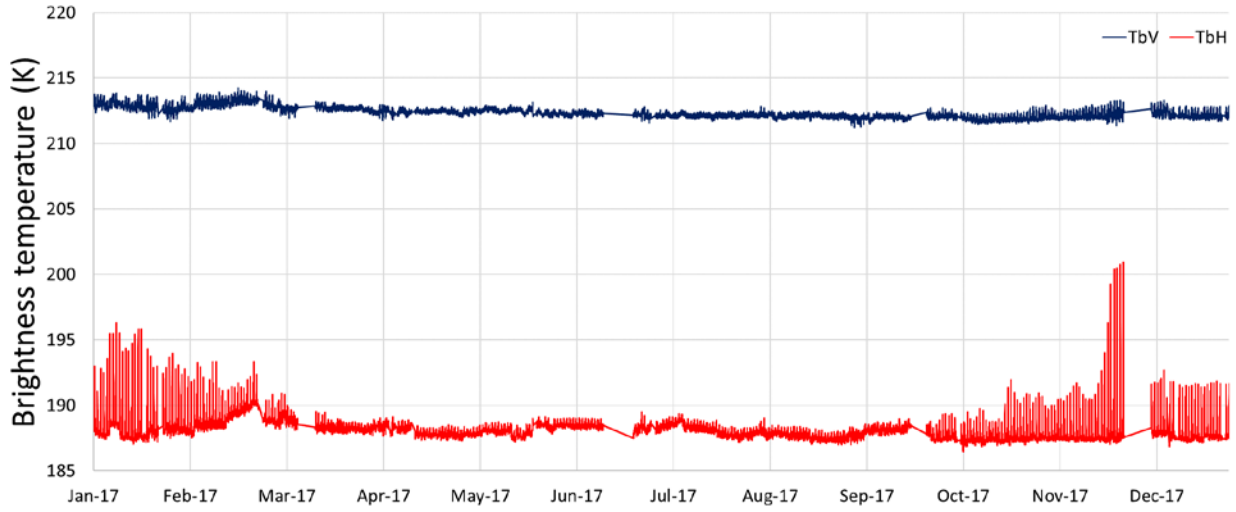

Figure 2-14; Brightness temperature recorded on 2016 for V- pol (blue) and H- pol (Red) at 42° observation

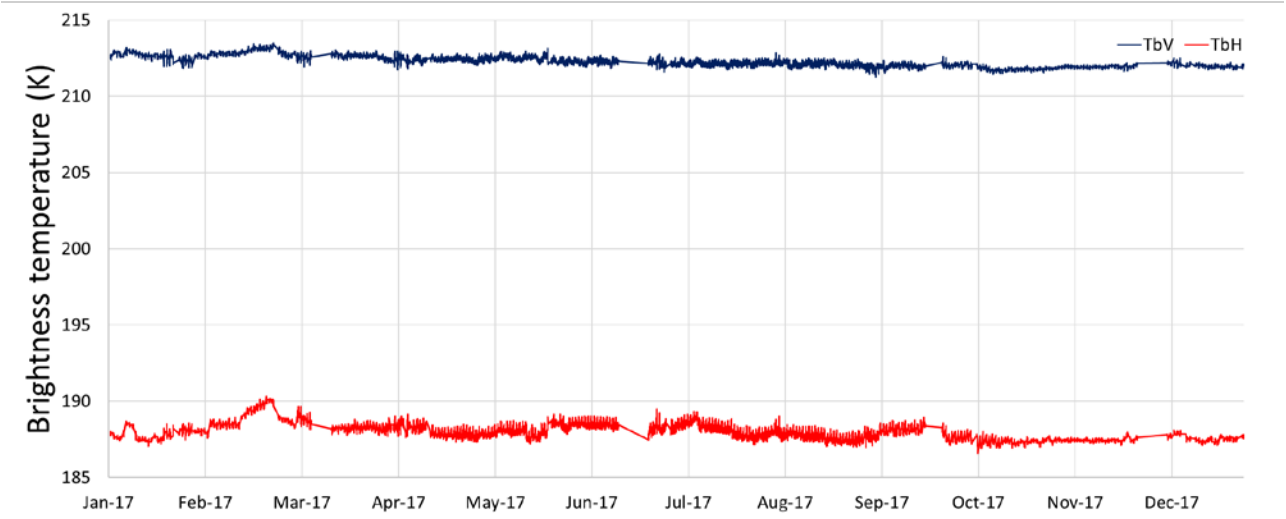

Figure 2-15: Brightness temperature at 42° after the removal of the effect of sun reflections.

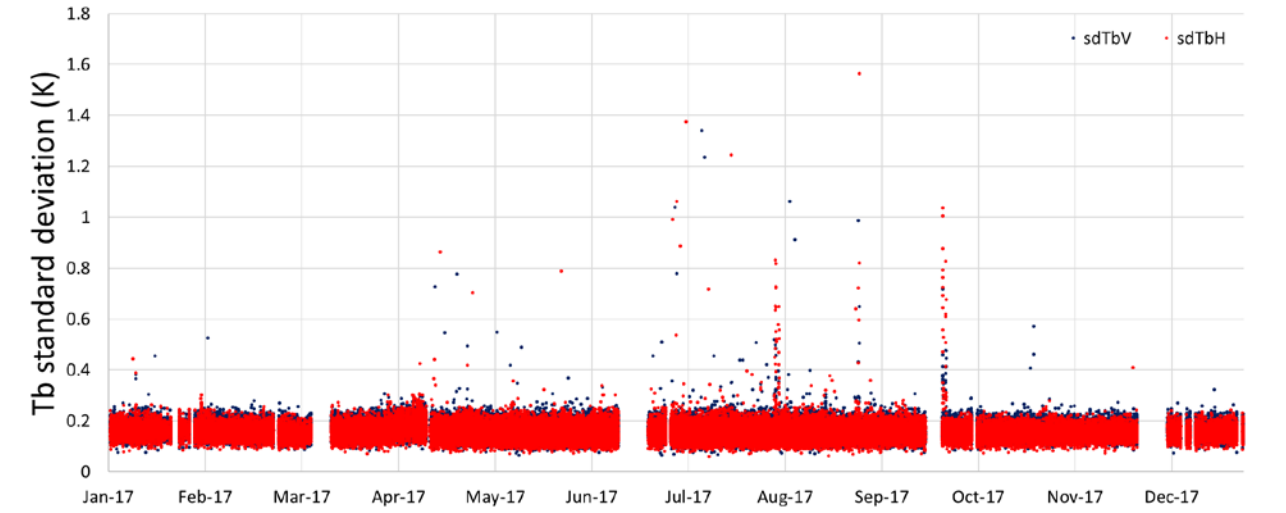

Figure 2-16: Standard deviation computed every 20 samples for the Tb collected at 42 deg incidence angle. V and H pol are represented in blue and red respectively.

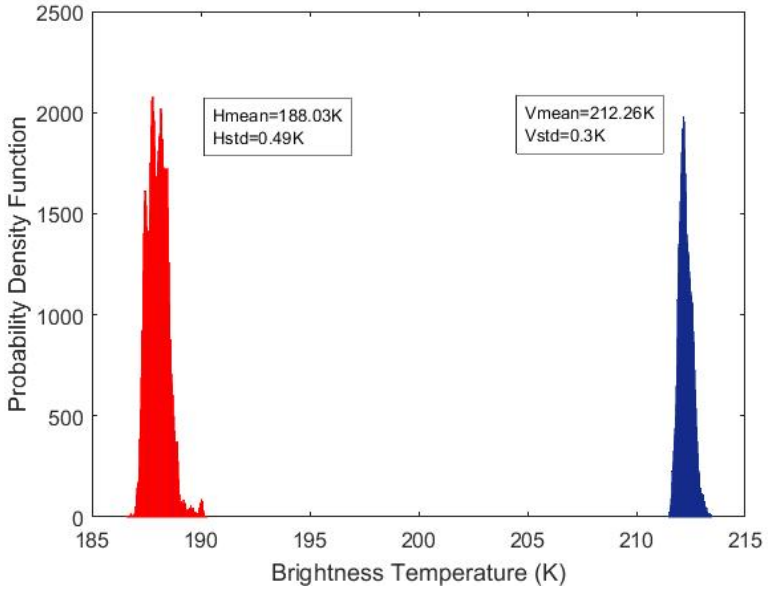

Figure 2-17: Statistics of TbV and TbH showing the probability density function of data acquired along the 2017 year. Average and standard deviations are reported on the plot.

The Polarization Index - PI (PI = 2* (Tbv-Tbh)/(Tbv+Tbh)) is represented in Figure 2-18. PI does not show appreciable fluctuations although some variations are present in February, May and September. The average value of the PI along the year is 0.121 and is slightly higher that the values observed in the past (0.116, 0.108, 0.110 for the year 2016, 2015 and 2014 respectively). However this fact could be due to the different absolute calibration procedure applied to the 2017 data. Conversely, the standard deviation of the PI is 0.0022, in line with the one derived in 2016 (0.0024) and 2014 (0.0028).

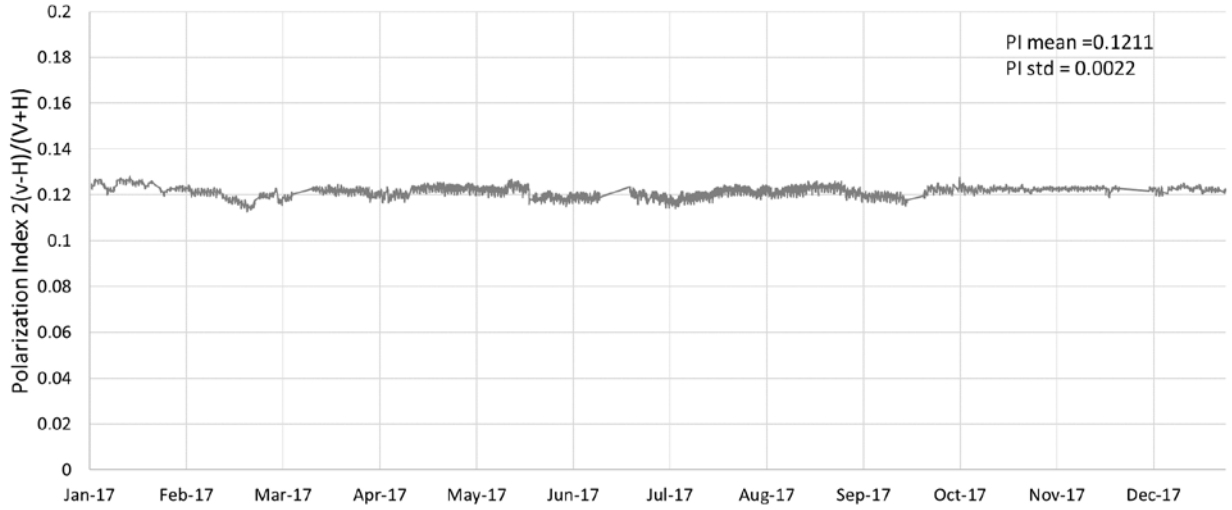

Figure 2-18: Polarization index as a function of time

The quality of instrument is also evaluated by its temperature stability in different control point.

The most relevant is the time series of thermometric temperatures inside the thermo-controlled RF-section provided in Figure 2-19. It is measured by PT100 probes stitched on the switch (red line) and on the noise source (blue line). It is worth recalling that the PT100 probe of the RF-section thermal control (a PID system) is located in the same point of the mw switch PT100 sensor. This is the reason for the higher stability of T_{sw} with respect to T_{NS}. The few interruption in the time series are due to the electrical blackouts.

The temperature inside of the RF section proved to be extremely stable (the NS that is located in the farthest point from the mw switch experienced an annual variation of 0.5°C while the external cables of 35°C), and a steady decreasing trend of 0.06°C (annual delta) can be noticed on T_{sw}. Once detrended, the standard deviation of T_{sw} resulted to be 0.027°C.

Temperatures measured on the RF cables at the antenna and the receiver sections, are shown in Figure 2-20. The temperatures have a fluctuation of about 5 °C during the winter that increases in the summer, when the internal temperature of the box get higher than the setpoints of the PID system and thus it cannot be controlled anymore. It should be noted that the maximum temperature value during the summer (until February and after December) is kept below of 20°C by the opening of the fresh air in/outlets that expel hot hair from the box and replace it with cool air from the outside.

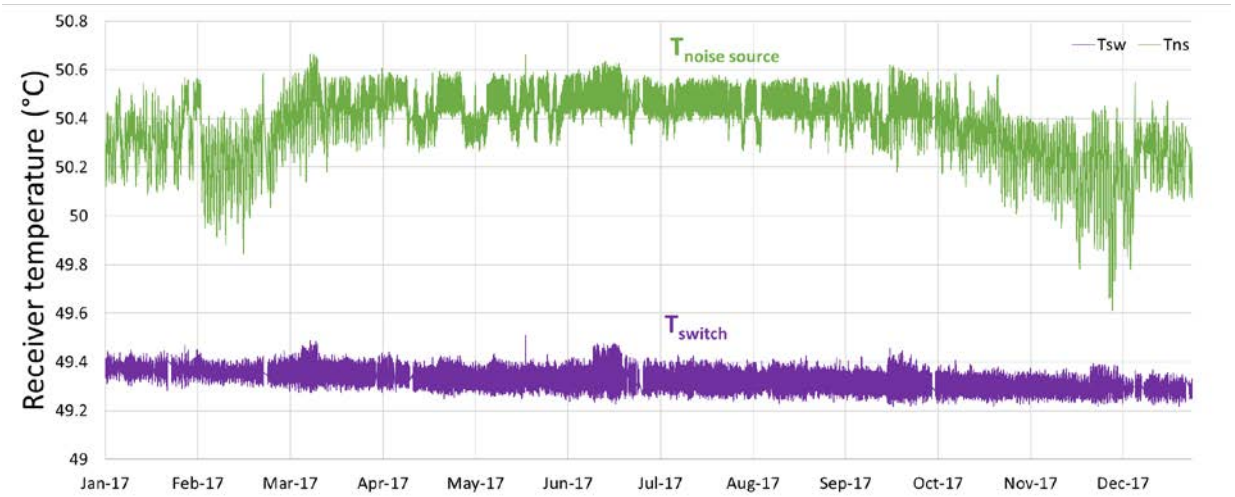

Figure 2-19: Temperature measure by PT100 inside the thermo-regulated box, on the switch (purple) and on the noise source (green).

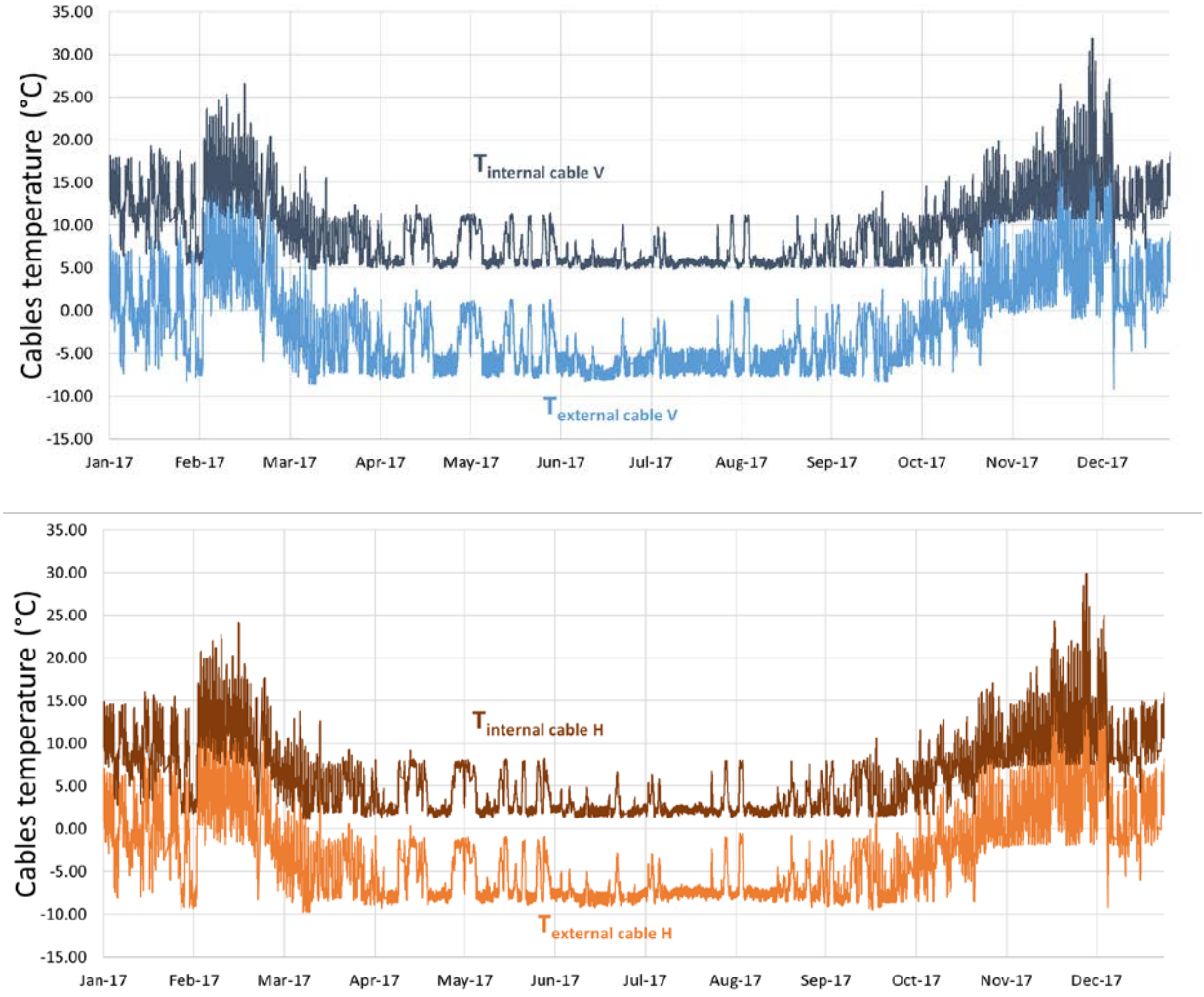

Figure 2-20: Temperature measured on the antenna cable and on the RF cable labelled as internal and external cable respectively. Cables associated to V and H polarizations are shown in the top and bottom charts.

2.3.1 Analysis of the full Domex-3 timeseries

The full series of brightness temperature data acquired spanning from the beginning of DomeX-3 experiment to the present date (January 2013 through December 2017) is provided in Figure 2-21. It should be noted that, as before explained, there is a bias between the old and new Tb resulted from the different calibration used (see [7]-[10] for the years before 2017). In order to be consistent with the values resulted from absolute calibration of the current year, data collected until December 2016 have been realigned by adding a bias of 4.53 K and 2.79 K to Tb collected before December 2016 at V and H polarization respectively. The resulting timeseries is provided in Figure 2-22.

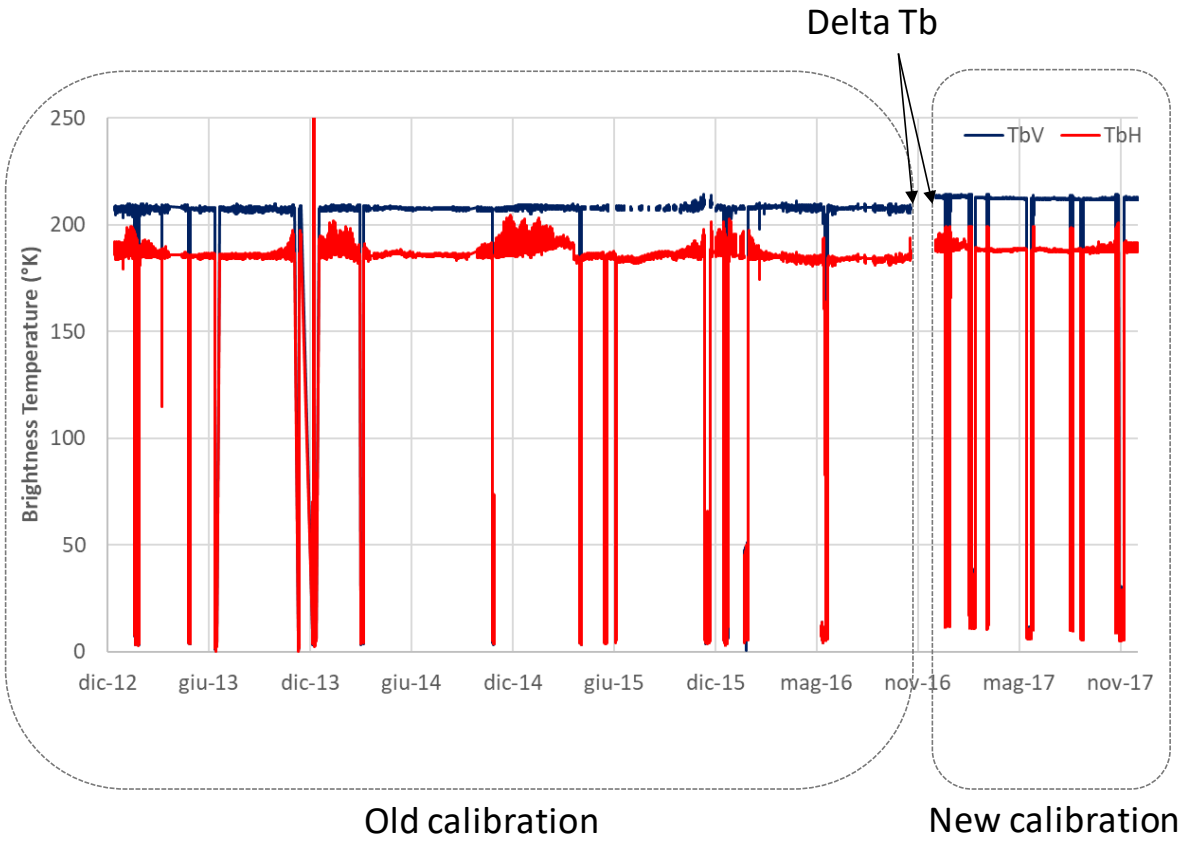

Figure 2-21: Entire Domex-3 dataset of brightness temperature at V (blue) and H polarization (red). The periods in which different calibration methods are used is highlighted by the blue boxes.

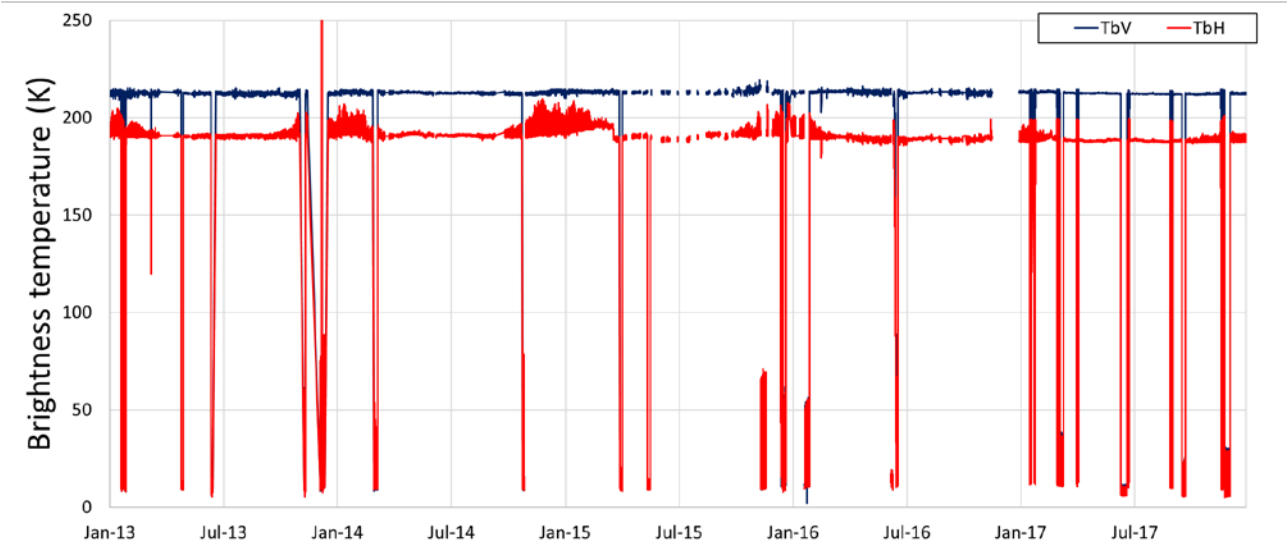

Figure 2-22: Full time series of Domex-3 brightness temperature spanning from January 2013 until December 2017.

A representation of the temporal trend of brightness temperature is provided at 42 degrees incidence angle by removing the data collected when the sun emission was reflected into the antenna by the ice sheet. The dataset is composed by a total of 873109 samples acquired every 3 minutes. The mean and the standard deviations over 20 samples are shown Figure 2-23 and Figure 2-24 respectively.

In line with the trend pointed out in the previous reports, it can be observed that V polarization is very stable (standard deviation 0.62 K) over the entire period. Moreover, if we consider two different time periods before and after Dec. 2016, the dispersion around the average decreases from 0.69 K to 0.41 K. This is addressed to a better stability of the new receiver and an improved correction of the cable losses.

Unlike V- pol, H-pol shows a more fluctuating trend. Excluding any instrumental issues since the radiometer acquired correctly, the variation is explained with the modification of the snow density in the first centimeters below the surface [7]. A sharp variation on H pol occurred between 20 March and beginning of April 2015 of around 5K change in few days. The event has been deeply investigated and reported in [18].

The standard deviation computed every 20 observations is provided in Figure 2-24. Taken apart the few periods when the calibration switched from T_{hot}/T_{cold} to $T_{hot}/T_{hot}+NS$ (from Apr 2013-Dec 2013, Aug 2014-Dec 2015) where the value is lower than 0.6-0.8 K, the cumulative value has mean of 0.15K and 0.20K for V and H polarizations.

The full time polarization index is shown in Figure 2-25.

The full time trend of temperatures measured on the RF cables at the antenna section is shown in Figure 2-26. Seasonal fluctuation from summer to winter are on the order of 35°C in the period until Dec 2016 while in the last season the delta decreases to 15 °C. The improvement have been achieved by opening the fresh

air inlet during the summer kept until March. As a consequence of a more stable temperature, the cable losses correction was more efficient.

The temperature measured inside the RF box over the 5 year data, is provided in Figure 2-27, and measured on the switch (purple line) and on the noise source (green line). The temperature have been stable (standard deviation lower than 0.06 °C) albeit a failure caused by unexpected power blackout in the base in Aug 2016 where the PID lost the thermal control. The nominal functioning was restored in Dec 2016 when the temperature was again very stable. Note that a higher set-point has been selected from this date.

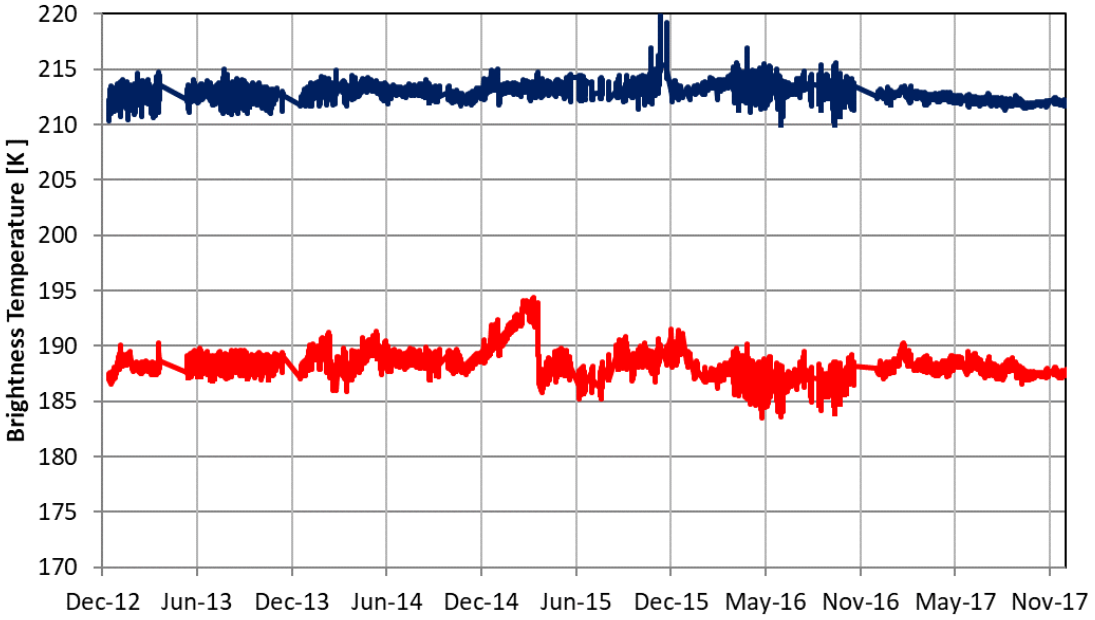

Figure 2-23: Full time brightness temperature from 1st Jan 2013 to 31 Dec 2017 considering only 42 deg incidence angle and removing the effect of sun reflections.

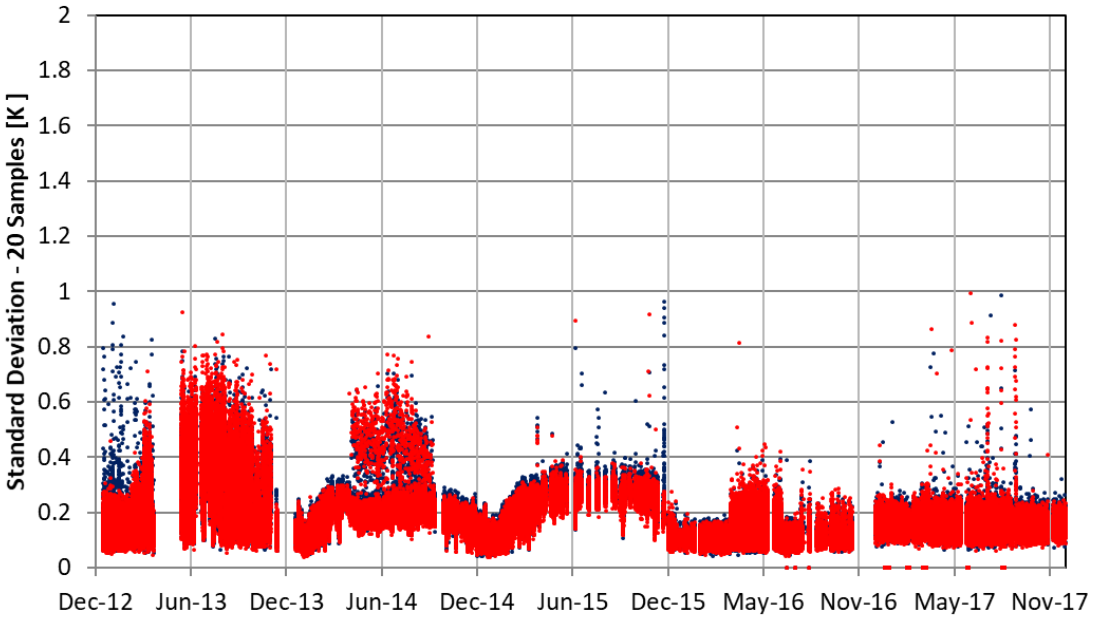

Figure 2-24: Standard deviation of brightness temperature from 1st Jan 2013 to 31 Dec 2017 considering only 42 deg incidence angle and removing the effect of sun reflections.

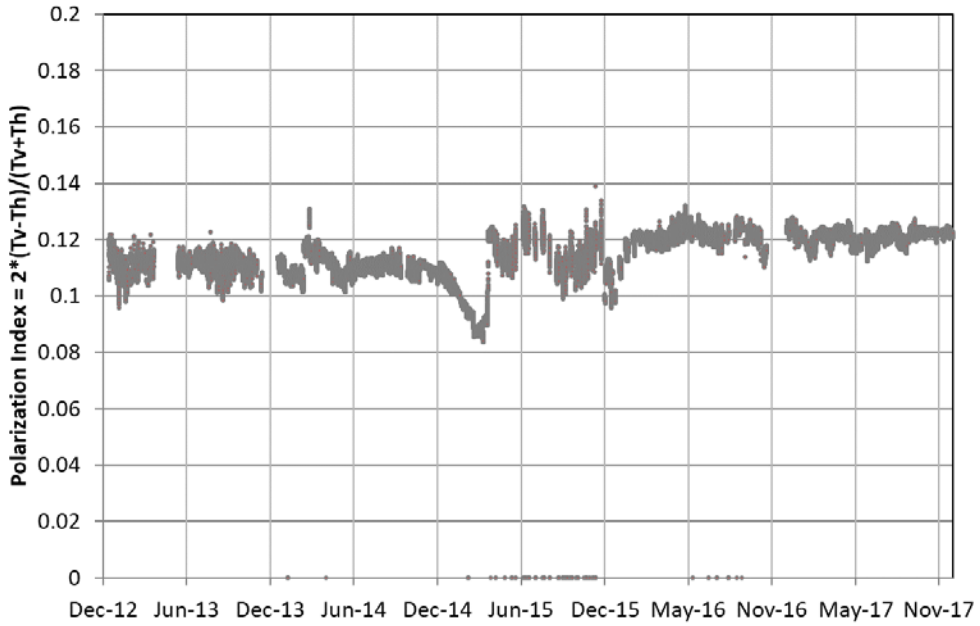

Figure 2-25: Polarization index from 1st Jan 2013 to 31 Dec 2017

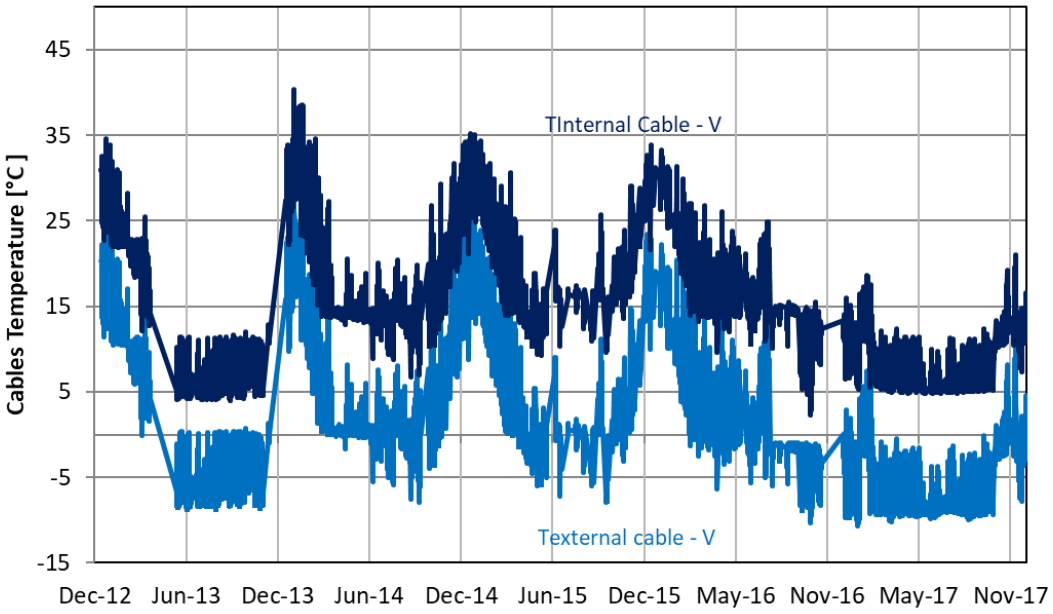

Figure 2-26: Antenna cables temperature from 1st Jan 2013 to 31 Dec 2017

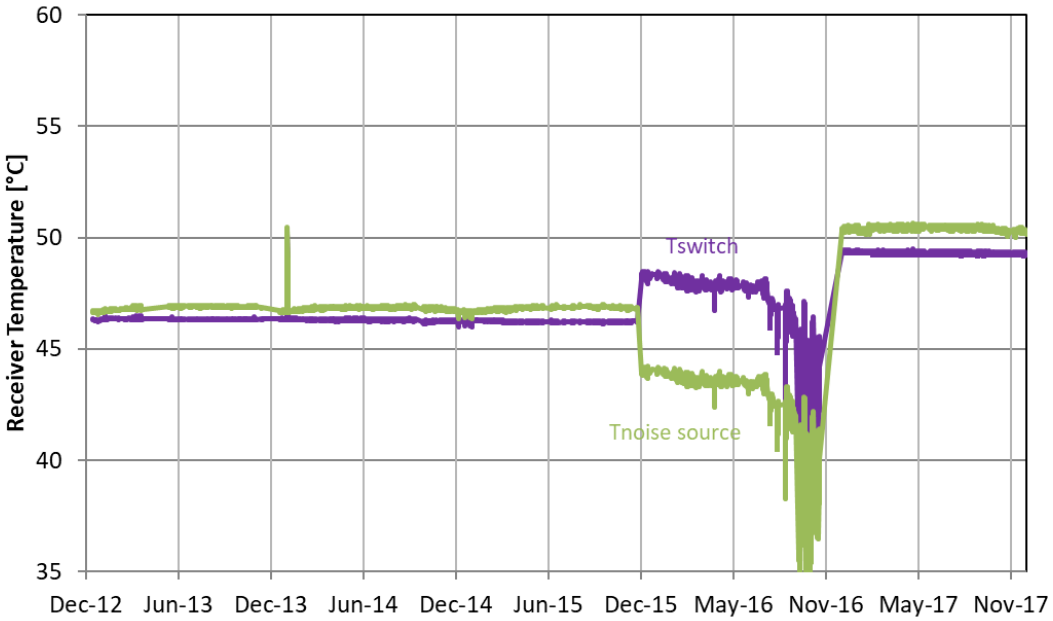

Figure 2-27: Physical temperature measure by PT100 inside the RF box, on the switch (purple) and on the noise source (green) from 1st Jan 2013 to 31 Dec 2017.

3 Intercomparison of Domex data

3.1 Temporal intercomparison

Temporal series of calibrated/deconvoluted/pseudo-TOA Domex data acquired at 42 degrees are compared with SMOS L1C v620 and SMAP L1B v3 [19] (see Figure 3-1). SMOS Tb are averaged over 9 dgg in the area around Concordia Station. It should also be noted that SMAP data reported here are collected at 40 deg incidence angle instead of 42 deg like for Domex and SMOS.

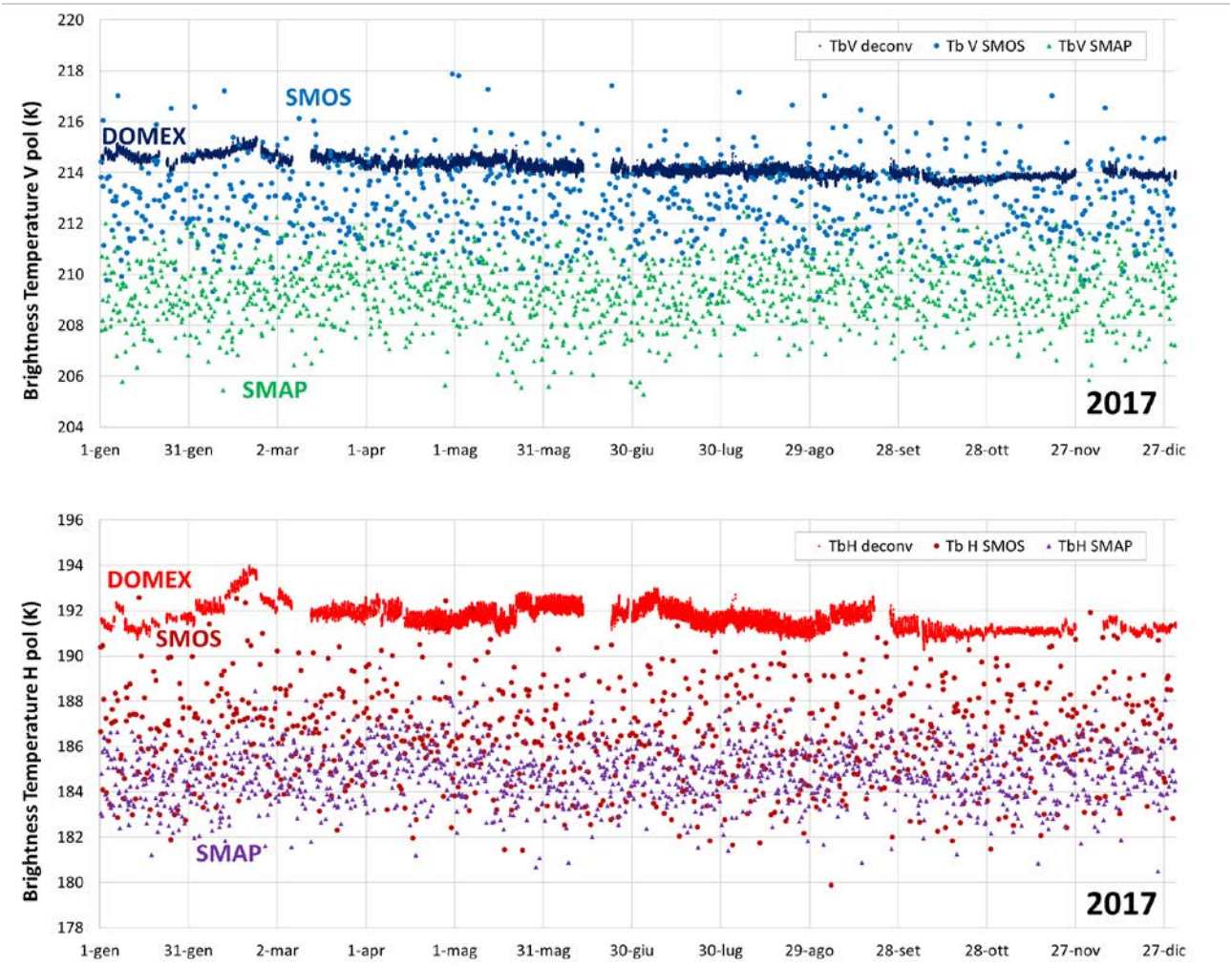

Figure 3-1: Comparison between Domex, SMOS v620 and SMAP v3 data. Top plot shows V polarization (Domex dark blue, SMOS light blue, SMAP green) while the bottom one shows the H pol (Domex red, SMOS magenta, SMAP purple). Domex and SMOS data were collected at 42 deg inc. ang. while SMAP at 40 deg.

Comparison show a good agreement between temporal trends for both V and H polarization while there are discrepancies for the absolute values. The relative statistics of the three datasets are reported in Table 3-1. In details, the average value of Domex is 1.41K higher than SMOS at V-pol and 5.31K higher at H pol. As explained beforethese values are different from the previous years, when Domex underestimated SMOS at

V-pol (approx. 2.7K lower) and overestimated at H pol (approx. 1.13K higher) [7]. It also should be noted that in the past the atmospheric correction was not implemented.. An assessment of the calibration methodology will be carried out after the 2018/19 summer campaign when absolute calibration test by using two independent targets, an Eccosorb wall and the sky, will be performed. SMAP data are generally lower than Domex and SMOS. This can be due to the slightly different viewing angle and to the peculiar characteristics of its absolute calibration (the radiometer is calibrated through the matchup of the the SSS product with the experimental data).

Table 3-1: Data statistics values for DOMEX (42 deg), SMOS (42 deg) and SMAP (40 deg) for 2017 acquisitions. Values are expressed in K.

	TbV μ	TbV σ	TbH μ	TbH σ
Domex TOA	214.21	0.3	191.71	0.49
SMOS L1C	212.8	1.5	186.4	2.11
SMAP L1B	209.6	1.19	184.9	1.16

In Figure 3-2 are reported the distribution of the different datasets considered. All the sensors have a gaussian shape more similar for SMOS and SMAP than for Domex which resulted to be one order of magnitude narrower. It should be noticed the standard deviation of SMAP at H pol is identical to the V pol. This has never been observed before by Domex, SMOS and Aquarius.

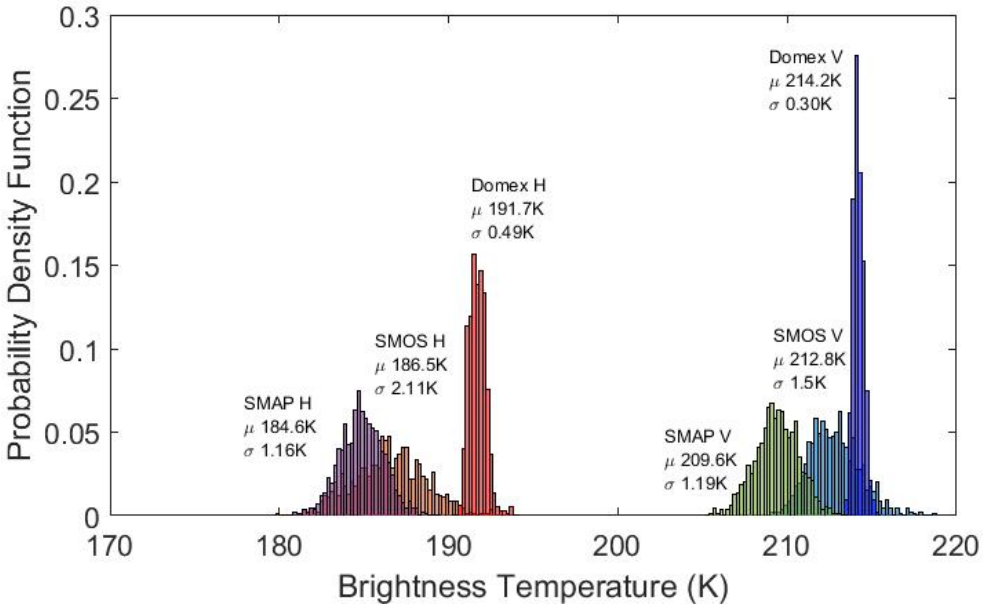

Figure 3-2: Normalized histograms of Domex, SMOS and SMAP time series. The labels report the statistics of each dataset.

Focusing on the daily averages (Figure 3-3), it is more evident the agreement of the temporal trend for the three radiometers, especially at V pol. Also, the variation at H pol measured in February-March by Domex becomes evident also in the SMOS and SMAP datasets, confirming that it not related to an instrumental issue of Radomex.

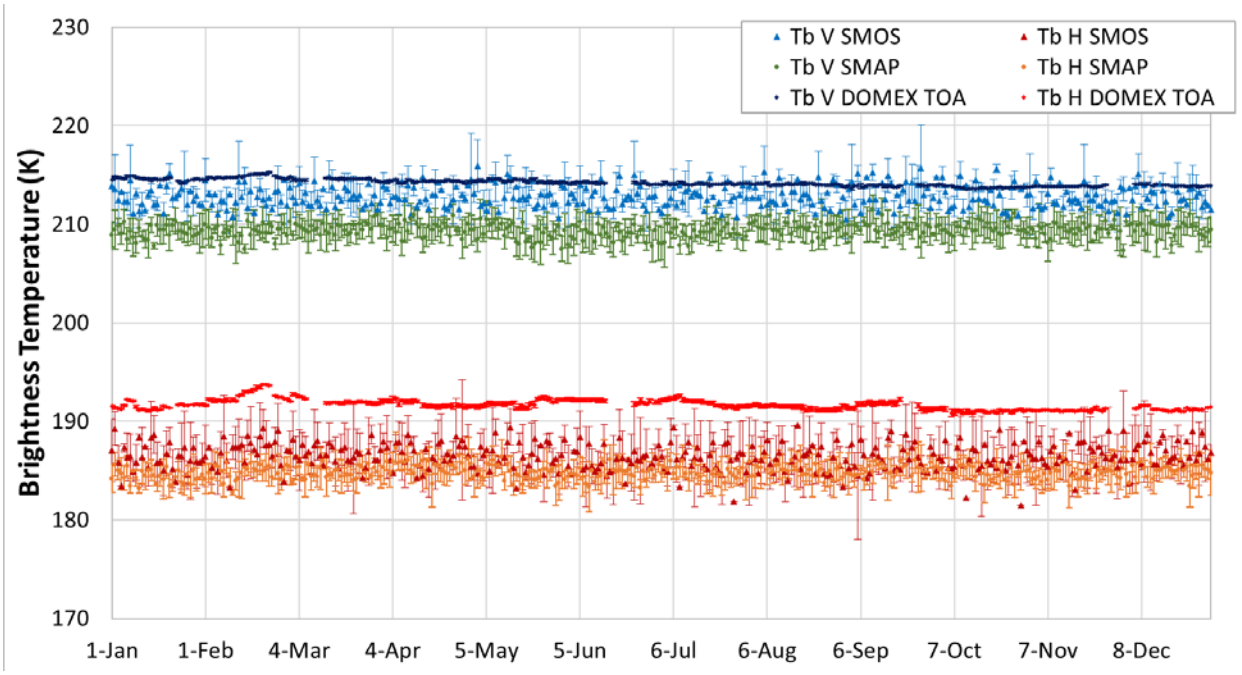

Figure 3-3: Time series of Domex, SMOS and SMAP daily averaged data. The error bars represent the daily standard deviation.

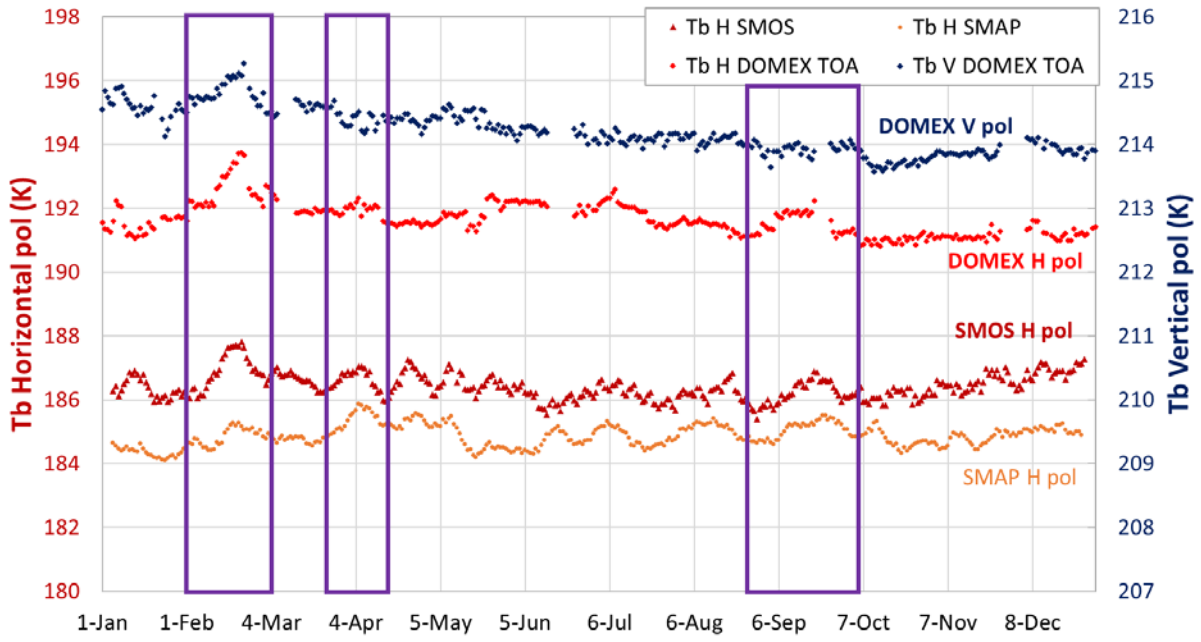

Figure 3-4: As Figure 3-3 without the error bars and with the Domex V pol moved on the right vertical axis to highlight the H pol temporal fluctuations. Purple boxes indicate the fluctuations clearly seen by more than one sensors.

By performing a detailed analysis of the temporal H pol temporal fluctuations (Figure 3-4) it is evident that some of them are due to modifications in the scenario (events highlighted by the purple boxes). Also it should be noted that SMAP seems to be more insensitive with respect to Radomex and SMOS to the Tb variations of the scenario. It is worth underlining that without an intercomparison of independent sensors, all of these fluctuations could be interpreted as malfunctioning of the instruments.

3.2 Angular trend intercomparison

The last analysis was devoted to the intercomparison of the angular trend of the Domex data with SMOS and DOMECAir datasets.

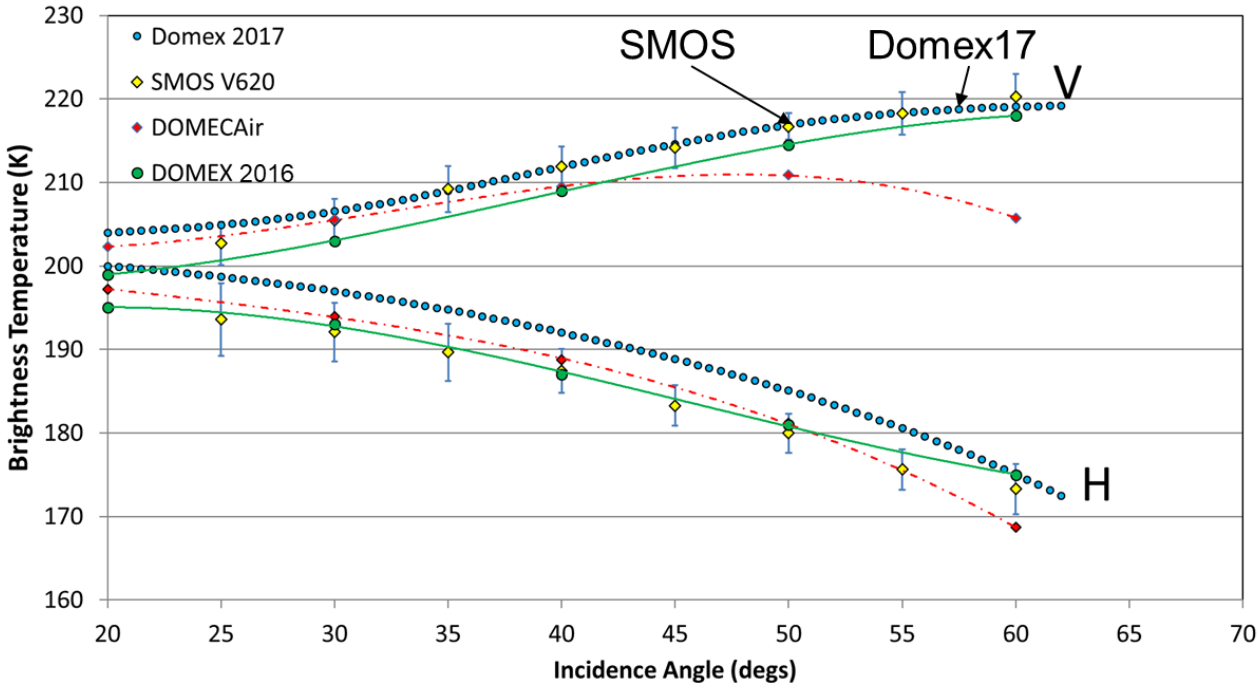

Figure 3-5: Angular trend of Domex 2016 (green circles and lines) and 2017 (blue circles) datasets, SMOS v620 (yellow diamonds) and DOMECair (red diamonds with dot-dashed lines) data. The error bars represent the standard deviations, although barely visible for DOMECAir and not for Domex.

Figure 3-5 shows the angular trend of Domex data acquired in 2016 and 2017 along with SMOS v620 and DOMECair datasets. The error bars representing the standard deviations are depicted, although barely visible for DOMECAir and not for Domex. Overall the 2017 dataset of Domex measurements is much in agreement with SMOS data than in 2016, especially at V pol. The statistics of the data computed at 40 deg incidence angle are represented in Table 3-2.

Table 3-2: Data statistics values for DOMEX, SMOS and DOMECAir datasets computed at 40 deg incidence angle.

	TbV (40 deg)	TbH (40 deg)
Domex 2017	213.1 K	193.8 K
SMOS v620	212 K	187.5 K
DOMECAir	209.5 K	188.9 K
Domex 2016	207.5 K	188.6 K

4 SNOW Data

Snow temperature measurements at Dome C are carried out continuously since the Domex-1 campaign in 2004. At present, the snow temperature is collected by means of a datalogger and a string of PT100 probes in the same site since Domex-2 (2009-10 summer campaign). The data collected during Domex-3 project are summarized hereinafter.

4.1.1 Snow temperature

The snow temperature measurement is collected continuously at different depths by means of permanent PT100 probes located in close to the US tower. The nominal depth of the probes is the following: 5, 10, 25, 75, 100, 150, 200, 250, 300, 400, 500, 600, 800 and 1000 cm. Due to the snow accumulation, the probes get deeper as time passed and snow accumulates. Only the probes placed in the first meter (up to 150 cm) are realigned on every summer campaign at their nominal depth. In 2016 Summer campaign a further probe was added and placed at 15 cm.

The annual series spanning from the 1st Jan 2017 to 1st March 2018 is shown in Figure 4-1. The temperature variability at different depth is highlighted in Figure 4-2 showing the mean and the standard deviation (error bars). It is evident that the surface probes are more affected by the seasonal variability of temperature at the air/snow interface. The deeper probes are more stable and not affected by the air gradient.

The full time acquisition from the beginning of DomeX-3 experiment is provided in Figure 4-3 and the values indicating the cumulative mean and standard deviations for each depth are summarized in Table 4-1.

For the same period, the IR temperature acquiring at the same angle of Domex is represented in Figure 4-4. The decreasing trend of the IR temperature which was noticed on the 2017 Domex annual meeting is of the order of 3K and maintained along the current year.

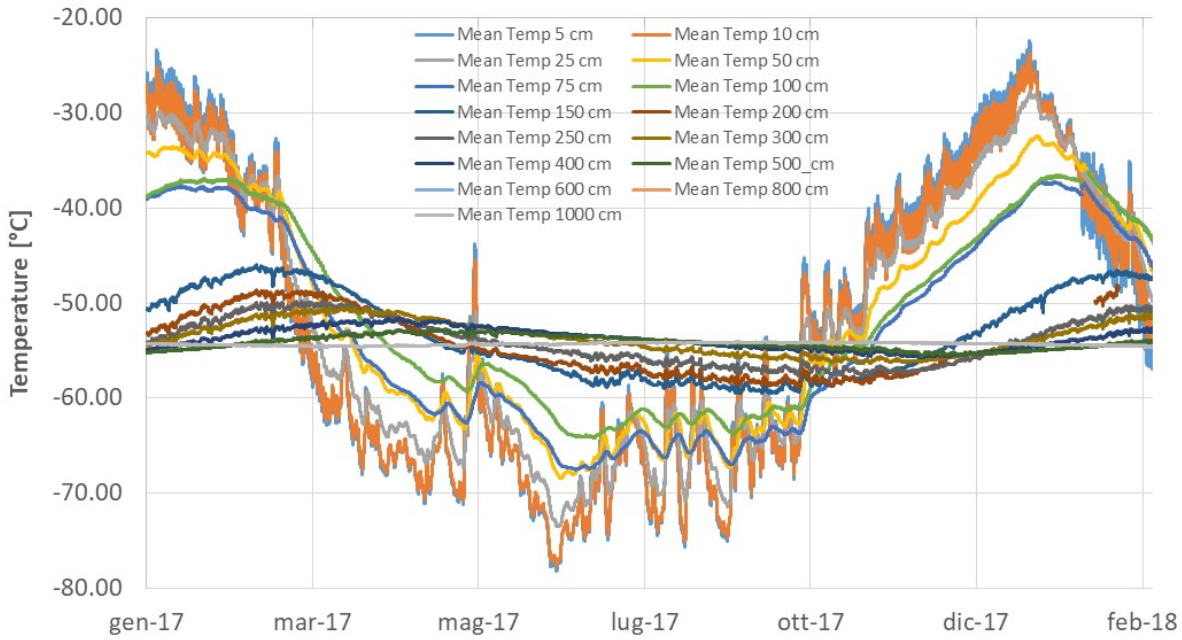

Figure 4-1: Snow temperature registered from 1 Jan 2017 to March 2018 at different depth (5 to 1000 cm)

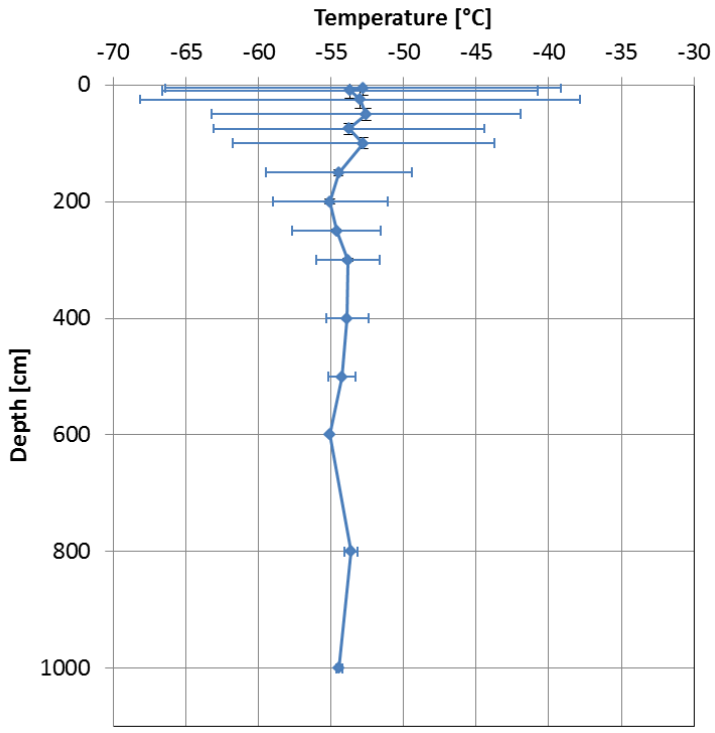

Figure 4-2: Variability of the snow temperature as a function of depth

Table 4-1: Average and Standard deviation temperature values measured by the snow probes at different depths from 2012 to March 2018.

Depth (cm)	Avg Temp (°C)	Std Dev Temp (°C)
5	-53.38	13.95
10	-53.96	13.28
25	-53.48	12.92
50	-52.98	10.69
75	-54.00	9.79
100	-52.99	9.04
150	-54.07	4.95
200	-54.83	3.82
250	-54.38	2.86
300	-53.77	2.10
400	-53.82	1.35
500	-54.22	0.87
600	-54.14	0.65
800	-53.73	0.32
1000	-54.41	0.19

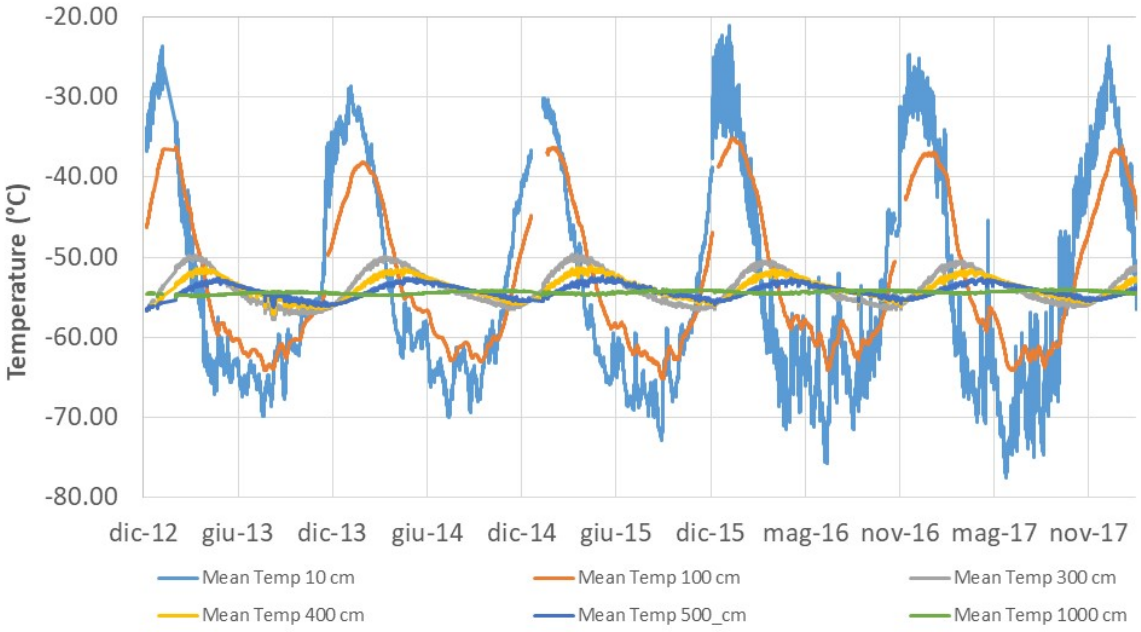

Figure 4-3: Snow Temperature measured at different depths since the beginning of DomeX-3 experiment.

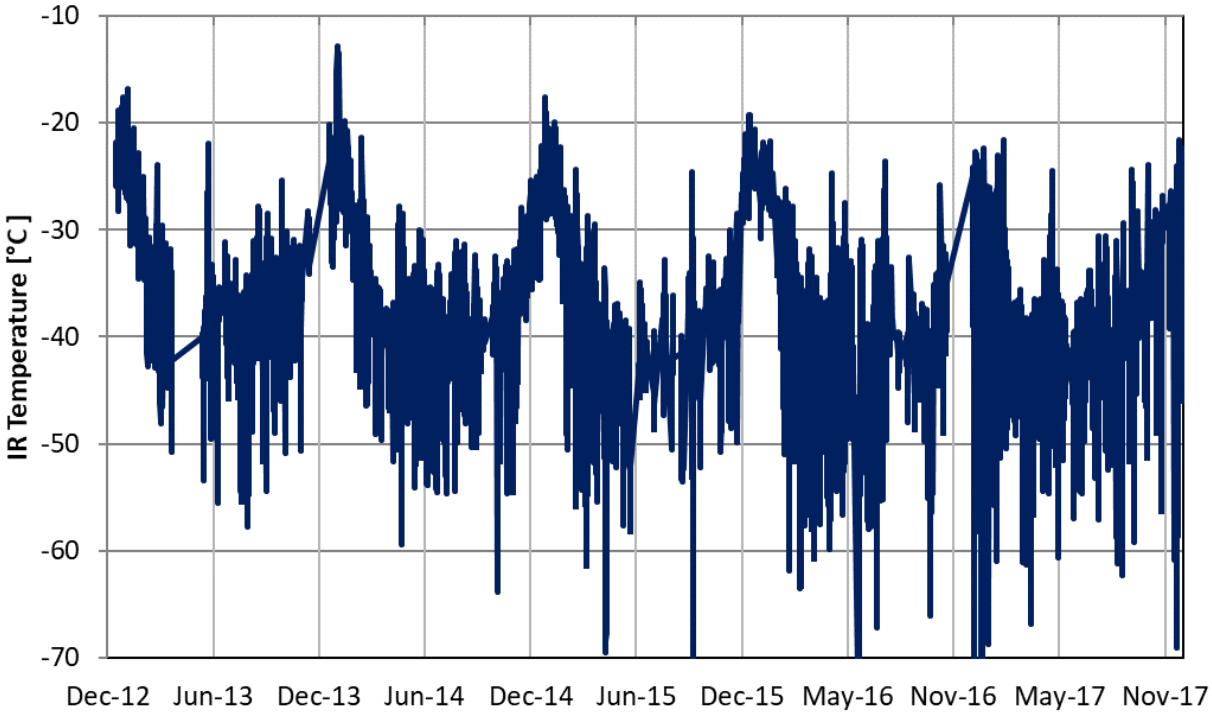

Figure 4-4: Infrared temperature from December 2012 to December 2017

5 References

[1] ESA-contract Technical Support for the Deployment of an L-band Radiometer at Concordia Station, Final Report, 2005

[2] ESA Contract:20066/06/NL/EL 22046/08/NL/EL, - Technical Support for the Deployment of an L-band radiometer at Concordia Station during DOMEX-2- - Final Report . 2011

[3] ESA Contract: 4000105872/12/NL/NF - Technical Support for the Deployment of an L-band radiometer at Concordia Station during DOMEX-2 – Proposal –July 2012

[4] ESA Contract: 4000105872/12/NL/NF - Technical Support for the Deployment of an L-band radiometer at Concordia Station during DOMEX-2 – Campaign Implementation Plan, Deliverable D2 – October 2012

[5] ESA Contract: 4000105872/12/NL/NF - Technical Support for the Deployment of an L-band radiometer at Concordia Station during DOMEX-2 – Readiness Review Report, Deliverable D3 – October 2012

[6] ESA-ESTEC Contract 4000105872/12/NL/NF Technical Support for the Long-Term Deployment of an L-Band Radiometer at Concordia Station, First Year Report , D6, February 2014

[7] ESA-ESTEC Contract 4000105872/12/NL/NF Technical Support for the Long-Term Deployment of an L-Band Radiometer at Concordia Station, Second Year Report , D6, June 2015

[8] ESA-ESTEC Contract 4000105872/12/NL/NF Technical Support for the Long-Term Deployment of an L-Band Radiometer at Concordia Station, Third Year Report , D6, June 2016

[9] ESA-ESTEC Contract 4000105872/12/NL/NF Technical Support for the Long-Term Deployment of an L-Band Radiometer at Concordia Station, Fourth Year Report , D6, March 2017

[10] ESA Contract 18060/04/NL/CB - Technical Support for the Deployment of an L-band radiometer at Concordia Station Final Report . May 2006

[11] ESA-ESTEC Contract 4000105872/12/NL/NFTN1 - Technical note on the absolute calibration strategies of Radomex, TN1, May 2018

[12] Marion Leduc-Leballeur, Ghislain Picard, Giovanni Macelloni, Marco Brogioni, Laurent Arnaud, Arnaud Mialon, Yann H. Kerr, “Modeling L-Band Brightness Temperature In Connection With Snow Surface Properties Variations At Dome C, Antarctica”, Microrad 2016

[13] J.A. Shroeder, and E.R. Westwater, “Users’ guide to WPL microwave radiative transfer software,” NOAA Technical Memorandum ERL WPL-213, October 1991.

[14] Data and information were obtained from IPEV/PNRA Project ‘Routin Meteorological Observation at Station Concordia’ - http://www.climantartide.it

[15] P.W. Rosenkranz, “Water Vapor Microwave Continuum Absorption: A Comparison Of Measurements And Models,” Radio Sci., vol. 33, no. 4, pp. 919–928, 1998

[16] M.T. Decker, E.R. Westwater, and F.O. Guiraud, “Experimental evaluation of ground-based microwave radiometric sensing of atmospheric temperature and water vapor profiles,” J. Appl. Meteor., no. 17, pp. 1788–1795, 1978

[17] Liebe, H. J., G. A. Hufford, and T. Manabe (1991), A model for the complex permittivity of water at frequencies below 1 THz, Int. J. Infrared Millimet. Waves, 12(7), 659–675

[18] M. Leduc-Leballeur, G. Picard, G. Macelloni, L. Arnaud, M. Brogioni, A. Mialon, Y.H. Kerr, Influence of snow surface properties on L-band brightness temperature at Dome C, Antarctica, Remote Sensing of Environment, Volume 199, 2017, Pages 427-436, ISSN 0034-4257.

[19] Piepmeier, J. R., P. Mohammed, J. Peng, E. J. Kim, G. De Amici, and C. Ruf. 2016. SMAP L1B Radiometer Half-Orbit Time-Ordered Brightness Temperatures, Version 3. 2017/01/01-2017/12/31. Boulder, Colorado USA. NASA National Snow and Ice Data Center Distributed Active Archive Center. doi: https://doi.org/10.5067/YV5VOWY5V446. accessed on 2018/03/01.

DOMEX related Publications

Leduc-Leballeur, M., Picard, G., Macelloni, G., Brogioni, M. IEEE NS and HM: Snowmelt in antarctica as derived from SMOS observations (2017) International Geoscience and Remote Sensing Symposium (IGARSS), 2017-July, art. no. 8127587, pp. 2829-2831.

Macelloni, G., Montomoli, F., Leduc-Leballeur, M., Brogioni, M., Ritz, C., Picard, G. Retrieval of ice sheet temperature profile in antarctica by using smos data: A combination of glaciological and microwave emission models (2017) International Geoscience and Remote Sensing Symposium (IGARSS), 2017-July, art. no. 8127582, pp. 2809-2812.

Leduc-Leballeur, M., Picard, G., Macelloni, G., Arnaud, L., Brogioni, M., Mialon, A., Kerr, Y.H. Influence of snow surface properties on L-band brightness temperature at Dome C, Antarctica (2017) Remote Sensing of Environment, 199, pp. 427-436.

Traversi, R., Becagli, S., Brogioni, M., Caiazzo, L., Ciardini, V., Giardi, F., Legrand, M., Macelloni, G., Petkov, B., Preunkert, S., Scarchilli, C., Severi, M., Vitale, V., Udisti, R. Multi-year record of atmospheric and snow surface nitrate in the central Antarctic plateau (2017) Chemosphere, 172, pp. 341-354.

ANNEXES

TN1 - Technical note on the absolute calibration strategies of Radomex

TN2 - Technical Note on the Acquisition Plan

This page is intentionally left blank

Technical Support for the Long-Term Deployment of an L-Band Radiometer at Concordia Station

TN1- Technical note on the absolute calibration strategies of Radomex

EUROPEAN SPACE AGENCY STUDY
ESTEC Contract 4000105872/12/NL/NF

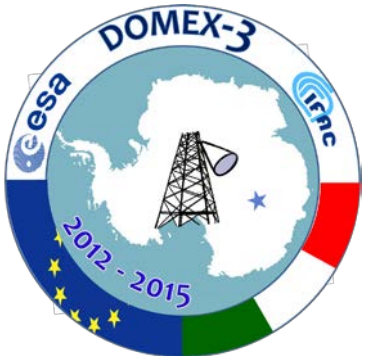

Prepared by

Giovanni MACELLONI, Marco BROGIONI, Francesco MONTOMOLI

IFAC- CNR, Florence, ITALY

DATE: 22/11/2017
Version: 1.1

Consiglio Nazionale delle Ricerche
Istituto di **F**isica **A**pplicata "Nello **C**arrara"

This page is intentionally left blank.

ESA STUDY CONTRACT REPORT

ESTEC Contract No:	Subject:		Contractor:
4000105872/12/NL/NF	Technical Support for the Long-Term Deployment of an L-Band Radiometer at Concordia Station		IFAC
ESA CR ( )No:	Star Code:	No of volumes: 1 This is volume no: 1	Contractor's Ref: Deliverable

ABSTRACT:

This technical note is related to the study *Technical Support for the Long-Term Deployment of an L-Band Radiometer at Concordia Station* (ESTEC contract 4000105872/12/NL/NF). It contains the description of the absolute calibration approaches that will be adopted for the data acquired with the new version of Radiometer, i.e. data acquired since the 2016/17 Antarctic summer campaign.

The work described in this report was carried out under ESA Contract. Responsibility for the contents resides in the author or organisation that prepared it.

Prepared by:

Giovanni MACELLONI, Marco BROGIONI, Francesco MONTOMOLI - IFAC

ESA STUDY MANAGER:	ESA BUDGET HEADING
Tania CASAL	

DOCUMENT CHANGE LOG

Issue/ Revision	Date	Observations
1/0	01/06/17	First issue
1/1	22/11/17	Revised version of first issue

ABBREVIATIONS

ACL	Active Cold Load
EAS	East Antarctic ice Sheet
ESA	European Space Agency
ESA –TEC	European Space Agency – Technical and Quality Management
IFAC-CNR	Institute of Applied Physics – National Research Council
IR	Infra-Red
LICEF	Light-weight Cost-Effective radiometer
LN2	Liquid Nitrogen
mw	Microwave
NS	Noise Source
OMT	OrthoMode Transducer
PNRA	Programma Nazionale Ricerche in Antartide (Italian National Research Programme in Antarctica)
Radomex	RADiometer for DOMEX experiment
UPC	Universitat Politecnica de Catalunya
VNA	Vectorial Network Analyzer

Applicable Documents

TN2	Technical Note on the Acquisition Plan, ESA Contract 4000105872/12/NL/NF – CCN6

This page is intentionally left blank.

TABLE OF CONTENTS

This page is intentionally left blank.

1 Purpose and structure of document

This technical note contains the description of two methodologies to be used operationally for the absolute calibration of Domex-3 data. It is introduced by a section in which the several parts of the instrument and the related thermal subsystems are detailed. Then the two different approaches are described with their pro and cons highlighted. At the end of the technical note there are three appendices in which the following are described: the theoretical relationship between the Tb of the scene and the several sections of the radiometer, the characterization of the lossy components at the input of the front end, and the temperature of the receiver.

This page is intentionally left blank.

2 Overview

The Domex-3 experiment is the continuation of two previous experiments called Domex-1 and Domex-2 that were successfully conducted at Concordia Station, Antarctica, by IFAC-CNR in collaboration with the Agency (contracts N. 18060/04/NL/CB [5] and N. 22046/08/NL/EL, 20066/06/NL/EL [3]) and PNRA.

An important part of the activity has been the preparation of an L-band radiometer to be used for the experiment that can reliably stand the Antarctic weather conditions present on the East plateau and that can work on the infrastructures of Concordia Station. The instrument was tested and calibrated in Italy before its shipping to Antarctica. However it must be underlined that the test conditions were not the same as those on the EAS. Also, the instrument underwent several improvements since the starting of the experiment, which thus necessitates a re-evaluation of the original calibration. These facts call for the development of new methodologies for obtaining the absolute calibration of the radiometer while it is operating on the tower.

In this technical note we report on the issues related to the absolute calibration of Radomex, pointing out the strategies for tackling them and the approach that can be followed for obtaining the operational absolute calibration of the data. In addition, the measurement incertitude associated with the proposed methodologies is reported.

This page is intentionally left blank.

3 Description of the instrument

Radomex is a multi-channel instrument, featuring one L-band and one IR radiometer. For the purposes of the present technical note, the IR will be ignored hereinafter.

The L-band radiometer is a total-power frequent-calibrated dual polarization instrument (i.e. at vertical and horizontal pols). The basic block diagram of the radiometer is represented in Figure 3-1, where the six port microwave switch connects the antenna (two ports for the V and H pols) and the four reference loads (namely Active Cold Load – ACL, cold load, hot load and Noise Source - NS) to the receiver chain composed of amplifiers and a filter. The blocks in red are the devices added in the last improvement of the radiometer, performed in 2016.

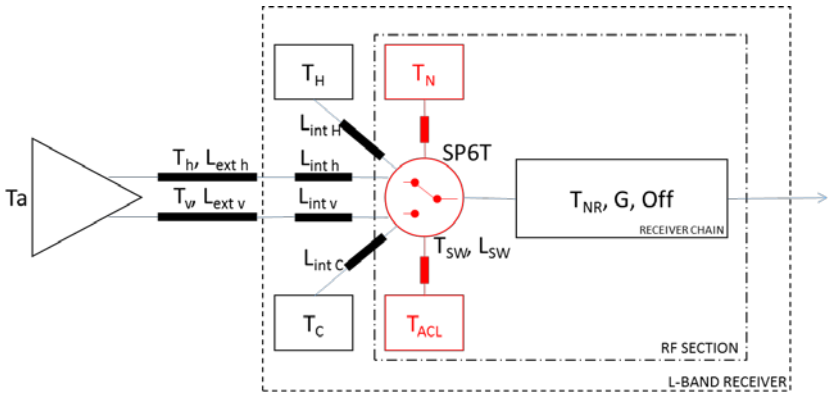

Figure 3-1 – Block diagram of the L-band radiometer

In order to determine the brightness temperature of the scene, the radiometer alternates the measurements on the antenna ports with the ones on the four reference loads. Each port is observed for an Integration Time of 2 seconds. This value was fixed in order to obtain a good radiometric sensitivity value (i.e. lower than 0.3 K) and established after the analysis carried out in the Domex-2 experiment [3]. Figure 3-2 reported the performed analysis for the sake of convenience.

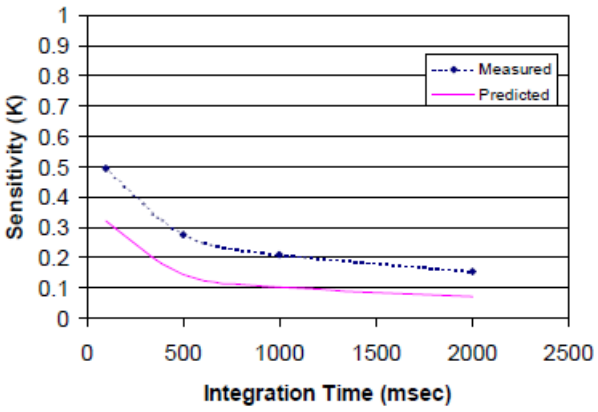

Figure 3-2 – Measured (blue) and predicted (pink) radiometer sensitivity [3]

The acquisition sequence is the following and a complete cycle will last for 12 seconds:

1- Cold load (a matched load kept at ambient temperature),
2- V polarization,
3- H polarization,
4- Noise Source,
5- Hot load (a matched load kept at ~70°C),
6- Active Cold Load (a mw amplifier identical to the ones in the receiver chain observed at the input port).

For any cycle, it is possible to compute the gain and offset of the receiver by using the reference load measurements (any combination of 2, 3 or 4 loads) and then to derive the Tb of the scene in front of the antenna. However, this procedure leads only to a calibration of the receiver section since the antenna losses (and mismatches) and the external cables losses (L_V, L_H) are not considered.

It is worth mentioning that the hot and cold loads, as well as the V and H input ports, are connected to the microwave switch by means of low-loss cables (Huber+Sunher Sucoform 141) that allow a minimal influence of the cable temperature on the mw measurements. The losses of these four cables are very similar, allowing for a good auto-compensation of the thermal effects. Instead, the ACL and the NS, which are located inside the thermo-controlled RF section, are connected by using standard RG316 cables properly characterized. Table 3-1 shows the losses of the cables measured by using a Agilent ENA E5071C VNA (calibrated with the Agilent 85052D cal kit) with a resolution bandwidth of 10 Hz over the range 1400-1427 MHz. The error of the VNA measurements is 0.05dB. Γ and τ are the average of the (S_{11}, S_{22}) and (S_{21}, S_{21}) parameters respectively

Table 3-1 – Losses of the internal cables connected to the SP6T switch

	Γ (dB)	τ (dB)
V pol	-40.5009	-0.10595
H pol	-42.7115	-0.10317
Noise Source	-42.8261	-0.28945
Active Cold Load	-33.8352	-0.22828
Hot Load	-34.7648	-0.13283
Cold Load	-36.5511	-0.13656

The external cables connecting the antenna to the receiver are a pair of 1 m long Phasetrack 210 cables manufactured by Times Microwave Systems that guarantees very stable electric characteristics as a function of the operating temperature. Table 3-2 reports the mean reflectivity and attenuation of the cable over the protected L-band measured in similar conditions as Table 3-1 but using the HP 85032B cal kit.

Table 3-2 – Losses of the external cables

	Γ (dB)	τ (dB)
V pol	-30.94	-0.409
H pol	-31.78	-0.403

These loss values are all quite low and comparable to the ones of the SMOS instrument (~ 0.15 ÷ 0.35 dB) as obtained by the UPC team.

3.1 Radiometric schematization

From the radiometric point of view, the various losses and mismatches that are relevant to the measurements of Radomex are represented in Figure 3-3. There, $S_{11\text{-}V,H}$ are the mismatches at the OMT ports, $L_{ext\ V,H}$ are the external cables losses (i.e. the Phasetrack 210), $L_{int\ V,H}$ are the internal cables losses (i.e. the Sucoform) and $S_{xy\text{-}V,H}$ are the microwave switch losses for each channel.

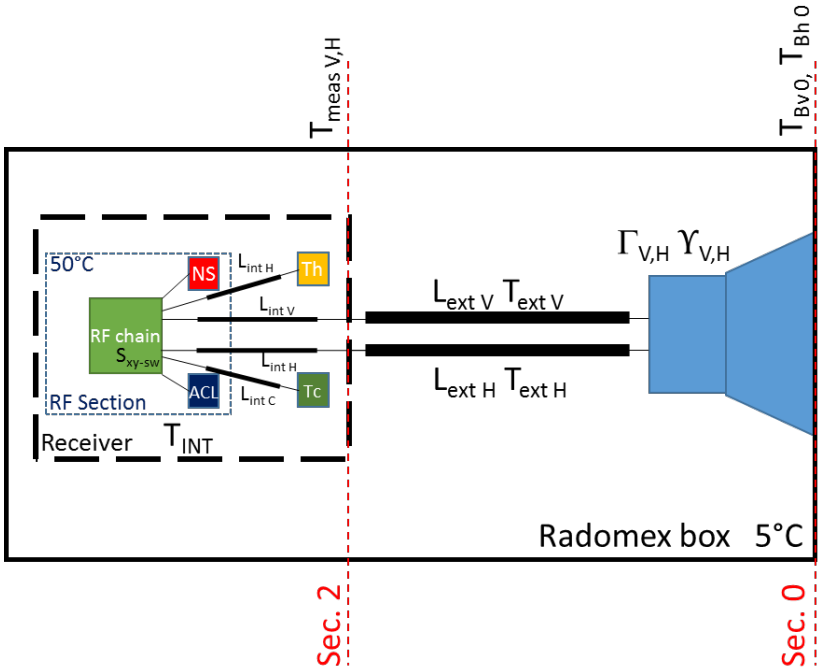

Figure 3-3 – The cable losses that are relevant for the Radomex measurement. Sections are labelled coherently with the analysis in Appendix 6.

The measurements obtained by means of the frequent calibration technique are referred to Section 2 of Figure 3-3, leaving the effect of the external cables and the antenna uncompensated. In Figure 3-3,

sections are labelled coherently with the analysis in Appendix 6. As detailed in Appendix 6, it is possible to derive the brightness temperature of the scene at Section 0 by using the Friis formula, thus deriving a compensation curve for each channel of the radiometer (in this case two: one for the V and one for the H polarization). The general equation relating $T_{meas\,v,h}$ (Sec. 2) with the $T_{Bv,h}$ of the scene (Sec. 0) are detailed in Appendix 6 and reported here for the sake of convenience.

$$T_{meas\,v} = L_{ext\,v}\,\Upsilon_v\,T_{Bv\,0} + L_{ext\,v}^2\,\Gamma_v\,T_{REC} + (L_{ext\,v}\,\Gamma_v + 1)\,(1 - L_{ext\,v})T_{ext\,v}$$

$$T_{meas\,h} = L_{ext\,h}\,\Upsilon_h\,T_{Bh\,0} + L_{ext\,h}^2\,\Gamma_h\,T_{REC} + (L_{ext\,h}\,\Gamma_h + 1)\,(1 - L_{ext\,h})T_{ext\,h}$$

By solving the previous equations for $T_{Bv\,0}$ and $T_{Bv\,0}$ (i.e. the brightness temperature of the scene), it is possible to compensate the losses of external cables and antenna. The values of L, Γ, Υ parameters are listed in appendix 6.

3.2 Thermal sections of Radomex

The design of a radiometer must take into account the thermal regimes inside the instrument since the temperature of each component of the radiometer affects the performance of the instrument. The structure of Radomex (i.e. the Domex-3 instrument) was designed for the Domex-2 experiments by leveraging the experience of the Domex-1 ESA project, with the help of the ESA TEC division regarding the thermal system design. It should be noticed that the design was constrained by some intrinsic limitations (e.g. limited available power supply at Dome-C, box dimensions and designs, resources) which in turn constrained the adopted technical solutions. This means that it was agreed that it was not possible to have an average temperature inside the box that remains 'within stable' in a small temperature range (i.e. < 5°C) for the whole year around. Moreover, because of the different conditions encountered in winter (no-sun, air temperature down to -90°C) and summer (24/24 h of sun, air temperature up to -18 °C), at the above mentioned constraints, it was decided that the system should have been temperature-controlled during winter but not in summer.

Radomex is composed of a main thermal insulator box that houses the antenna (Figure 3-4), the RF receiver and control systems (see Figure 3-5). This solution has been adopted for protecting the various components from the extreme Antarctic weather, in particular from the high temperature variations between winter and summer. Indeed, whereas the Potter antenna can be assumed lossless it is not strictly required to be kept thermally stable (e.g. like in the case of other L-band SMOS instruments like Elbara or Lewis radiometers), the temperature variations of the EAS environment can appreciably stress the structure of the antenna leading to a non-stable electromagnetic performance.

Figure 3-4 – Radomex enclosure

To avoid this problem, the interior of the box is kept at a minimum temperature of +5°C, thus limiting the annual thermal excursions of the systems.

The electric actuator allowing for the angular scanning is installed outside of the box, on the left side (i.e. on the hidden side of Radomex as represented in Figure 3-4) and is covered by an insulating crankcase. In this case, the interior of the crankcase is kept at a minimum temperature of 0°C. In order to have a more homogeneous thermal dynamics inside of the box, another insulated heated empty crankcase is installed on the opposite side of the box.

The interior of the Radomex box is heated by two thermal subsystems: one located on the bottom part and one on the ceiling. Each subsystem is driven by separate PID controllers whose PT100 probes are located on the orthomode feed horn and on the radiometer receiver (see Figure 3-5). In order to homogenize the internal temperature and avoid vertical gradients, the circulation of air is obtained by using three fans: two in the front pushing the air downward and one in the rear of the box with an upward airflow. Also, all the components housed in the Radomex enclosure that are sensitive to thermal variations were painted with a black thermal conductive paint, in order to render the internal heating more effective.

Nevertheless, temperature differences still exist inside of the instruments (4°C were measured at the ends of the V pol external cable and 7°C for the H pol one).

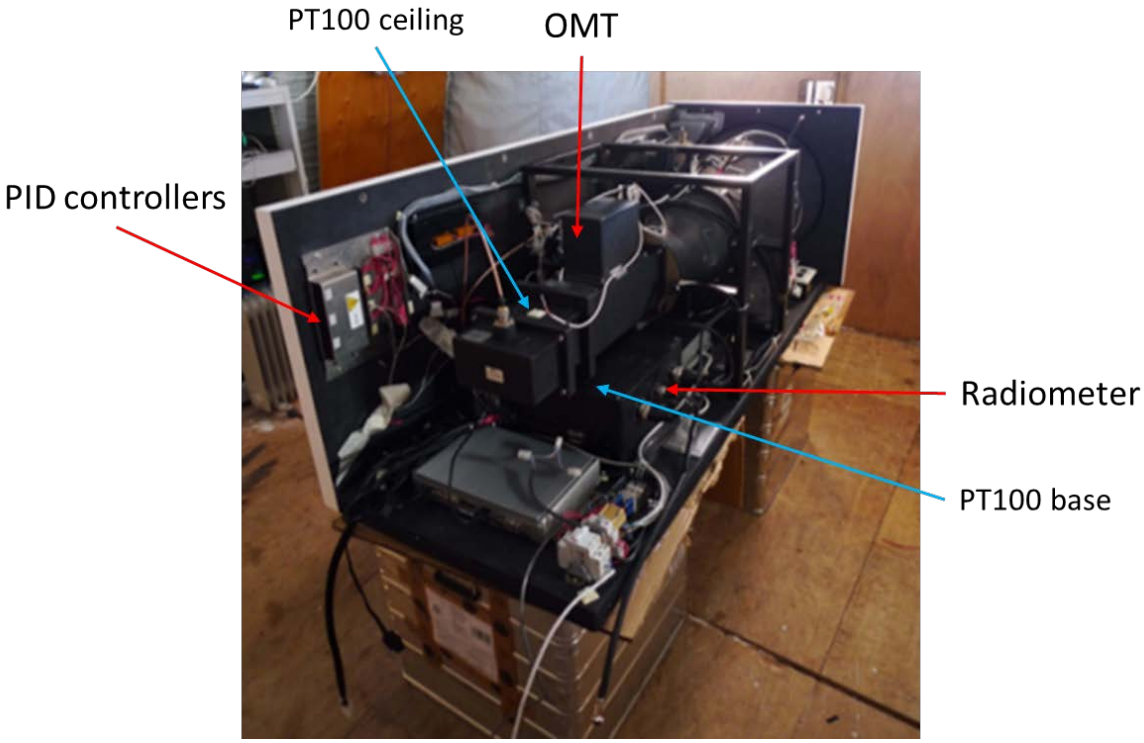

Figure 3-5 – Interior of Radomex

From a thermal point of view, Radomex can be represented as three nested sections (see Figure 3-6):

- the RF section, which has a temperature of 50°C ±0.1°C regulated by a PID controller
- the external box section, kept at a minimum temperature of 5°C ± 2.5°C regulated by two PID controllers,
- the receiver case section which is not thermo-controlled: slightly warmer than the external enclosure temperature due to the dissipation of the receiver power suppliers.

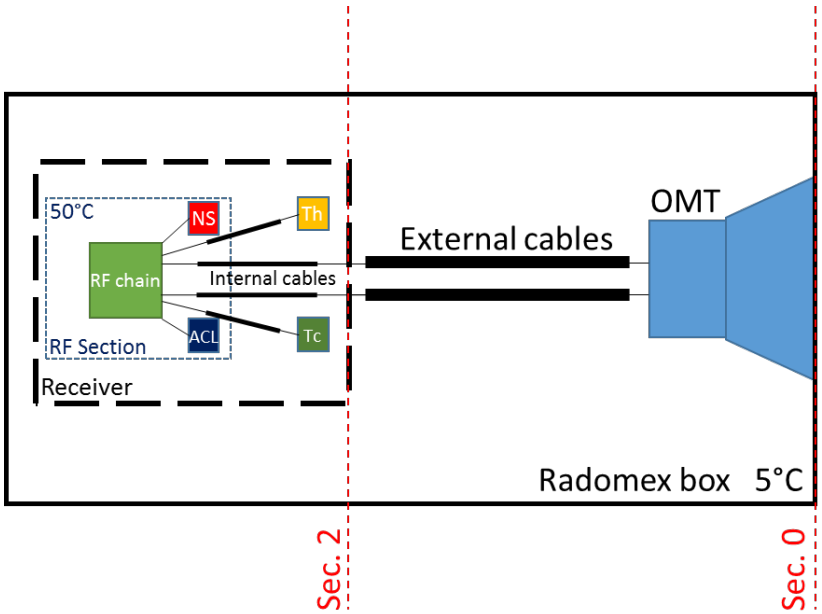

Figure 3-6 – Sketch of the thermal sections of Radomex

The temperature of the cables and antenna inside Radomex is monitored in several points, as depicted in Figure 3-7. More precisely, the temperature of each component that has losses or mismatches is monitored (inner and outer cables and antenna). The temperature of the external cables is monitored at two points since they can experience a temperature gradient.

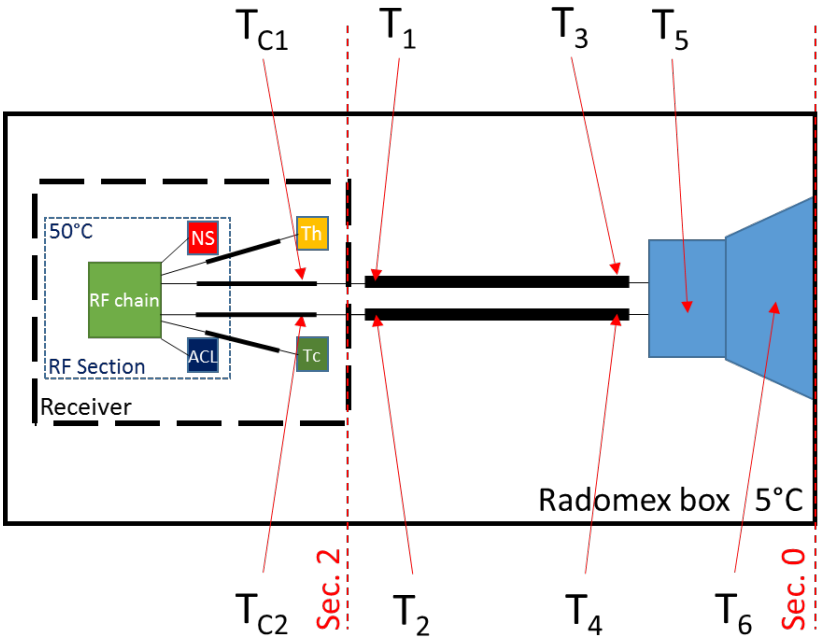

Figure 3-7 – The temperature measurement points inside Radomex. The name of the probes is the same as in the datasets.

This page is intentionally left blank.

4 Absolute calibration

Radiometers are extremely sensitive instruments whose measurements are strongly influenced by any change of the components' characteristics (e.g. due to the aging or to their final coupling, or to the operative thermal and mechanical conditions), by the temperature variations, the incertitude in the measurements of the devices' temperatures (especially of the reference loads), etc. Despite the existence of all of the strategies that can be planned for decreasing the sensitivity of the radiometer to these nuisance factors (like the frequent calibration, the use of stable reference loads, the choice of high quality components), some incertitude on the absolute value measured still persists and strategies to re-compute the absolute calibration of the instrument must be set out.

The absolute calibration of a radiometer is usually obtained by measuring the emission of two well-characterized targets at different temperatures (usually called cold and hot reference targets) and verifying that the instrument has a linear behavior over the operative range (or at least well-characterized). Depending on the accuracy required, a radiometer should need to be absolutely calibrated at regular intervals.

Radomex was fully calibrated prior to the shipment to Antarctica in 2012 by observing the deep sky, a water body at several incidence angles and the walls of the anechoic chamber at IFAC. However, this calibration cannot be considered reliable anymore for several reasons:

- Absolute calibration was performed without the white external enclosure to avoid overheating the internal parts, thus resulting in a different thermal operating environment than the Antarctic one, especially for the microwave cables and connectors. Albeit allowing a quite good absolute accuracy, this calibration is not precise enough to provide data to be compared with SMOS ones. Furthermore, the original aim of Domex-3 was the continuous monitoring of the emission trends of the plateau, with a lesser importance on the absolute values of the measurements.
- The receiver and the RF cables have been updated several times in the past 6 years in order to improve the accuracy of the measurements, the reliability and the failure-tolerance of the instrument. All of these changes, albeit improving the capability of the instrument in collecting longer time-series of data (the last failures were due to unpredictable problems in the station power grid), call for a new absolute calibration of the radiometer.

In summary, a new absolute calibration is needed to correct the Radomex accurate relative measurements. The data collected over the waterbody in 2012 are still very useful and will be used for the deconvolution of the antenna lobe.

In order to perform this task, two strategies have been developed for Radomex. One leverages the receiver calibration performed in 2016 before the shipment to Concordia Station. The other one is based on the use of the noise source turned off for obtaining a matched load at a high stable temperature directly connected to the microwave switch as in the LICEF of SMOS. Hereinafter the two approaches are detailed.

4.1 First methodology

This approach relies on the fact that the receiver itself has already been absolutely calibrated at IFAC laboratories by using a high-stability high-accuracy thermal bath and a matched load put inside of the liquid nitrogen (i.e. calibrated at Section 2 in Figure 3-7). The main hypothesis underlying this method is that the founded relationship does not change in time, because the condition of the RF section remains the same, and it can be applied in Antarctica. Under this assumption, it is possible to get the absolute calibration of Radomex (i.e. at section 0) by observing a well-characterized target, e.g. the sky, and then estimating the losses $L_{EST\,V,H}$ between sections 1 and 2. Then by using these derived losses, it is possible to get the absolute calibrated Tb of the ice sheet.

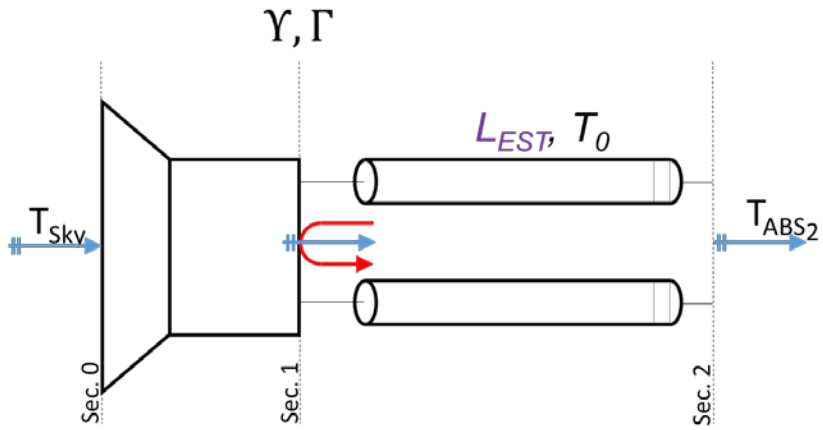

Figure 4-1 Radiometric schematization of the losses chain for the first methodology

By using the relationships derived in Appendix 6 the losses $L_{EST\,V,H}$ can be derived for each channel from

$$T_{ABS_2} = L_{EST}\,\Upsilon\,T_{Sky} + L_{EST}^2\,\Gamma\,T_{REC} + (L_{EST}\,\Gamma + 1)\,(1 - L_{EST})T_0$$

which gives (only the positive solution must be chosen)

$$L_{EST} = \frac{(\Gamma - 1)T_0 + \Upsilon\,T_{Sky} \pm \sqrt{-4\,\Gamma\,(-T_0 + T_{ABS_2})(T_0 - T_{REC}) + [(\Gamma - 1)T_0 + \Upsilon\,T_{Sky}]^2}}{2\,\Gamma\,(T_0 - T_{REC})}$$

In the previous equation T_0 is an average of the temperatures measured at the ends of each cable, T_{REC} is estimated in Appendix 8 and Γ, Υ are given in Appendix 7. The main reason why the brightness temperature measured at section 2 (i.e. the input ports of the radiometer) is different to the one at section 0 (i.e. antenna aperture) is in the losses of the cables and the mismatches of the connectors and OMT and receiver ports. These losses should be quite constant in time since they are due mainly to the aging of components. Given that a negligible energy flows thorough the cables and the antenna, and that the working temperature range is between 5°C and 20°C the aging of these components is expected to be very slow. Finally, we verify the derived losses with the ones obtained with VNA measurements reported in Appendix 7.

As said previously, the calibration of the radiometer receiver at sec.2 has been performed by using a high stable thermal bath. After having compensated the cable losses the calibration curves are shown below (see Figure 4-2)

$$\begin{cases} T_{B\,Vpol} = 0.9544\,T_{meas\,Vpol} + 5.0874 \\ T_{B\,Hpol} = 0.9856\,T_{meas\,Hpol} - 5.9789 \end{cases}$$

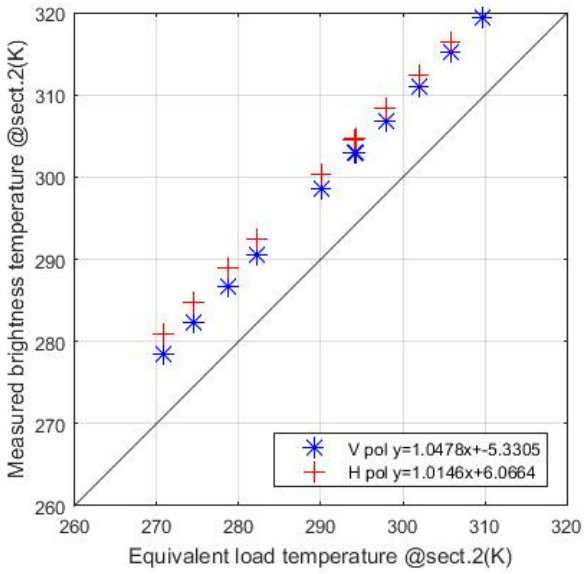

Figure 4-2 Calibration curves for the receiver at section 2

Then, we tested the previous calibration curves, by using a nitrogen calibrator coupled with a noise source. A schematic representation of the test is represented in Figure 4-3 along with the test obtained by varying the attenuator in the range 0 dB ÷ -30 dB. One channel of the radiometer (H pol) was measuring a matched load dip in the liquid nitrogen while the other one was kept observing a termination in the thermal bath. This arrangement was intended for checking the linearity of the instrument over a wide Tb input range while measuring a target with a known behavior. The test results give a RMSE between measured and equivalent load temperature of 0.76 K at section 2 (and a R^2=1). Also, the linear interpolant has a slope of 0.997 and a bias of 0.169 K.

This latter verification is a test for the calibration of real Radomex data collected in Antarctica, when the Tb of the deep sky will be used in lieu of the LN2 and the losses between section 0 and 2 evaluated.

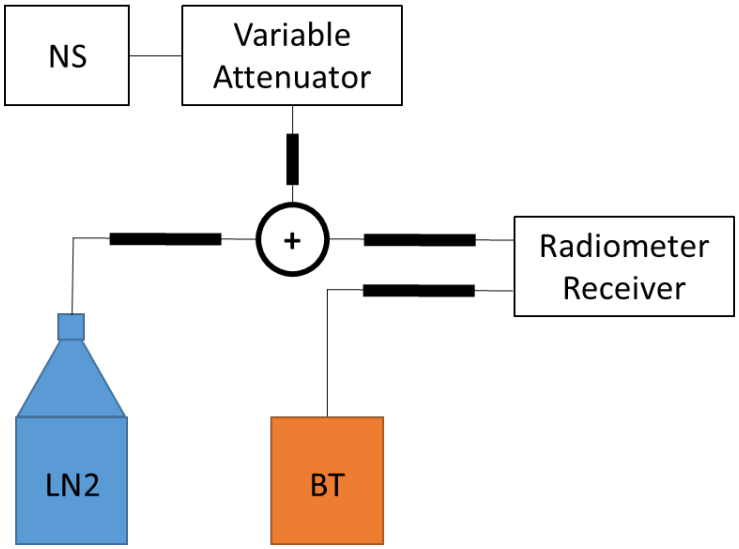

Figure 4-3 Scheme of the liquid nitrogen test

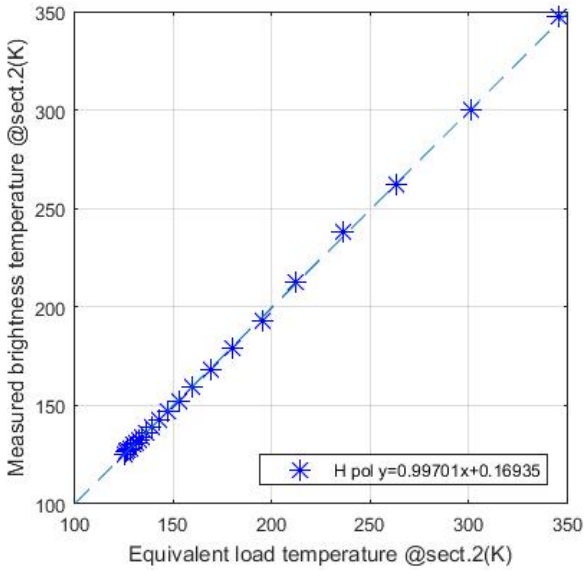

Figure 4-4 Verification curve for the LN2 test at section 2

Despite the simplicity of the method, it main weakness is represented by the fact that the absolute calibration curves need to be determined over the entire Tb range by compensating the targets for the testing cables at sec.2 under the same operative conditions as in Antarctica in order to have a useful accuracy (i.e. <1K). Because the LN2 measurements were conducted in laboratory, and then the reproducibility of Antarctic system was not possible, we concluded that the developed method cannot be used for absolute calibration. Indeed, while it provides reliable information on the RF section of RADOMEX it is not possible to provide an estimate of the error on the measured Tb values (i.e. including cables and losses) in Antarctica.

4.2 Second methodology

This second approach is similar to the one developed by the UPC team for the SMOS LICEF radiometers and makes use of the matched load connected to the microwave switch at the beginning of the RF chain.

This approach for the absolute calibration is similar to the traditional one that relies on the measurement of two stable targets (one cold, one hot) outside to the system having a well-known Tb for re-calibrating the collected data. Moreover, it does not make any assumption on the a-priori absolute calibration of the various Radomex sections.

As a cold target, the deep sky can be used since it has a stable Tb. Obviously the plane of the galaxy and other RF emitting sources (e.g. Cygnus) must be avoided during the measurements. To observe the sky it is sufficient to rotate Radomex at its highest elevation over the horizon.

Unfortunately, a direct measure of a hot target is not possible for Radomex and, like SMOS, an "artificial" one must be simulated. In the case of Radomex, one of the internal reference loads can be used. Indeed, the new version of the radiometer has been equipped with four reference loads in order to perform a better frequent calibration and improve the failure-tolerance of the instrument. The four loads are (see sketch in Figure 3-1):

- Active Cold Load, a mw amplifier (the same model of the ones in the RF chain) observed at the input port, with an equivalent brightness temperature of 62.8 K,
- Cold load, a matched load kept at the ambient temperature ~ 5°C ÷ 20°C,
- Hot load, a matched load kept at ~70°C by an electronic linear controller,
- A noise source with an equivalent brightness temperature of ~480 K that can be electronically switched on and off.

The ACL and the noise source are located inside of the RF section whose temperature is kept stable at +50°C ± 0.05°C. The noise source (whose characteristics are reported in Table 4-1) can be turned on and off via software. When it is turned off it becomes a matched load at a very stable temperature.

Table 4-1 – Characteristics of the Noise Source

ATM NX1512X noise source generator	
Input power	+28 A, 25mA max (typ < 10mA)
Noise output variation with temperature	less than 0.01 DB/°C
Noise output variation with voltage	less than 0.1 dB/%V
Operating temperature range	-55°C to +85°C
Noise output rise time and fall time	< 1 µsec
Noise Output ENR (dB)	15.5 +/- 0.5
VSWR Max. (ON/OFF)	1.20:1

By considering the switch port losses L_{SW}, internal cable losses $L_{INT\,V,H}$, external cable losses $L_{EXT\ V,H}$ and antenna ports mismatch $S_{11\,V,H}$ it is possible to simulate a load at the antenna plane, i.e. in similar conditions of the sky. The procedure for obtaining the relationships for the V and H channels is outlined in Appendix 6. In this case the radiometric schematization of the chain is represented in the following Figure 4-5.

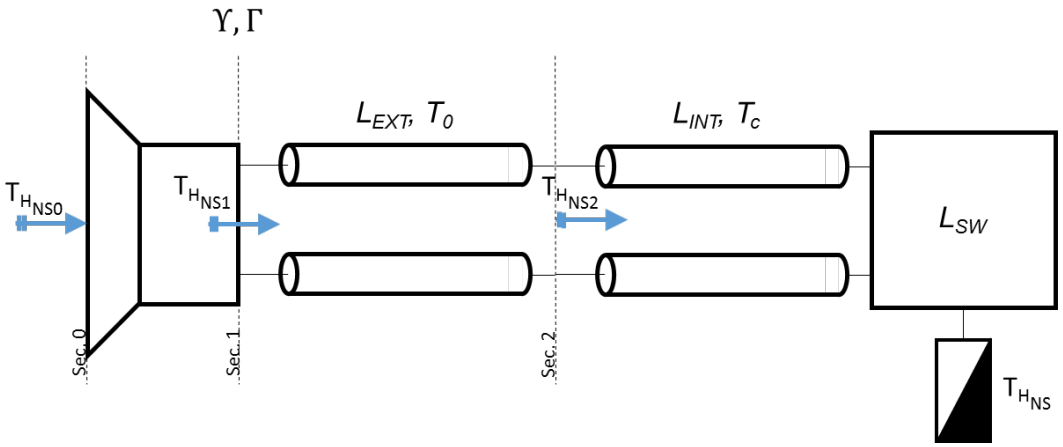

Figure 4-5 Radiometric schematization of the chain losses for the second methodology

In Figure 4-5 the switched-off noise source can be considered a matched load at the RF chain temperature. Since also the switch is at the NS temperature, the chain can be further simplified.

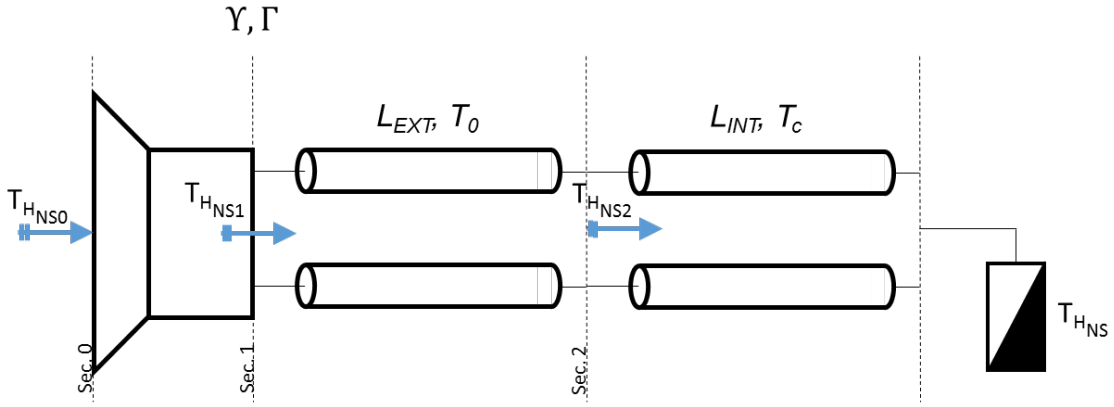

Figure 4-6 Simplified radiometric schematization of the chain losses for the second methodology

Thus, by following the approach of Appendix 6 it is possible to write the relationship between $T_{H_{NS}}$ and the one of the "pseudo-hot target" in front of the antenna $T_{H_{NS0}}$

$$T_{H_{NS}} = L_{INT}\left[L_{EXT}\left(\Upsilon\, T_{H_{NS0}} + \Gamma\, T_{REC1}\right) + (1 - L_{EXT})T_0\right] + (1 - L_{INT})T_c$$

with

$$T_{REC1} = L_{EXT}[L_{INT}\, T_{REC1} + (1 - L_{INT})T_c] + (1 - L_{EXT})T_0$$

By solving previous equation for $T_{H_{NS0}}$ with the values of the components detailed in Appendix 7 and 8 for the V and H channel it is possible to derive the values of the pseudo-hot target.

$$T_{H_{NS0\ \mathrm{v,h}}} = \frac{\beta_{\mathrm{v,h}} - \Gamma_{\mathrm{v,h}}\, T_{REC1}}{1 - \Gamma_{\mathrm{v,h}}}$$

where

$$\beta_{\mathrm{v,h}} = \frac{\alpha_{\mathrm{v,h}} - \left(1 - L_{EXT\ \mathrm{v,h}}\right)\, T_0}{L_{EXT}}$$

$$\alpha_{\mathrm{v,h}} = \frac{T_{H_{NS}} - \left(1 - L_{INT\ \mathrm{v,h}}\right)\, T_c}{L_{INT\ \mathrm{v,h}}}$$

For the sake of convenience, the values of the component losses are reported here too (see Table 4-2).

Table 4-2 – Values of the losses of the components

	V pol	H pol
Internal cable losses L_{int}	0.976	0.977
External cable losses L_{ext}	0.910	0.911
Antenna ports mismatch Γ	0.0134	0.0052

Obviously, the main assumption of this method is that the characterization of any components (between the microwave switch and the antenna aperture) performed in laboratory at ~20°C when they were brand new keep on being the same while in operating condition. In addition, it must be considered that the measurements performed with the VNA have an intrinsic absolute error. The VNA manual reports a total error of 0.1 dB at the transmitting and receiving power levels used at the IFAC labs. By considering this incertitude in the determination of the equivalent hot load at section 0 it emerges that assuming a $T_{H_{NS}}$=323.15 K, $T_{H_{NS0}}$=332.21K ± 2.3K for the V pol channel and $T_{H_{NS0}}$=330.30K ± 2.3K for the H pol one. By considering the Tb of the deep sky to be known exactly (the CMB value is very accurate from radioastronomy and the small atmosphere emission is very stable), an estimate of the downward cold sky measurements at the incidence angle of 115 deg is provided in the first annual report of Domex-3 [11] and is T_{SKY}=5.01K. Then we convolved the antenna lobe with the ice sheet and sky emissions to get an accurate estimate of Tb measurements at 115 deg incidence angle. By using this value for the cold reference and the ones of $T_{H_{NS0}}$ plus and minus the incertitude it is possible to estimate the total error on the ice sheet measurements.

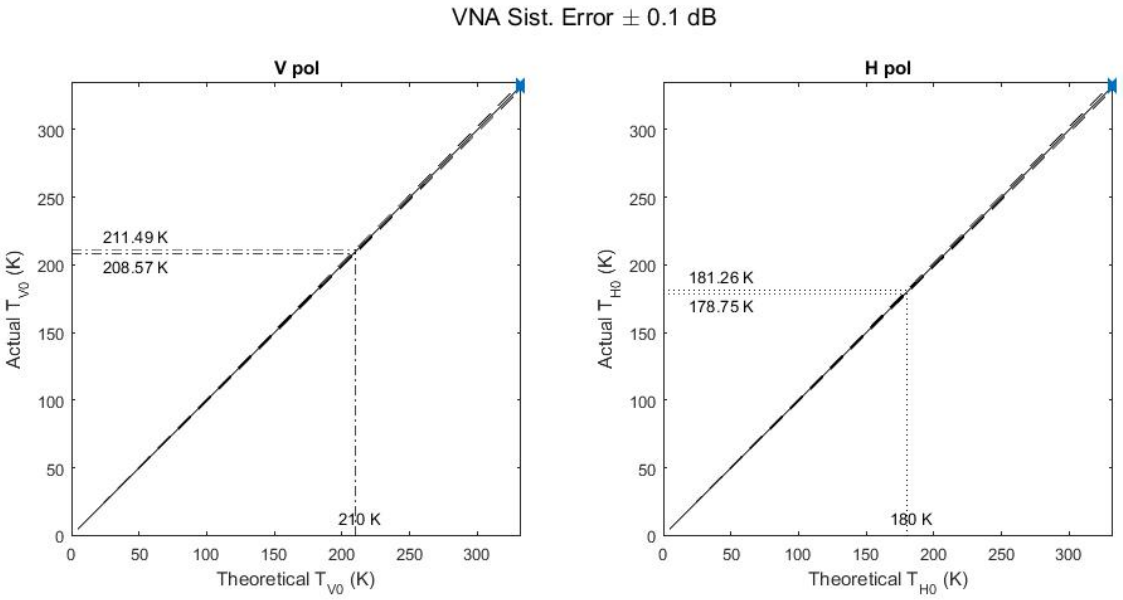

Figure 4-7 Effect of uncertainties of the S parameters of the cables and antenna on the ice sheet measurements

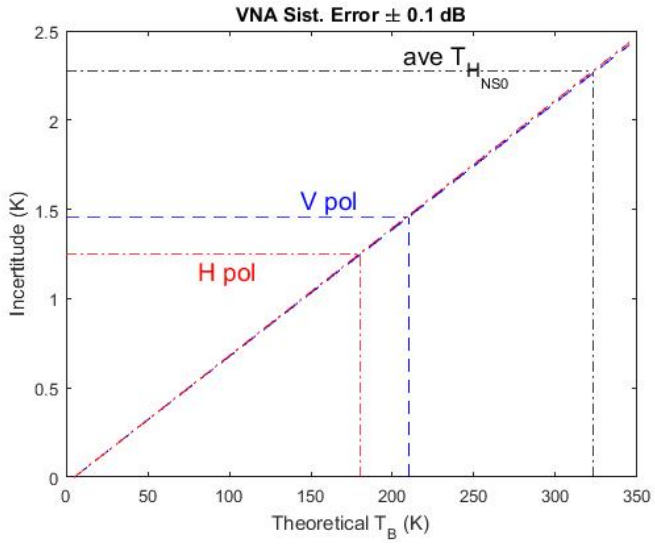

Figure 4-8 Incertitude on the T_b measurements of the ice sheet for the two channels. For the equivalent hot load an average value has been reported.

Assuming a TbV=210K and a TbH=180K the incertitude on the absolute Tb values due to the incertitude on the equivalent hot load are ± 1.4K and ± 1.2K for the V and H pol respectively (see Figure 4-7 and Figure 4-8).

Because previous results demonstrated that the losses between sections 1 and 2 can change in time (e.g. see report [11]), the calibration should be repeated after a given time lapse as described in [TN2].

It should be noted that also the internal cold load could be used for this kind of calibration since its temperature is continuously measured. However, since its temperature is not stable and is located outside of RF section, it is expected that its performances for the absolute calibration will be worse with respect to the noise source because of the fluctuating temperature and of the further loss introduced by the cable connecting Tc to the mw switch.

4.2.1 Absolute calibration results

The previously described approach has been tested by using the data collected from 31 May to 7 July 2017. On June 14-23, Radomex acquired data looking at the sky with an incidence angle of 115 deg while the internal noise source was switched off (see Figure 4-9).

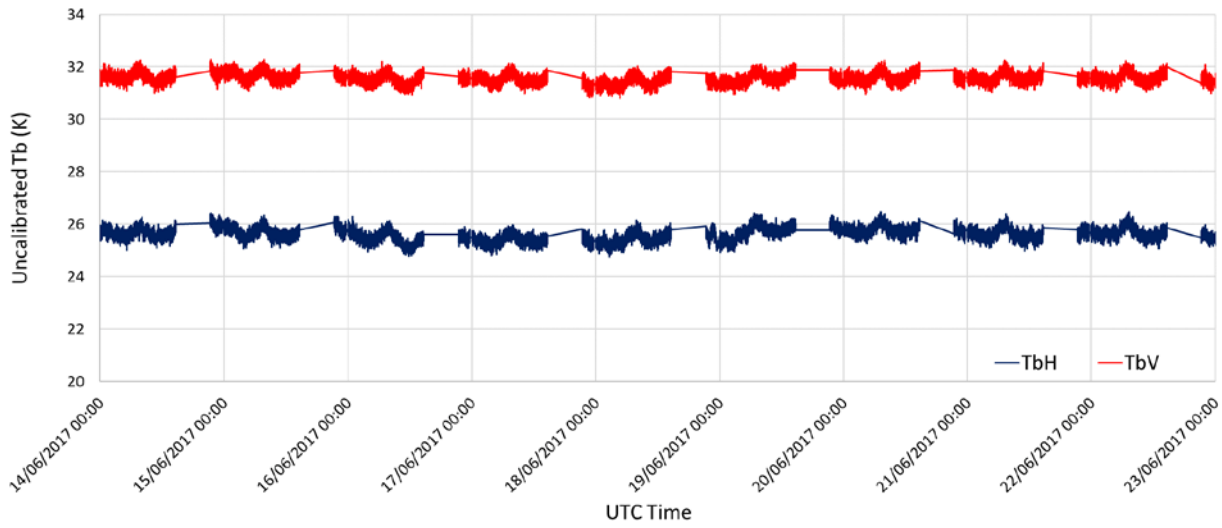

Figure 4-9 Data collected on Jun 14-23 2017 for the absolute calibration test.

Only data collected from 21:30 to 14:30 (i.e. sun azimuth lower than 90deg or higher than 200deg) were used since the center of the galaxy is outside the antenna lobe in this period. The Tb of the sky measurements were 31.6K and 21.6K for the V and H pol respectively (standard deviations 0.2K and 0.24K).

The equivalent hot targets derived from the procedure of section 4.2 were 333.8K and 331.9K for the V and H polarization respectively (standard deviation 0.11K and 0.12K). To obtain the "real" Tb value of the cold target we proceed as follows. Given that the radiometer was measuring at an elevation of 25 deg above the horizon, the antenna lobe still collected energy coming from the ice sheet (albeit very small). Thus, in order to derive a proper cold reference value we convolved the antenna lobe with the Tb of a proper synthetic scene. For the ice sheet the Tb simulated by using the WALOMIS model [12]

was used. Sky emission was obtained by using a radiative transfer model under the assumption of non-scattering plane parallel atmosphere in local thermodynamic equilibrium [13] and two years of Radio-Echo Sounding collected at Dome C by the Italian Meteorological observatory from Jan 2012 to Dec 2013 [14]. Gaseous absorption/emission (mainly water vapor and oxygen) formulas were developed by Rosenkranz [15], cloud layers are identified from RAOBs when the atmospheric RH profile exceeds a suitable threshold function [16], absorption/emission from Liebe [17] and further modifications. The final scenario is represented in Figure 4-10 along with the antenna gain (Radomex antenna has a symmetrical lobe on the V and H planes).

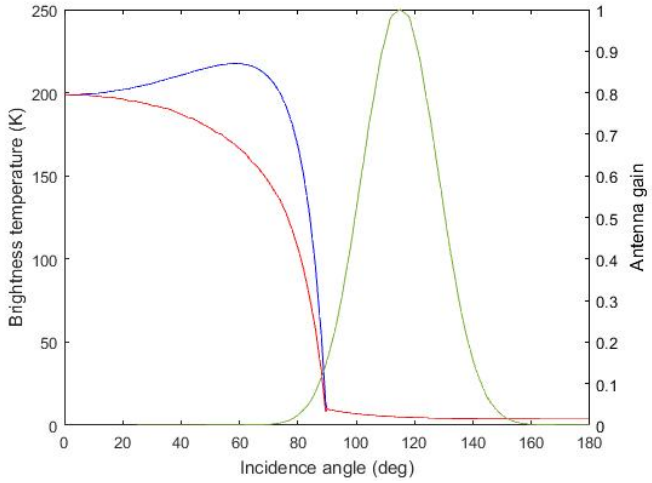

Figure 4-10 The angular trend of the synthetic scenario at V- (blue) and H-pol (red) plotted along with the antenna gain (green) in a linear scale.

By convolving the V- and H-pol Tb angular trends with the antenna gain it is possible to derive the true Tb values observed by the radiometer while looking at 115deg. They resulted in being 7.51K and 6.65K for the V and H pol respectively.

With the hot and cold reference target characterized, it was possible to calibrate absolutely Radomex data. As a first test, the data collected fourteen days before (from May 31 00:00 to June 13 10:00) and after (from June 23 3:50 to July 7 23:36) the sky measurements while looking at the ice sheet at 42 deg incidence angle were calibrated absolutely. The average Tb values obtained were 211.14K and 186.32K (pre-calibration period, σ 0.22K and 024K) and 211.04K and 186.22K (post-calibration period, σ 0.21K and 0.33K) for the V and H pol respectively.

These values resulted in being slightly higher with respect to those obtained during the 2016 Antarctic campaign (see Table 4-3) and in line with SMOS data, especially at V-pol. Albeit being slightly higher, Tb obtained with the new procedure showed a polarization difference higher than before (24K Vs 22K) and more in line with SMOS data. It must be underlined that Domex data were not deconvoluted for the antenna pattern, thus the Tb values will likely increase by a few K.

Table 4-3 – Values of Tb after the absolute calibration

Dataset	Tb (K)	
	H pol	V pol
Domex 2017 new procedure	186.27	211.09
Domex entire 2016 (no sun)	185.24	207.73
SMOS entire 2016	186.3	212.37

It is worth outlining that absolute calibration strongly relies on the value of Tb for the sky measurement. The atmosphere model used in this TN assumed plane parallel layers, however this assumption can be too strong for measurements carried out at low elevation angles. A more accurate model can provide a different value for T_{sky}, resulting in a different absolute calibration curve. However, this difference is expected to be small since the atmospheric water vapor content in over the Antarctic plateau is quite negligible.

A last exercise was carried out by evaluating how many sky acquisitions are necessary for the absolute calibration of the data. The entire dataset described before was considered. It was calibrated by using sky Tb collected only for 1 day, 2 days, 3 days, and so on until the use of the full sky time series. The results of the analysis are represented in Figure 4-10 and show a very small dependence of the Tb on the days of sky acquisitions used in determining the absolute calibration curve. Although a variation in Tb can be noted, its amplitude is negligible (less than 0.1K).

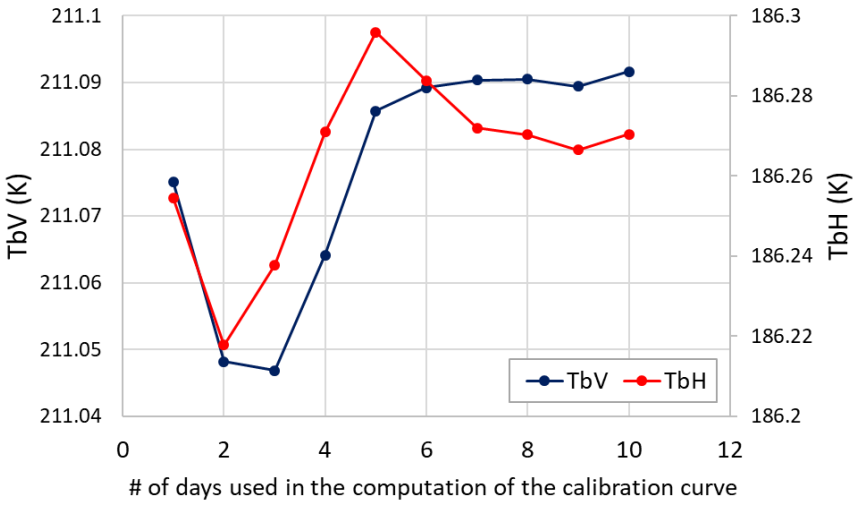

Figure 4-11 Variation of Tb as a function of the days of sky measurements used in the determination of the absolute calibration curve

4.2.2 Quantification of the total incertitude

In order to quantify the total accuracy associated with absolute calibration the sources of incertitude in the process must be identified. In section 4.2, the parameter values that determine the absolute calibration are:

- cable losses $L_{INT\ v,h}$ and $L_{EXT\ v,h}$,
- reflection coefficients at the antenna ports $\Gamma_{v,h}$,
- temperature of the internal and external cables T_C and T_0,
- temperature of the noise source T_{NS},
- energy emitted from the input ports of the RF section toward the antenna T_{REC},
- brightness temperature of the sky at the calibration incidence angle T_{sky} .

Cable losses $L_{INT\ v,h}$, $L_{EXT\ v,h}$ were measured prior to their deployment at Dome C by using an Agilent ENA E5071C VNA. The measurements were collected at constant ambient temperature around 20°C. The IF frequency was set to 10 Hz and the input power to -5 dBm in order to have the most accurate measurements as possible. For these conditions, the VNA datasheet reports an absolute accuracy of 0.1dB on the S parameters.

The antenna ports reflection coefficients $\Gamma_{v,h}$ were measured before the beginning of the Domex-3 experiment in the IFAC anechoic chamber by using an Anritsu MS2026A VNA. The accuracy of these measurements is 0.2 dB.

The noise source is used in the absolute calibration procedure as a matched load at a very stable thermometric temperature. For this reason it is turned off during the calibration acquisitions. Its temperature is controlled by a PID regulator manufactured by Jumo Gmbh (model 702040) coupled with a three-wire PT100 probe. The temperature of the noise source T_{NS}, as well as the one of the internal T_C and external cables T_0, is measured by means of PT100 transmitters manufactured by Edif Instruments s.r.l (model RTDTX1). Their accuracy is reported to be <0.05°C.

The value of T_{REC} has been determined by using the procedure outlined in appendix 8 with the attenuation values of the cable and the isolator measured by the previously described VNA. By using the VNA accuracy, the incertitude on T_{REC} value can be estimated to be 62.8K ± 11.9K. It is worth underlining that this is the value of the Tb emitted by the ACL, not the Tb of the entire system ACL+isolator+cable which was determined accurately with LN2 measurements and used in the relative calibration of the radiometer.

The last parameter that influences the absolute calibration accuracy is the true value of the Tb of the scene during the sky measurements. The simulations provided the values of T_{sky} as a function of the elevation angle with an incertitude due to RAOB variations (see Figure 4-12 and Table 4-4). However an estimate of the absolute accuracy of T_{sky} is not available. In [18] an estimation of the atmosphere emission contribution at nadir in similar conditions of dry atmosphere is provided by extrapolating the Tb from measurements at S-, X- and W-band. The resulting value was 0.83 K ± 0.1 K and is concordantly in line with our model results.

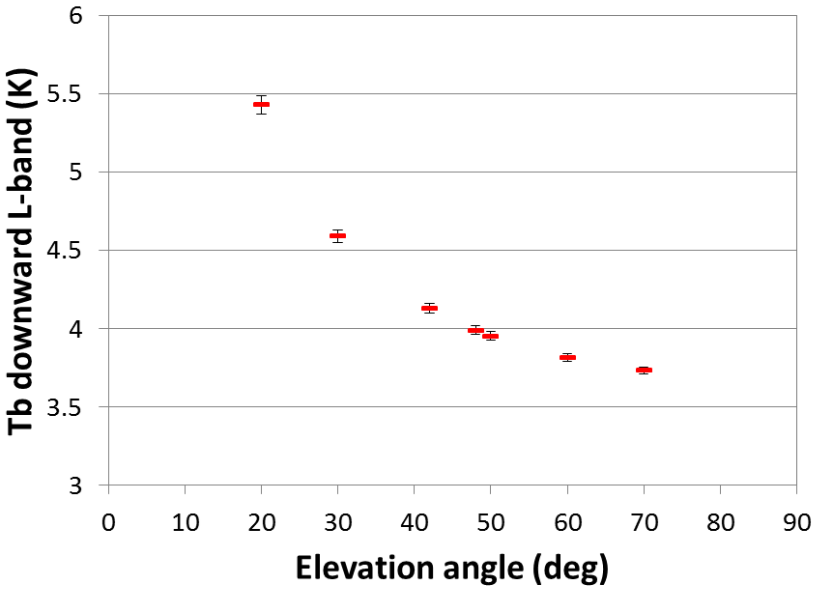

Figure 4-12 Modeled Tb emitted downward from the atmosphere as a function of the elevation angle. Cosmic Background Radiation contribution is included

Table 4-4 – Values of sky Tb emitted downward

Elevation (deg)	Mean Tb (K)	Std Dev (K)
20	5.43	0.060
30	4.59	0.041
42	4.13	0.031
48	3.99	0.028
50	3.95	0.027
60	3.82	0.024
70	3.73	0.022

Table 4-5 shows the absolute accuracies to which the parameters involved in the absolute calibration are known.

Table 4-5 – Values of parameter accuracy used in the determination of calibration incertitude

Parameter	Accuracy
$L_{INT\ v,h}$, $L_{EXT\ v,h}$	0.1 dB
$\Gamma_{v,h}$	0.2 dB
T_C, T_0, T_{NS}	0.05°C
T_{REC}	11.9 K
T_{sky}	0.02K

Since all of the parameters previously listed can be assumed to vary independently in the operative conditions, the accuracy of the absolute calibration can be expressed by

$$A_{T_b} = \sqrt{\left(\frac{\partial T_b}{\partial L_{INT}(A_{L_{INT}})}\right)^2 + \left(\frac{\partial T_b}{\partial L_{EXT}(A_{L_{EXT}})}\right)^2 + \left(\frac{\partial T_b}{\partial \Gamma(A_\Gamma)}\right)^2 + \left(\frac{\partial T_b}{\partial T_C(A_{T_C})}\right)^2 + \left(\frac{\partial T_b}{\partial T_0(A_{T_0})}\right)^2 + \left(\frac{\partial T_b}{\partial T_{NS}(A_{T_{NS}})}\right)^2 + \left(\frac{\partial T_b}{\partial T_{REC}(A_{T_{REC}})}\right)^2 + \left(\frac{\partial T_b}{\partial T_{sky}(A_{T_{sky}})}\right)^2}$$

where A_γ indicates the accuracy of a given parameter γ. Each term represents the variation of Tb w.r.t. to a given parameter γ when this latter is known with an incertitude A_γ. Obviously, previous equation must be specified for each channel of the radiometer. The incertitude introduced in the absolute calibration by each parameter of Table 4-5 is reported in Table 4-6 along with the total one.

Table 4-6 – Incertitude introduced in the absolute calibration by each parameter of Table 4-5

Source of incertitude	Tb incertitude (K)	
	H pol	V pol
Antenna cables losses	0.84	0.94
Internal cables losses	0.70	0.70
Antenna reflection coeff	0.03	0.09
Tns	0.03	0.04
Tc	0.00	0.00
T0	0.02	0.00
Trec	0.03	0.08
Tsky	0.01	0.01
Total incertitude	1.10	1.18

5 References

[1] ESA Contract:20066/06/NL/EL - Technical Support for the Deployment of an L-band radiometer at Concordia Station during DOMEX-2 – Report 1 –Sept 2006

[2] ESA Contract:20066/06/NL/EL - Technical Support for the Deployment of an L-band radiometer at Concordia Station during DOMEX-2 – Report 2 –Aug 2007

[3] ESA Contract:20066/06/NL/EL - Technical Support for the Deployment of an L-band radiometer at Concordia Station during DOMEX-2 – Report 3 –Sep 2008

[4] ESA Contract:20066/06/NL/EL and 20046/08/NL/EL - Technical Support for the Deployment of an L-band radiometer at Concordia Station during DOMEX-2 and Data Analysis – Final Report – Oct 2011

[5] ESA Contract: 4000105872/12/NL/NF - Technical Support for the Long-Term Deployment of an L-Band Radiometer at Concordia Station – Yearly Report – Data Acquisition and Processing Report First Year – D3- D6 –2014

[6] M. Leduc-Leballeur et al., "Modeling L-Band Brightness Temperature at Dome C in Antarctica and Comparison With SMOS Observations," in IEEE Transactions on Geoscience and Remote Sensing, vol. 53, no. 7, pp. 4022-4032, July 2015, doi: 10.1109/TGRS.2015.2388790

[7] J.A. Shroeder, and E.R. Westwater, "Users' guide to WPL microwave radiative transfer software," *NOAA Technical Memorandum* ERL WPL-213, October 1991

[8] Data and information were obtained from IPEV/PNRA Project 'Routin Meteorological Observation at Station Concordia' - http://www.climantartide.it

[9] P.W. Rosenkranz, "Water Vapor Microwave Continuum Absorption: A Comparison Of Measurements And Models," *Radio Sci*., vol. 33, no. 4, pp. 919–928, 1998.

[10] M.T. Decker, E.R. Westwater, and F.O. Guiraud, "Experimental evaluation of ground-based microwave radiometric sensing of atmospheric temperature and water vapor profiles," *J. Appl. Meteor.,* no. 17, pp. 1788–1795, 1978

[11] Liebe, H. J., G. A. Hufford, and T. Manabe (1991), A model for the complex permittivity of water at frequencies below 1 THz, *Int. J. Infrared Millimet. Waves*, *12*(7), 659–675

[12] Levin S. M., C. Witebsky, M. Bensadoun, M. Bersanelli, G. de Amici, A. Kogut, "A measurement of the cosmic microwave background radiation temperature at 1.410 GHz", Astrophysical Journal, Part 1 (ISSN 0004-637X), vol. 334, Nov. 1, 1988, p. 14-21.

[13] Ulaby F.T., R. K. Moore, A. K. Fung, "*Microwave remote sensing – Active and passive*", Addison-Wesley Publishing Company, Volume 1, 1981

[14] Søbjærg S. S., S. S. Kristensen, J. E. Balling and N. Skou, "The airborne EMIRAD L-band radiometer system," 2013 IEEE International Geoscience and Remote Sensing Symposium - IGARSS, Melbourne, VIC, 2013, pp. 1900-1903, doi: 10.1109/IGARSS.2013.6723175

[15] Pablos M., I. Durán, "Analysis of amplitude calibration drift in SMOS", SMOS-BEC Workshop "One year of SMOS data", 5/12/2010

This page is intentionally left blank.

6 Appendix – Effects of lossy passive devices on the Tb measurements

The effect of a cable or an antenna on the brightness temperature can be estimated by using the Friis formula [19]. Indeed, these passive devices can be modelled as potentially mismatched lossy devices.

In the case of a lossy device with matched ports (e.g. a cable can be assumed with these characteristics, see Figure 6-1)

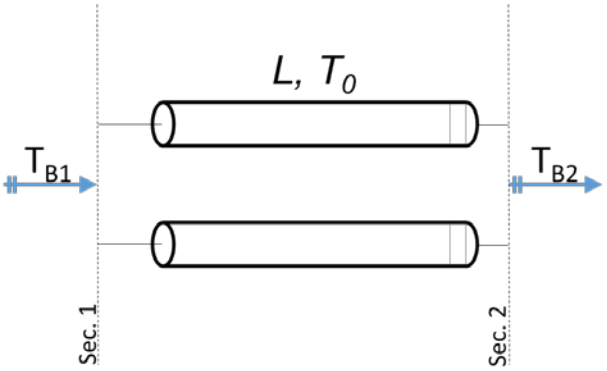

Figure 6-1 – Sketch of a lossy transmission line. *L* and T_0 indicate the losses and the transmission line temperature respectively.

the brightness temperature measured at section 2 is

$$T_{B2} = L\,T_{B1} + (1 - \mathrm{L})T_0$$

and

$$L = 10^{-S_{21}(dB)/10}$$

In the previous formula, $S_{21}(dB)$ are the attenuation losses in dB of the device (a positive value), e.g. as measured with a vectorial network analyzer. In the case of a cascade of two perfectly matched lossy devices (e.g. like in the case of a cable connected to an antenna, see Figure 6-2) it is possible to apply the previous Friis formula iteratively.

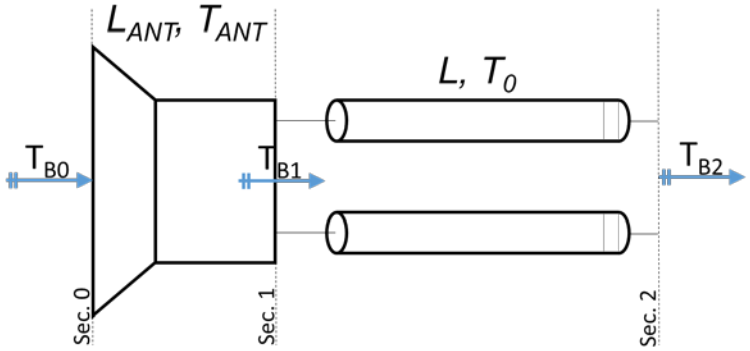

Figure 6-2 – Sketch of a cascade of lossy antenna and transmission line. L_{ANT}, T_{ANT}, L and T_0 indicate the losses and the temperature of the antenna and the transmission line respectively.

In this case

$$T_{B1} = L_{ANT}\, T_{B0} + (1 - L_{ANT})T_{ANT}$$

which gives

$$T_{B2} = L\, L_{ANT}\, T_{B0} + L\, (1 - L_{ANT})T_{ANT} + (1 - \mathrm{L})T_0$$

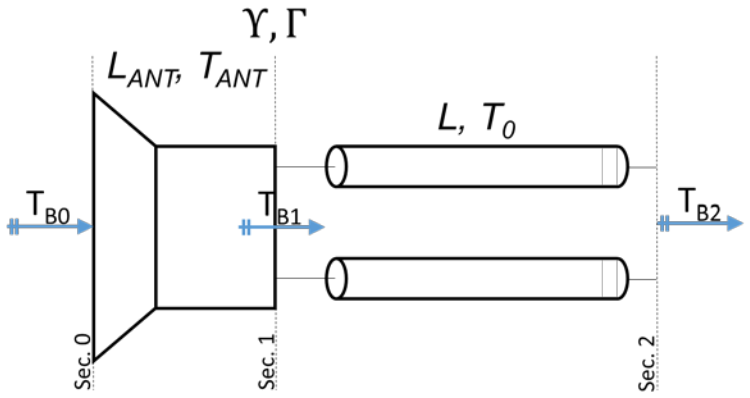

Figure 6-3 – Sketch of a cascade of lossy antenna and transmission line with a mismatch on section 1. □ and □ are the transmissivity and the reflectivity respectively.

In the case of a mismatch between the two devices (i.e. a mismatch at section 1, see Figure 6-3 where □ and □ are respectively the transmission and reflection coefficients at section 1, a common approximation is □=1-□) the energy that is fed into section 1 from section 0 is lower than the one impinging in the section of a factor □. At the same time the energy coming from section 2 to section 1 is reflected

backward and dumped by a factor □. This is the case of a radiometer receiver connected at section 2, that will feed its own emitting power T_{REC} into section 2 toward section 1, that will be reflected by the mismatch at section 1 towards section 2 (see Figure 6-4). A quantification of this quantity is provided in appendix 8.

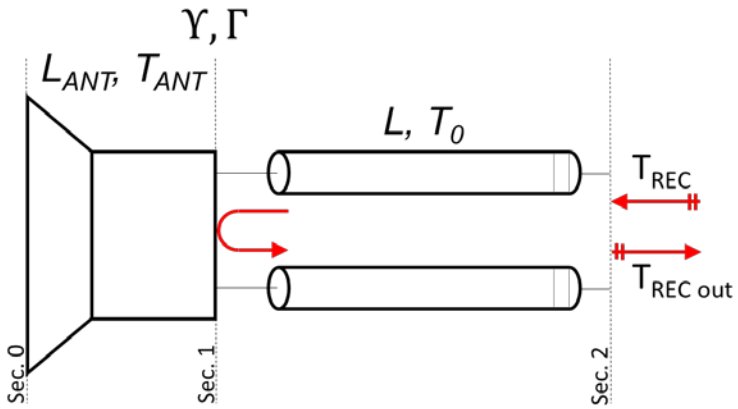

Figure 6-4 – Sketch of the energy emitted by the receiver inside of the transmission line and reflected by the mismatch.

In this case the brightness temperature measured at section 2 will be

$$T_{B2} = L\,(\Upsilon\,T_{B1} + \Gamma\,T_{REC1}) + (1-\mathrm{L})T_0$$
$$= L\,(\,(1-\Gamma)\,T_{B1} + \Gamma\,T_{REC1}\,) + (1-\mathrm{L})T_0$$

in which

$$T_{B1} = L_{ANT}\,T_{B0} + (1-L_{ANT})T_{ANT}$$

and

$$T_{\mathrm{REC1}} = L\,T_{REC} + (1-\mathrm{L})T_0$$

It should be noticed that previous equations easily reduce to the initial case when the antenna port is matched with the transmission line (□=0 and □=1).

In the case of a lossless antenna ($L_{ANT} = 1$, the Potter antenna of Radomex can be assumed thus), the previous equation simplifies to

$$T_{B2} = \mathrm{L}\Upsilon\,T_{B0} + \mathrm{L}^2\,\Gamma\,T_{REC} + (\mathrm{L}\,\Gamma + 1)\,(1-\mathrm{L})T_0$$

This page is intentionally left blank.

7 Appendix – Parameters of the Radomex components

During the design of Radomex, particular care has gone into selecting the better components available on the market.

The antenna is a Potter horn (the same used in the Emirad radiometer [20]) coupled with an OMT manufactured by Pasquali Microwave Systems. The characterization of the two coupled devices provides the following parameters

$$L_{ANT} = 0$$
$$\Gamma_V = 0.0134 \quad \Gamma_H = 0.0052$$
$$\Upsilon_V = 0.9866 \quad \Upsilon_H = 0.9948$$

The external cable S parameters have been measured prior to the installation in the instrument and their values are listed in Table 3-2 and reported here for the sake of convenience.

Table 7-1 – Losses of the external cables

	S_{11} (dB)	S_{21}(dB)
V pol	-30.94	-0.409
H pol	-31.78	-0.403

Given the low values of S_{11} it is correct to assume that the cables are perfectly matched. The attenuation losses L are:

$$L_{ext\,V} = 0.910$$
$$L_{ext\,H} = 0.911$$

Regarding the internal antenna cables (the ones connecting the N-ports to the SP6T microwave switch), also in this case it is possible to consider the cables perfectly matched and the L values are

$$L_{int\,V} = 0.976$$
$$L_{int\,H} = 0.977$$

It is worth underlining that these values have been measured at an ambient temperature of about 20°C. However the radiometer works over a much broader temperature range. Thus the impact the temperature has on these values should be evaluated.

This page is intentionally left blank.

8 Appendix – Computation of T_{REC}

In order to derive the brightness temperature of the scene in front of the antenna it is important to estimate the energy emitted by the radiometer and reflected by the antenna mismatches. This value can be obtained by measuring the brightness temperature emitted by the radiometer under test by using a calibrated one. However, since the ACL is an amplifier like the ones in the RF chain (same brand, model and operating conditions) it is possible to assume that T_{REC} is the same as T_{ACL} providing the compensation of the losses introduced by the ACL and the cable.

In summary, it is possible to model the cable and the isolator between the ACL and the switch as loss devices and use 2-stages Friis equation to get the effective T_{ACL} (see Figure 8-1). T_{ACL} was obtained during the laboratory calibration phase by using the liquid nitrogen test.

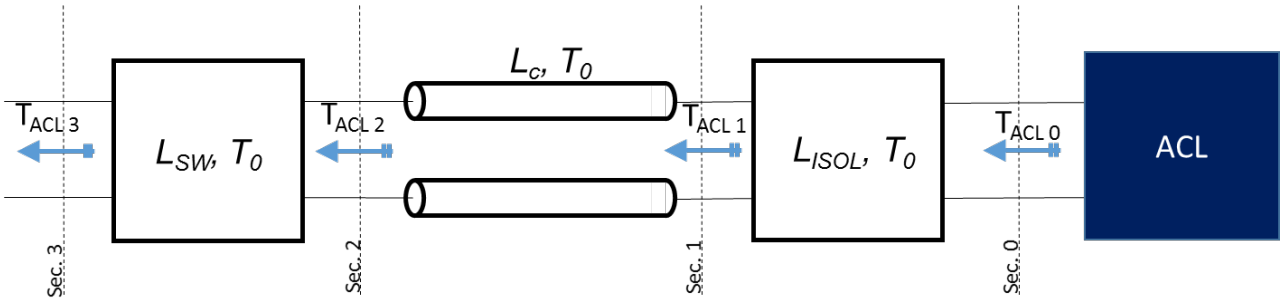

Figure 8-1 – The ACL chain

The parameters of the devices represented in Figure 8-1 in the chain are listed in Table 8-1, where L_c is the excess of attenuation with respect to the Sucoform cables of the antenna and LSW is the excess of loss of the sixth switch channel with respect to the other channels (all very similar).

Table 8-1 – Losses of the devices in the ACL chain

T_0	49.37 °C
L_{ISOL}	0.186 dB ↔ 0.958
L_c	0.083 dB ↔ 0.981
L_{SW}	0.422 dB ↔ 0.907

From the laboratory measurements it is shown that:

$$T_{ACL\,3} = 101K$$

Then, by using the equations developed in Appendix 6

$$T_{ACL\,2} = L_{sw}^{-1}\,[\,T_{ACL\,3} - (1 - L_{sw})\,T_0\,] = 78.39\;K$$

$$T_{ACL\,1} = L_{c}^{-1}\,[\,T_{ACL\,2} - (1 - L_{c})\,T_0\,] = 73.68\;K$$

$$T_{ACL\,0} = L_{ISOL}^{-1}\,[\,T_{ACL\,1} - (1 - L_{ISOL})\,T_0\,] = 62.8\;K$$

The temperature emitted by the receiver toward the antenna can be assumed

$$T_{REC} = 62.8\;K$$

Technical Support for the Long-Term Deployment of an L-Band Radiometer at Concordia Station

TN2 - Technical Note on the Acquisition Plan

EUROPEAN SPACE AGENCY STUDY
ESTEC Contract 4000105872/12/NL/NF
CCN 6

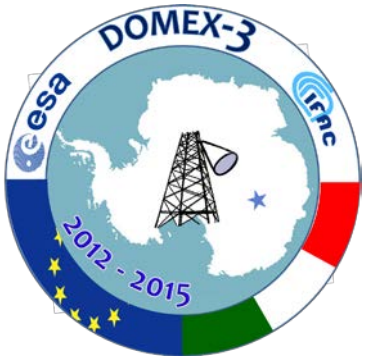

Prepared by

Giovanni MACELLONI, Marco BROGIONI, Francesco MONTOMOLI

IFAC- CNR, Florence, ITALY

Date: 31/8/2017

Version: 1.0

Consiglio Nazionale delle Ricerche
Istituto di **F**isica **A**pplicata "Nello **C**arrara"

This page is intentionally left blank.

ESA STUDY CONTRACT REPORT

ESTEC Contract No:	Subject:		Contractor:
4000105872/12/NL/NF	Technical Support for the Long-Term Deployment of an L-Band Radiometer at Concordia Station		IFAC
ESA CR ( )No:	Star Code:	No of volumes: 1 This is volume no: 1	Contractor's Ref: Deliverable

ABSTRACT:

This technical note is related to the study *Technical Support for the Long-Term Deployment of an L-Band Radiometer at Concordia Station* (ESTEC contract 4000105872/12/NL/NF). It contains the description of the angular scan and sky measurements scheduling to be carried out for fulfilling the requirement of a better absolute calibration and for improving the capability to compare ground and satellite observations.

The work described in this report was done under ESA Contract. Responsibility for the contents resides in the author or organisation that prepared it.

prepared by:

Giovanni MACELLONI, Marco BROGIONI, Francesco MONTOMOLI - IFAC

ESA STUDY MANAGER:	ESA BUDGET HEADING
Tania CASAL	

DOCUMENT CHANGE LOG

Issue/ Revision	Date	Observations
1/0	31/08/2017	First issue

ABBREVIATIONS

ESA	European Space Agency
IFAC-CNR	Institute of Applied Physics – National Research Council
PNRA	Programma Nazionale Ricerche in Antartide (Italian National Research Programme in Antarctica)
Radomex	RADiometer for DOMEX experiment
TN	Technical Note

Applicable Documents

CCN6	ESA Contract. 4000105872/12/NL/FF/FK – Contract Change Note 6, dated 17/10/2016
RD1	Campaign Implementation Plan October 2012, Deliverable D2 of "Technical Support for the Long-Term Deployment of an L-Band Radiometer at Concordia Station'', ESA Contract 4000105872/12/NL/NF, Version 2.0, dated 22/10/2012.
TN1	Technical Note on RADOMEX high level radiometer architecture and absolute calibration strategy, ESA Contract 4000105872/12/NL/NF

This page is intentionally left blank.

TABLE OF CONTENTS

This page is intentionally left blank.

1 Purpose and structure of document

This technical note is focused on the angular scan and sky measurements scheduling to be performed in the framework of the Domex-3 experiment to fulfil the requirement of a better absolute calibration and to improve the capability to compare ground and satellite observations. It is strongly related to TN1 in which the absolute calibration strategies of Radomex are detailed. The present TN summarize the angular measurement scans to be performed during the 2017, highlighting the ones to be used for the calibration along with an assessment of the risks linked to the angular scans.

This page is intentionally left blank.

2 Overview

The Domex-3 experiment is the continuation of two previous experiments called Domex-1 and Domex-2 that were successfully conducted at Concordia Station, Antarctica, by IFAC-CNR in cooperation with the Agency (contracts N. 18060/04/NL/CB [5] and N. 22046/08/NL/EL, 20066/06/NL/EL [4]) and PNRA (Italian Antarctic National Research Programme).

The acquisition configuration of Radomex consists in a fixed azimuth direction (north-west direction) and a variable incidence angle between 30deg and 130deg. Form the beginning of the experiment until the Austral summer 2016, Radomex acquisitions were carried out at a fixed angle of 42deg (the same of the SMOS browse product). Angular scans were sporadically carried out to check the relative calibration of the radiometer (i.e. to identify any drift in the RF chain or in the thermal system) and changes in the angular signature of the ice sheet emission. Usually, around five angular scans per year were carried out.

In order to improve the monitoring of the ice sheet and to develop a new absolute calibration methodology for Radomex (as described in TN1), it was decided to modify the acquisition plan as described in [RD1] (see [CCN6]). In the next section the new acquisition plan is described as long as the description of the measurements performed until summer 2017.

This page is intentionally left blank.

3 Description of new acquisition plan

3.1 Old acquisition plan

The acquisition plan implemented in the period November 2012 – December 2016 is described in the Domex-3 Campaign Implementation Plan [RD1]. Every year of campaign is divided into two periods, each with a particular geometry acquisition plan:

- ***Intensive Operational Period (IOP),*** beginning of the summer when a qualified operator will be at Concordia station
- ***Normal Operational Period (NOP),*** the rest of the year.

During the IOP , three different angular acquisitions were performed:

- 42deg incidence angle ice sheet measurements
- Sky Measurements
- Incidence angle scan

The objective of the sky measurements was the verification of radiometer performances over a low temperature target. The sky is observed for 24 hours per day at a fixed incidence angle of 120° taking into consideration the sun contamination and the sky emission and the mechanical limitations.

The incidence angle scan were intended to compare DOMEX-3 data to SMOS one and to monitor the angular emission of the ice sheet along the years. For these specific measurements, a procedure similar to that used during the first phase of Domex-2 experiment was adopted:

- Phase 1: Ice-sheet Acquisition : data are acquired in the incidence angle range 90°- 30° using 7 steps of 10°, at each incidence angle the period of observation is 10 minutes in order to acquire a sufficient number of data. The total duration of this phase is 70 minutes and it appeared to be sufficiently short to satisfy the constraints 3 described above.
- Phase 2: Sky acquisition: data are acquired in the incidence angle range 110°- 120° using 3 steps of 5°, at each incidence angle the period of observation is 10 minutes in order to acquire a sufficient number of data
- Phase 3: Ice-sheet SMOS angle: data are acquired at a fixed incidence angle of 42° for a period of 70 minutes.

With this angular scheduling, a total number of 8 complete cycles per day can be performed. This number was large enough to control the daily physical processes of the snow surface and to evaluate the effect of sun in the different period of the day.

The sky measurements last for 4 days and are performed at the beginning and at the end of the IOP. The incidence angle scans also last 4 days and are performed after each sky acquisition.

The NOP is considered when the instrument operates during winter time (i..e from February to November) or in summer when the qualified operator will not be at the base. Due to the limited possibility of operation on the field and the extreme weather conditions (highlighted in [RD1]) Radomex was let collecting data will be acquired at a fixed incidence angle of 42° 24 h per day.

Incidence angle scans were performed occasionally in late spring and early autumn if the weather conditions allowed them.

3.2 New Acquisition Plan

The old acquisition plan was established in order to cope with the main object of the Domex-3 experiment, i.e. the long term monitoring of the ice sheet emission at Dome C. In the last years a new need has emerged: the accurate absolute calibration of the Radomex acquisition in order to support SMOS MIRAS instrument. To perform such task, the acquisition plan of the experiment has been reviewed according to the suggestion of the Agency in order to allow for new calibration techniques described in [TN1].

The requirement of the new acquisition plan strategy, as described in the [CC6], were the following:

1) During the intensive operational period (Austral Summer)
   a. Cold Sky acquisitions at 70° elevation angle by manually resetting the pointing of RADOMEX at the lower range of its mechanical actuator. Cold Sky acquisition to be performed during the month when IFAC personnel is available at Dome-C base camp (the goal is to perform four (4) Cold Sky measurements)
   b. Extended scans to improve the antenna deconvolution calculations, from 50° incidence to 80° elevation (hence, over a 120° angular range), with 5° resolution, performed with the mechanical actuator in Cold Sky configuration, i.e. as part of a Cold Sky acquisition
   c. Incidence angle scans from 20° to 60° for comparison with SMOS, with an improved sampling of 2° resolution. These scan are to be performed once per day (TBC).
   d. 42° fixed incidence angle pointing in between any angular scans or Cold Sky views.
   e. All angular scans and Cold Sky views shall be carried out during the local morning time when the Sun is at the back of RADOMEX (i.e. close to opposite azimuth angle) and the galactic plane is far from the Cold Sky pointing direction (i.e. the Galactic Pole is within 60° of the Cold Sky pointing direction) to minimise their influence.

2) During the normal operational period (Austral Winter)
   a. Incidence angle scans from 20° to 60° for comparison with SMOS, with an improved sampling of 2° resolution. A total of three (3) (TBC) of these scan are to be performed.
   b. 42° fixed incidence angle pointing the remaining time.

A suggested draft Acquisition Plan is described in Annex 1 of CCN6.

Starting from the austral summer campaign of 2016/17, the new acquisition plan has been implemented. A summary of the measurement performed until 31/07/2017 is given in Table 3-1 and Table 3-2.

Table 3-1 – Summary of acquisition geometry performed during the 2016/17 Austral summer

Period	Acquisition Type	Date	Duration (hh:mm)	Angle (deg – start/stop/step)
intensive operational period (Austral Summer)	DECONV #1	28/11/2016	01:10	60/160/ 5
	DECONV #2	28/11/2016	01:16	60/160/ 5
	ICE SHEET #1	29/11/2016	01:34	20/60/2
	ICE SHEET #2	30/11/2016	01:34	20/60/2
	ICE SHEET #3	01/12/2016	01:34	20/60/2
	ICE SHEET #4	03/12/2016	02:30	20/60/2
	ICE SHEET #5	04/12/2016	02:30	20/60/2
	ICE SHEET #6	04/12/2016	02:30	20/60/2
	DECONV #3	05/12/2016	01:16	60/160/ 5
	DECONV #4	06/12/2016	01:16	60/160/ 5
	ICE SHEET #7	06/12/2016	02:30	20/60/2
	ICE SHEET #8	07/12/2016	02:30	20/60/2
	ICE SHEET #9	07/12/2016	02:30	20/60/2
	ICE SHEET #10	08/12/2016	02:30	20/60/2
	ICE SHEET #11	09/12/2016	02:30	20/60/2
	ICE SHEET #12	10/12/2016	02:30	20/60/2
	DECONV #5	10/12/2016	01:16	60/160/ 5
	DECONV #6	11/12/2016	01:16	60/160/ 5
	ICE SHEET #13	11/12/2016	02:30	20/60/2
	ICE SHEET #14	12/12/2016	02:30	20/60/2
	ICE SHEET #15	12/12/2016	02:30	20/60/2
	ICE SHEET #16	13/12/2016	02:30	20/60/2
	ICE SHEET #17	16/12/2016	02:30	20/60/2
	ICE SHEET #18	17/12/2016	02:30	20/60/2
	ICE SHEET #19	18/12/2016	02:30	20/60/2
	ICE SHEET #20	19/12/2016	02:30	20/60/2
	ICE SHEET #21	20/12/2016	02:30	20/60/2
	ICE SHEET #22	21/12/2016	02:30	20/60/2
	ICE SHEET #23	22/12/2016	02:30	20/60/2

In Table 3-1 are listed all the acquisitions performed in the 2016/17 austral summer that are different to the 42deg incidence angle measurements. In the column Acquisition Type is reported the target of the measurement along with a progressive number. “DECONV” referred to the requirement at points 1-a) and 1-5) of the previous list while “ICE SHEET” to the point 1-c).

Table 3-2 is similar to Table 3-1 but it described the acquisition performed in the winter period. “FULL SCAN” referred to the point 2-a) of the above list. In March and in June, 2 long-time measurements of the sky has been performed for calibration purposes.

Table 3-2 – Summary of acquisition geometry performed during the 2017 Austral winter

Period	Acq Type	Date	Duration (hh:mm)	Angle (deg – start/stop/step)
Normal operational period (Austral Winter)	FULL SCAN #1	18/01/2017	04:01	20/110/2
	FULL SCAN #2	19/01/2017	04:01	20/110/2
	FULL SCAN #3	20/01/2017	04:01	20/110/2
	FULL SCAN #4	24/01/2017	04:01	20/110/2
	FULL SCAN #5	25/01/2017	04:01	20/110/2
	FULL SCAN #6	26/01/2017	04:01	20/110/2
	FULL SCAN #7	02/03/2017	04:01	20/110/2
	FULL SCAN #8	03/03/2017	04:01	20/110/2
	FULL SCAN #9	04/03/2017	04:01	20/110/2
	FULL SCAN #10	05/03/2017	04:01	20/110/2
	FULL SCAN #11	06/03/2017	04:01	20/110/2
	SKY #1	07/3 - 13/3	7 days	110
	FULL SCAN #12	02/04/2017	04:01	20/110/2
	FULL SCAN #13	03/04/2017	04:01	20/110/2
	FULL SCAN #14	04/04/2017	04:01	20/110/2
	FULL SCAN #15	06/04/2017	04:01	20/110/2
	SKY #2	13/06 - 23/06	10 days	115
	FULL SCAN #16	25/06/2017	04:01	20/110/2
	FULL SCAN #17	26/06/2017	04:01	20/110/2

For the remaining part of the 2017 campaign the acquisition will follow the same schedule used up to now and described above.

TECHNICAL SUPPORT FOR THE LONG-TERM DEPLOYMENT OF AN L-BAND RADIOMETER AT CONCORDIA STATION

DATA DESCRIPTION: MW –IR TEMPERATURE

MAY 2018

EUROPEAN SPACE AGENCY STUDY CONTRACT REPORTS

ESTEC CONTRACT 4000105872/12/NL/NF

PREPARED BY

Giovanni Macelloni, Francesco Montomoli and Marco Brogioni

IFAC – CNR – SESTO FIORENTINO – ITALY

DATE: 28/05/ 2018

This page is intentionally left blank

ESA STUDY CONTRACT REPORT			
EUROPEAN SPACE AGENCY STUDY CONTRACT REPORTS ESTEC CONTRACT 4000105872/12/NL/NF	TECHNICAL SUPPORT FOR THE LONG-TERM DEPLOYMENT OF AN L-BAND RADIOMETER AT CONCORDIA STATION		CONTRACTOR: IFAC-CNR
ESA CR ( )NO:	STAR CODE:	No of volumes: 1 This is volume no: 1	CONTRACTOR'S REF: MW-IR Temperature DataBase
ABSTRACT: This report contains the information of the MW-IR temperature data collected during DOMEX-3 experiment.			
The work described in this report was done under ESA Contract. Responsibility for the contents resides in the author or organisation that prepared it.			
AUTHORS: G. Macelloni, M. Brogioni, F.Montomoli (IFAC-CNR)			
ESA **STUDY MANAGER**: T.Casal		ESA BUDGET HEADING	

This page is intentionally left blank

1 TITLE

1.1 Data set identification

DOMEX-3 Microwave and Infrared Radiometers data.

1.2 Revision date of this document (dd/mm/yyyy)

14/05/2018

1.3 INVESTIGATOR(S)

Dr. Giovanni Macelloni
Earth Observation Department
Istituto di Fisica Applicata (IFAC)
Consiglio Nazionale delle Ricerche
Via Madonna del piano 10 - 50019 -Sesto Fiorentino (Fi) - Italy
Tel. + 39 055 5226495 – Fax + 39 055 5226467
E-mail: G.Macelloni@ifac.cnr.it

2 EQUIPMENT

2.1 Instrument description.

The measurements were carried out with IFAC microwave radiometer called RADOMEX, please refers to the Year report 2017 of the project for more information.

2.2 Platform (Satellite, Aircraft, Ground).

Ground

2.3 Key variables.

Microwave brightness temperature at 1.4 GHz (L-band), horizontal and vertical polarization, Infrared temperature (8-14 μm).

2.4 Instrument measurement geometry.

Data were collected from the tower-mounted radiometer from January 2017 to December 2017 at different incidence angles within the 30° - 115° range with respect to nadir (i.e 0° = nadir view) in the North-West direction. Different procedure have been followed for the acquisition as described in the Final Report and in the Experiment Support Plan of the project.

2.5 Manufacturer of instrument.

Instruments were designed and developed at IFAC CNR Firenze Italy

2.6 ABSOLUTE CALIBRATION DISCLAIMER

The absolute calibration procedure used for the 2017 dataset differ from the one used in the past and is described in DOMEX-3, "Yearly Report - Data Acquisition and Processing Report - Fifth Year", D3- D6, May 2018. Thus the brightness temperature values are higher than the ones of past Domex-3 dataset showing a bias of 4.53K at V pol and 2.79K at H pol (i.e. 2017 Tb are higher than the ones of previous years). In order to compare previous data these biases need to be considered.

3 PROCEDURE

3.1 Data acquisition methods.

Data were collected automatically from the tower-mounted radiometer 24 hours/day. Data acquisition and platform movement were automatically controlled by means of a PC placed in the box; and the experiment was monitored remotely using a Local Area Network connection.

The following parameters were used for the acquisitions:
Integration time (measurement and calibration): 2 second
Number of measurements between calibration: 2 (1 V and 1 H)
Measurement Time (for each position): variable

IMPORTANT NOTE : In the dataset is represented the number of measurements, Tb mean value and standard deviation collected at each single position.

3.2 Spatial characteristics.

3.2.1 Spatial coverage.

Data were acquired at a fixed position at:

Coordinates: 75.0989°S 123.3005°E

Altitude: 3250 M

The antenna foot-print (HPBW) ranged from 10x14 m^2 at θ = 20° to 10 x 160 m^2 at θ = 70° .

3.2.2 Spatial resolution.

Please refers to Experiment Implementation Plan

3.2.3 Temporal characteristics.

Please refers to Experiment Implementation Plan

3.2.4 Temporal coverage.

Data represented in this dataset were acquired from January 2017 to December 2017

4 DATA DESCRIPTION

4.1 Table definition with comments.

The data base is contained in the file DOMEX_3_FIFTHYEAR_2017_MWDATA.txt in ASCII format.

It could be easily opened with MS Excel or Matlab.

The files are composed by a table of 345444 Rows + 1 (header) and 37 Columns

Column description:

c1 = Date – time DD/MM/YY hh:mm
c2 = Number of samples
c3 = Sun zenith position (degs)
c4 = Sun angular position (degs)

c5 = Quality flag; 0 = quality check passed; 1 = quality check not passed only for V-pol; 2 = quality check not passed only for H-pol; 3 = quality check not passed
c6 = sun flag; 0 = sun not in front of the antenna; 1 = sun in the antenna pattern
c7 = calibration scheme; 1 = frequent calibration hot and cold load; 2 = frequent calibration fixed gain, cold load; 3 = frequent calibration cold load and noise source.
c8 = TVL= Brightness Temperature L band – Vertical polarization (K)
c9 = Stdev TVL= Standard deviation of #c8 (K)
c10 = THL= Brightness Temperature L band – Horizontal polarization (K)
c11 = Stdev THL= Standard deviation of #c10 (K)
c12 = Theta = Incidence Angle (degrees)
c13 = SdevTheta = Standard deviation of #c12 (degs)
c14 = Theta = Azimuth Angle (degrees)
c15 = SdevTheta = Standard deviation of #c14 (degs)
c16 = Tir= Temperature of the calibrator of IR sensor (°C)
c17 = Stdev Tir= Standard deviation of #c16 (°C)
c18 = Temperature of Tns internal to the Radiometer receiver
c19 = Stdev Tns= Standard deviation of #c18 (°C)
c20 = Temperature of Tsw internal to the Radiometer receiver
c21 = Stdev Tsw= Standard deviation of #c20 (°C)
c22 = Temperature of Tcables1 internal to the Radiometer receiver
c23 = Stdev Tcables= Standard deviation of #c22 (°C)
c24 = Temperature of Tcables2 internal to the Radiometer receiver
c25 = Stdev Tcables= Standard deviation of #c24 (°C)
c26 = Temperature of T_H_omt connector
c27 = Stdev T_H_omt= Standard deviation of #c26 (°C)
c28 = Temperature of T_V_omt connector
c29 = Stdev T_V_omt= Standard deviation of #c28 (°C)
c30 = Temperature of T_H_rad connector
c31 = Stdev T_H_omt= Standard deviation of #c30 (°C)
c32 = Temperature of T_V_rad connector
c33 = Stdev T_V_rad= Standard deviation of #c32 (°C)
c34 = Temperature of T_OMT
c35 = Stdev T_ant= Standard deviation of #c34 (°C)
c36 = Temperature of Antenna front part
c37 = Stdev T_ant= Standard deviation of #c36 (°C)

- Missing data are identified as NaN

5 DATA QUALITY

5.1 Data Manipulations

As described in detail in the DOMEX Final Report the data at L band were processed and calibrated.

5.2 Sources of error.

The errors in the measurement were mainly related to the data post-processing. The adopted procedure is described in the Final Report of the project.

5.3 Quality assessment.

The minimum detectable temperature variation of the radiometer (sensitivity) was 0.3 K (with $\tau = 2$ sec), and the accuracy (repeatability) was better than 0.5 K over a period of 30 days.

5.4 Quality flag definition.

The quality flag (column # c5 of the file) is defined as follows:
0 - Tb standard deviation computed over number of samples defined in column # c2 at V and H pol. Is lower than 1 K
1 - Tb standard deviation computed over number of samples defined in column # c2 at V pol. Is higher than 1 K
2 - Tb standard deviation computed over number of samples defined in column # c2 at H pol. Is higher than 1 K
3 - Tb standard deviation computed over number of samples defined in column # c2 at V and H pol. Is higher than 1 K.

A value higher than 0 imply a degradation of the measure.

6 REFERENCES

Technical Support for the Long-Term Deployment of an L-Band Radiometer at Concordia Station Yearly Report – Fifth Year Report, May 2018 ESA-ESTEC Contract 4000105872/12/NL/NF – Macelloni et al.

7 DATA POLICY

The participants (IFAC and CVA) have the exclusive right of access to and exploitation of data lather than 6 months after the end of the project (presentation of the final report). After this date dissemination of the dataset will be performed by ESA under the control and with the approval of IFAC.

TECHNICAL SUPPORT FOR THE LONG-TERM DEPLOYMENT OF AN L-BAND RADIOMETER AT CONCORDIA STATION

DATA DESCRIPTION: SNOWTEMPERATURE

MAY 2018

EUROPEAN SPACE AGENCY STUDY CONTRACT REPORTS

ESTEC CONTRACT 4000105872/12/NL/NF

PREPARED BY

Giovanni Macelloni, Simone Pettinato, Francesco Montomoli and Marco Brogioni

IFAC – CNR – SESTO FIORENTINO – ITALY

DATE: May 2018

This page is intentionally left blank

ESA STUDY CONTRACT REPORT			
EUROPEAN SPACE AGENCY STUDY CONTRACT REPORTS ESTEC CONTRACT 4000105872/12/NL/NF	TECHNICAL SUPPORT FOR THE LONG-TERM DEPLOYMENT OF AN L-BAND RADIOMETER AT CONCORDIA STATION		CONTRACTOR: IFAC-CNR
ESA CR ( )NO:	STAR CODE:	No of volumes: 1 This is volume no: 1	CONTRACTOR'S REF: Snow Temperature DataBase
ABSTRACT: This report contains the information of the snow temperature data collected during DOMEX-3 experiment.			
The work described in this report was done under ESA Contract. Responsibility for the contents resides in the author or organisation that prepared it.			
AUTHORS: S.PETTINATO, G. Macelloni, M. Brogioni, F.Montomoli (IFAC-CNR)			
ESA **STUDY MANAGER**: T.Casal		ESA BUDGET HEADING	

This page is intentionally left blank

1 TITLE

1.1 Data set identification

DOMEX-3 Snow Temperature Data

1.2 Revision date of this document (yyyy/mm/dd)

2018/05/28

2 INVESTIGATOR(S)

Dr. Giovanni Macelloni
Earth Observation Department
Istituto di Fisica Applicata (IFAC)
Consiglio Nazionale delle Ricerche
Via Madonna del piano 10 - 50019 -Sesto Fiorentino (Fi) - Italy
Tel. + 39 055 5226495 – Fax + 39 055 5226467
E-mail: G.Macelloni@ifac.cnr.it

3 EQUIPMENT

3.1 Instrument description.

The measurements were carried out with LSI LASTEM –data logger. –Model EL 305 and EL 105, Probes: PT100 Din-A
Please refers to http://www.lsi-lastem.it for more information.

3.2 Platform (Satellite, Aircraft, Ground).

Ground

3.3 Key variables.

Snow Temperature measured at different depth (range 0-10 m)

3.4 Instrument measurement geometry.

The temperature profile of the first 10 m of the snow pack was measured by using 16 probes. The probes (PT100 –DIN-A) were placed at different depths as described Table 1

Table 1

Probe N	Depth (cm)
1	5
2	10
3	25
4	50
5	75
6	100
7	150
8	200
9	250
10	300
11	400
12	500
13	600
14	800
15	1000
16	AIR

3.5 Manufacturer of instrument.

Instruments were designed and developed by LSI-LASTEM (Italy).

4 PROCEDURE

4.1 Data acquisition methods.

Data were collected automatically by the data logger.

Data were acquired at each minute and recorded at each hour.

IMPORTANT NOTE : In the dataset is represented the mean value and its standard deviation along one hour of acquisition registered every minute.

4.2 Spatial characteristics.

Spatial coverage.

Data were acquired at a fixed position at,:

Coordinates: 75.0989°S, 123.3005°E.

Altitude: 3250 m

Please refers to the Final Report of the project for more information

4.3 Temporal characteristics.

Temporal coverage.

Data represented in this dataset were acquired from January 1, 2017 to December 31, 2017.

5 5. DATA DESCRIPTION

Snow temperature probe collected at at 600 and 800 cm was damaged after 23/11/2016.
Air Temperature must be intended as experimental

5.1 Table definition with comments.

The data base is contained in the file **DOMEX3_snowtemp_database3.txt** as ASCII format.

It could be easily opened with MS Excel or Matlab.

The file is composed by a table 10468 rows + 1 (header) and 33 Columns.
Columns description:
c1 =Date – time YYYYMMDDTHHMMSS
c2 = T1= Mean Temperature Probe 1 (5 cm) (°C)
c3 = T1= Standard Deviation Temperature Probe 1 (5 cm) (°C)
c4 = T2= Mean Temperature Probe 2 (10 cm) (°C)
c5 = T2= Standard Deviation Temperature Probe 2 (10 cm) (°C)
c6 = T3= Mean Temperature Probe 3 (25 cm) (°C)
c7 = T3= Standard Deviation Temperature Probe 3 (25 cm) (°C)
c8 = T4= Mean Temperature Probe 4 (50 cm) (°C)
c9 = T4= Standard Deviation Temperature Probe 4 (50 cm) (°C)
c10 = T5= Mean Temperature Probe 5 (75 cm) (°C)
c11 = T5= Standard Deviation Temperature Probe 5 (75 cm) (°C)
c12 = T6= Mean Temperature Probe 6 (100 cm) (°C)
c13 = T6= Standard Deviation Temperature Probe 6 (100 cm) (°C)

c14 = T7= Mean Temperature Probe 7 (150 cm) (°C)
c15 = T7= Standard Deviation Temperature Probe 7 (150 cm) (°C)
c16 = T8= Mean Temperature Probe 8 (200 cm) (°C)
c17 = T8= Standard Deviation Temperature Probe 8 (200 cm) (°C)
c18 = T9= Mean Temperature Probe 9 (250 cm) (°C)
c19 = T9= Standard Deviation Temperature Probe 9 (250 cm) (°C)
c20 = T10= Mean Temperature Probe 10 (300 cm) (°C)
c21 = T10= Standard Deviation Temperature Probe 10 (300 cm) (°C)
c22 = T11= Mean Temperature Probe 11 (400 cm) (°C)
c23 = T11= Standard Deviation Temperature Probe 11 (400 cm) (°C)
c24 = T12= Mean Temperature Probe 12 (500 cm) (°C)
c25 = T12= Standard Deviation Temperature Probe 12 (500 cm) (°C)
c26 = T9= Mean Temperature Probe 13 (600 cm) (°C)
c27 = T9= Standard Deviation Temperature Probe 13 (600 cm) (°C)
c28 = T10= Mean Temperature Probe 14 (800 cm) (°C)
c29 = T10= Standard Deviation Temperature Probe 14 (800 cm) (°C)
c30 = T11= Mean Temperature Probe 15 (1000 cm) (°C)
c31 = T11= Standard Deviation Temperature Probe 15 (1000 cm) (°C)
c32 = T12= Mean Temperature Probe 16 (Air Temperature) (°C)
c33 = T12= Standard Deviation Temperature Probe 16 (Air Temperature) (°C)

- Missing data are identified as NaN

6 *DATA QUALITY*

6.1 Data Manipulations

Data were not manipulated

7 Sources of error.

Please refers to LSI-Lastem information

8 Quality assessment.

Please refers to LSI-Lastem information

9 REFERENCES

[1] LSI-LASTEM user manual (http://www.lsi-lastem.it/pdf/instum00031.pdf)

[2] TECHNICAL SUPPORT FOR THE LONG-TERM DEPLOYMENT OF AN L-BAND RADIOMETER AT CONCORDIA STATION

10 DATA POLICY

The participants (IFAC and CVA) have the exclusive right of access to and exploitation of data lather than 6 months after the end of the project (presentation of the final report). After this date dissemination of the dataset will be performed by ESA under the control and with the approval of IFAC.